

Aus dem Institut für Klinische Neuroimmunologie,

Ludwig-Maximilians-Universität München

Direktor: Prof. Dr. Reinhard Hohlfeld

**Gen-Expressionsanalyse aus autoptischen Formalin-fixierten und
Paraffin- eingebetteten Gewebeproben von Multiple Sklerose Patienten**

Dissertation

zum Erwerb des Doktorgrades der Medizin

an der Medizinischen Fakultät der

Ludwig-Maximilians-Universität zu München

vorgelegt von

Sylvia Christine Eisele

aus

Schwäbisch Gmünd

2013

Mit Genehmigung der Medizinischen Fakultät
der Universität München

Berichterstatter: Prof. Dr. Edgar Meinel

Mitberichterstatter: Priv. Doz. Dr. Rupert Egensperger
Prof. Dr. Ortrud Steinlein
Priv. Doz. Dr. Stefan Kastenbauer

Dekan: Prof. Dr. med. Dr. h.c. Maximilian Reiser, FACR, FRCR

Tag der mündlichen Prüfung: 18.04.2013

Gewidmet
meinen Eltern und
meiner lieben Großmutter Elfriede,
die mein Interesse für die Medizin geweckt hat.

Table of Contents

1	Introduction.....	5
1.1	Pathological concepts of multiple sclerosis based on tissue analysis.....	5
1.2	Tissue specimens for pathological investigation of multiple sclerosis.....	5
1.3	Transcript expression analysis in FFPE tissue.....	6
1.4	Micro-RNAs and their potential role in multiple sclerosis.....	7
1.5	Alteration of the extracellular matrix in multiple sclerosis brain tissue.....	8
2	Summary.....	9
2.1	Scope of this study.....	9
2.2	Results.....	9
3	Zusammenfassung.....	12
3.1	Fragestellung.....	12
3.2	Ergebnisse.....	12
4	Publications	15
4.1	“Prospects of transcript profiling for mRNAs and microRNAs using formalin fixed and paraffin embedded dissected autoptic multiple sclerosis lesions”.....	15
4.2	„Extracellular matrix in multiple sclerosis lesions: fibrillar collagens, biglycan and decorin are upregulated and associated with infiltrating immune cells“	16
4.3	„Micro RNA profiling of multiple sclerosis lesions identifies modulators of the regulatory protein CD47”	17
5	Abbreviations	18
6	References	19
7	Acknowledgement	27
8	Curriculum Vitae.....	28

1 Introduction

1.1 Pathological concepts of multiple sclerosis based on tissue analysis

Josephine Paget was 38 years old when she presented with left sided hemiparesis, gait imbalance and painful right hand numbness. When she died one year later, pathological examination of her spinal cord revealed a patchy degeneration of the nervous tissue reaching from superficial white matter into the deep gray matter. This was the first clinic-pathological description of the disease which is known today as multiple sclerosis (MS) and was published in 1842 by Cruveilhier (18). Later on, Charcot, Bourneville, Babinski and others have referred to and have extended the description of „la sclerose en plaques“ (4, 9, 15).

Over 150 years later, tremendous efforts have been made to elucidate the causes and the mechanisms of this chronic demyelinating disease of the central nervous system (CNS). Today, MS is considered an autoimmune disease, which is driven by an immune cell mediated injury of the myelin sheath (50, 70). The brain parenchyma is invaded mainly by T cells and macrophages, but also by B cells and plasma cells (8, 24, 32, 50, 64, 80) which travel across a disrupted blood-brain barrier (84). This process is orchestrated by a multitude of adhesion molecules, chemokines/cytokines, cleaving enzymes and other immune related molecules (13, 20, 38, 58). Beyond the aspect of demyelination of the white matter, other hallmarks of the disease (re)gain more and more attention such as neuronal and axonal injury (5, 16, 25-27, 30, 31, 45, 47, 65, 79), grey matter pathology (6, 7, 12, 43, 48, 57, 69) and normal appearing white matter pathology (2, 28, 49). In addition, there are controversial discussions, whether or not there are inter-individual and even inter-lesional variations in the pathology of MS lesions (10, 56).

Despite all these valuable contributions, conclusions and hypotheses, one is still far from a complete and detailed understanding of the causes and the pathogenesis of MS. Last but not least, there remains a need for effective and targeted therapy strategies to potentially influence or even halt the progression of this chronic debilitating disease.

1.2 Tissue specimens for pathological investigation of multiple sclerosis

Modern molecular biology techniques such as quantitative polymerase chain reaction (qPCR), multiplex PCRs and microarrays are inevitable tools for the investigation of MS pathology and pathogenesis. These techniques require good quality tissue specimens. In general, fresh frozen biopsy specimens are considered to have best tissue quality,

followed by fresh frozen autopsy specimens and formalin fixed and paraffin embedded (FFPE) specimens. The term FFPE refers to the conservation process of formalin fixation and embedment in paraffin. Most MS tissue samples are obtained by autopsy whereas biopsy specimens are very rare.

The vast majority of MS tissue samples obtained by autopsy are stored as formalin fixed and paraffin embedded (FFPE) specimens (77). Whereas good preservation of tissue structures in FFPE specimens allows for precise histological and immunohistochemical evaluation, the investigation of RNA expression levels is challenging due to impaired RNA quality even if the tissue is fixed immediately (44). Hence, for investigations using molecular research technology, frozen tissue specimens are in general preferred over FFPE tissue, because of the better preservation of ribonucleic acids. However, there is increasing evidence that reliable gene expression analysis can also be performed in FFPE tissue, especially when highly sensitive techniques such as qPCR are used (17, 68, 77). Most of these prior studies have been performed in cancer tissue obtained by surgical biopsy, therefore representing high-quality, cell-rich tissue which contains high amounts of undegraded ribonucleic acids. In contrast, there is only little known about the reliability of gene expression analysis in FFPE tissue specimens obtained by autopsy and even less about prospects and limitations of transcript analysis in archival MS tissue samples of autoptic origin.

Modern investigation strategies to investigate MS pathology require application of a combined approach including detailed histological analysis and sensitive molecular research technologies such as qPCR, microarrays and multi-gene PCR assays (14, 36, 46, 55, 72). Neuro-pathological collections all over the world contain highly valuable FFPE specimens and represent treasures of different disease subtypes and variants. These specimens are awaiting discovery for molecular investigations.

1.3 Transcript expression analysis in FFPE tissue

RNA isolation from FFPE tissue is possible and several efficient protocols have been developed (34, 40, 82). RNA expression levels in archival tissue samples can be measured using reverse transcription (RT)-PCR technology (1, 34, 52).

In tissue samples of autoptic origin, RNA degradation by terminal hypoxia and post mortem autolysis add to the inevitable RNA destruction and modification during

formalin fixation and paraffin embedment (11, 17, 29, 54, 60, 67) and therefore complicate transcript expression analysis.

However, the short transcript fragments left after RNA degradation can still be detected with quantitative PCR technology because the amplicon length of commonly used gene assays is rather small and ranges from 50-150 only (1, 33, 51, 77, 83). Therefore qPCR has been shown to be particularly suitable for RNA analysis in archival tissue specimens. With this technology, effective gene expression analysis in FFPE specimens has been demonstrated in various types of human tissues obtained by surgical biopsy. These studies have shown that results from FFPE tissue reliably reflect results obtained in frozen tissue samples (1, 33, 51, 77, 83). Also, investigations of RNA stability in frozen brain samples obtained by autopsy have shown that brain tissue is quite robust in this regard even with long time period between death and tissue fixation (19, 41, 75, 90).

Over the past years, broad-spectrum gene expression assays such as micro-arrays and multi-gene PCR assays have been widely accepted for investigation of various diseases including MS (14, 46, 72). This technology allows for evaluation of gene expression patterns or “thumbprints” of the investigated disease in includes different gene families and genes of differential abundance. Therefore, a multi-gene PCR assay appears suitable to analyse how reliable gene expression patterns can be detected in FFPE compared to frozen tissue and whether there are differences in usability of FFPE tissue specimens based on abundance of the target gene and amplicon length of the used gene detection assay.

1.4 Micro-RNAs and their potential role in multiple sclerosis

Micro-ribonucleic acids (miRNAs) have increasingly been recognized as important players in physiology and pathology of many diseases including MS (21, 22, 53). Since little is known about these recently identified molecules, they are currently the subject of intensive investigations using transcript profiling technology.

In FFPE tissues, expression levels of miRNAs have been investigated using microarray and qPCR technology in various human organs (78, 85, 87) including the brain (62). In these studies, detectability of miRNAs has been shown to be enormously stable despite formalin fixation and paraffin embedment, and miRNA expression results were nearly identical compared to frozen tissue (62, 78, 85, 87). These findings could

make archival MS lesion samples a valuable and extensively available resource for further investigation of the role of miRNAs in MS pathology.

Based on an analysis in frozen MS and healthy brain tissue, two of the miRNAs, miR-181a and miR-124, were found to be very abundant and stably expressed in both, diseased and healthy brain tissue (own data). Therefore, these miRNAs were selected to investigate the differential amplifiability in FFPE compared frozen tissue. Further, it was of interest to learn whether miRNA profiling can be applied to archival MS lesions of differential disease activity and if the miRNA expression profiles change based on the stages of activity.

1.5 Alteration of the extracellular matrix in multiple sclerosis brain tissue

The structural organization of the extracellular matrix (ECM) in the brain is mainly based on hyaluronan (or hyaluronic acid/hyaluronate), a linear polysaccharide and glycosaminoglycan (63, 71, 73, 81). Hyaluronan acts as the backbone molecule to which proteoglycans are attached with the help of linking proteins such as the tenascins C and R. Prominent proteoglycans in the brain are the lectican family including brevican and neurocan (59, 88) and the “small leucine rich proteoglycans” (SLRPs) such as decorin and biglycan (39, 74).

So-called fibrous glycoproteins (e.g. collagens, laminins and fibronectin) are expressed at relatively low levels in the healthy adult brain. All these components form a scaffold which provides physical support to the resident cells and directly influences re-modelling processes, cell division and motility (81).

Previous work showed that expression of these ECM components as well as of ECM modifying enzymes may be altered in MS. For example: tenascin C and the matrix metalloproteinase 2 (MMP-2) are upregulated components of the gliotic scar in chronic MS lesions (3, 35). In active demyelinating lesions neurocan and MMP-2 are induced during ongoing re-modeling processes (76). Neurocan is further associated with T cell activation (66). The SLRP decorin may act as a scavenger protein for TGF- β (89) and possibly promotes survival and adhesion of macrophages (86). It has also been described to rescue a suppressed T cell response (37).

Since ECM components are relatively abundant in the brain and may be easily detected in FFPE tissue, expression results for this group of genes were investigated in further detail by comparing FFPE and frozen tissue.

2 Summary

2.1 Scope of this study

The aim of this study was to evaluate the usage of archival MS tissue specimen for transcript profiling of mRNAs and miRNAs using qPCR technology.

Specifically, the following issues were addressed:

- (1) Application of a feasible protocol to isolate RNA from FFPE brain tissue and comparison of the RNA yield in FFPE and frozen material
- (2) Usability of randomly selected archival FFPE tissue samples for transcript analysis by investigating the amplifiability of a housekeeping gene and two miRNAs
- (3) Effect of length of formalin fixation on transcript amplifiability
- (4) Implementation of an experimental setup for dissection of defined MS lesion areas in FFPE tissue for subsequent qPCR
- (5) Comparison of gene expression results of 84 extracellular matrix related genes using TaqMan[®] qRT-PCR Low Density Arrays in FFPE and frozen tissue samples
- (6) Validation of the upregulation of the extracellular matrix component decorin on protein level by immunohistochemistry
- (7) Application of this methodological progress to obtain the first miRNA profile of MS lesions

2.2 Results

A protocol for RNA isolation from FFPE brain tissue was introduced and optimized in the laboratory. It was demonstrated that both, RNA yield and the ratio of light absorption at 260 nm vs. 280 nm (OD 260/280) in FFPE tissue are comparable to frozen tissue (23).

A total of 27 archival brain specimens of 11 MS donors obtained from different brain banks were screened for the ability to amplify the housekeeping gene PPIA as well as miRNA 181a and miR 124. Results were compared to amplification of the same transcripts in 9 frozen MS tissue samples of 9 MS patients. The ability to amplify PPIA in FFPE tissue specimens was very heterogeneously distributed and the loss of amplifiable transcript copies ranged from 45 fold to 200 000 fold as compared to frozen tissue. In some archival samples PPIA could not be detected at all. These specimens were considered not suitable for further qPCR analysis. In contrast, the amplification of

miRNA 181a and miR 124 in FFPE tissue was tremendously stable with an average loss of amplifiability of 1.7 fold only (23).

Among several factors which possibly have an influence on impaired transcript amplification in FFPE tissue, the effect of length of formalin fixation was investigated in more detail. It was shown that duration of formalin fixation had great impact on loss of subsequent amplification of coding transcripts (e. g. PPIA). Compared to frozen tissue, PPIA amplification was reduced by ~15 fold in samples which were formalin-fixed for a day-long period, which is in contrast to a reduction of PPIA amplification by ~200 fold in specimens which had been fixed for years (23). Here again, miRNA amplification was demonstrated to be remarkably stable in the same FFPE tissue samples (23).

Based on the stable miRNA detection in FFPE tissue specimens, 18 FFPE tissue specimens (MS n=13, healthy donor n=5) were included in a study which compared the miRNA expression pattern in MS lesions to healthy brain tissue by qPCR analysis of 365 mature miRNAs (42).

Furthermore, an experimental setup was established which allows for precise dissection of MS lesions from surrounding normal appearing white matter (NAWM). To this end, FFPE sections were obtained using a microtome, were flattened in a DEPC water bath and mounted on PEN membrane coated slides. RNA yield and amplification of PPIA were not altered by this approach. Parallel tissue sections were stained with Luxol Fast Blue (LFB) and served as a model to help with the precise dissection of MS lesions. This setup was applied to 5 FFPE tissue samples (MS lesion n=3, healthy donor n=2). RNA was isolated from the dissected tissue specimens to analyse differential expression of 84 extracellular matrix (ECM) related genes in MS lesions compared to healthy tissue using TaqMan[®] Low Density Array qPCR technology. This was compared to a data set derived from frozen tissue samples that had been processed in a similar way. Detection of gene regulation (MS/healthy) in FFPE tissue was found to be reliable and comparable to frozen tissue, provided that the selected genes were of sufficient abundance (23).

The up-regulation of the extracellular matrix component decorin could be validated on protein level by immuno-histochemistry in the same FFPE MS lesions. This result was published as part of a study which investigated the expression of several extracellular matrix related genes in MS lesions with frozen tissue, e.g. collagens and the protein biglycan (61). Furthermore this study showed that fibrillar collagens, biglycan and decorin are part of the perivascular fibrosis. These molecules are expressed in

proximity to tissue invading immune cells, therefore suggesting a possible disease modifying function (61).

In summary, this work presents a detailed protocol for the use of autoptic FFPE tissue specimens to obtain gene expression profiles from dissected MS lesions (23). This protocol was implemented as part of a study which investigated alterations of ECM in MS lesions (61) and contributed to obtain the first miRNA profile in MS lesions (42).

3 Zusammenfassung

3.1 Fragestellung

Ziel der vorliegenden Doktorarbeit war es, die Verwendbarkeit von archivierten Multiple Sklerose (MS)-Gewebeproben zur Transkriptionsprofil-Analyse von mRNA und miRNA mittels qPCR Technologie zu untersuchen.

Insbesondere wurden hierzu folgende Punkte adressiert:

- (1) Anwendung und Optimierung eines Protokolls zur RNA-Isolierung aus FFPE Hirngewebe und Vergleich der RNA-Ausbeute und -Qualität in FFPE- und Gefrier-Proben
- (2) Verwendbarkeit von zufällig ausgewählten Archiv-Gewebeproben für qPCR-Genexpressionsanalysen anhand der Amplifizierbarkeit eines *housekeeping* Gens und zwei miRNAs
- (3) Auswirkung der Formalin-Fixationsdauer auf die Transkript-Amplifizierbarkeit
- (4) Erarbeitung eines Versuchsaufbaus, der die makroskopische Dissektion von MS-Läsionen und anschließende qPCR-Analyse erlaubt
- (5) Vergleich der Expressionsanalyse von 84 Genen der extrazellulären Matrix in MS Läsionen mittels TaqMan[®] qRT-PCR Low Density Arrays in FFPE- und Gefriergewebeproben
- (6) Bestätigung der dabei gefundenen Hochregulierung der extrazellulären Matrix-Komponente Decorin auf Proteinebene mittels Immunhistochemie
- (7) Anwendung der erarbeiteten Methodik um das erste miRNA-Profil in MS Läsionen zu erhalten

3.2 Ergebnisse

Zunächst wurde ein zuverlässiges Protokoll zur RNA-Isolierung aus FFPE Hirngewebe eingeführt und optimiert. Dabei war sowohl die RNA-Ausbeute als auch das Verhältnis der Lichtabsorption bei 260 nm beziehungsweise 280 nm (OD 260/280) in FFPE Hirnproben vergleichbar zu Gefrierproben (23).

Insgesamt wurden 27 archivierte Hirnproben von 11 MS-Spendern aus verschiedenen Hirnbanken auf die Amplifizierbarkeit des *housekeeping* Gens Peptidyl-Propyl-Isomerase A (PPIA) und der miRNAs 181a und 124 hin untersucht und zur

Amplifizierbarkeit derselben Transkripte in 9 tiefgefrorenen Gewebeproben von 9 MS Spendern verglichen. Die Amplifizierbarkeit von PPIA in den FFPE Proben war dabei sehr heterogen verteilt und der Verlust an nachweisbaren Transkripten im Vergleich zu Gefrierewebe reichte von ~45- bis ~2000-fach. In einigen Archiv-Proben konnte PPIA überhaupt nicht nachgewiesen werden und diese Proben erschienen für weitere qPCR-Untersuchungen ungeeignet. Im Gegensatz hierzu war die Amplifizierbarkeit der miRNAs 181a und 124 in FFPE Gewebe sehr stabil mit einem durchschnittlichen Amplifikationsverlust von ca. 1,7 fach (23).

Unter verschiedenen Faktoren, die die Beeinträchtigung der Gen-Amplifikation in FFPE-Proben möglicherweise beeinflussen, wurde die Bedeutung der Fixationsdauer in Formalin genauer untersucht. Dabei konnte gezeigt werden, dass die Fixationszeit einen großen Einfluss auf die anschließende Amplifizierbarkeit von genkodierenden Transkripten (z.B. PPIA) hat. Im Vergleich zu Gefrierproben war die PPIA-Amplifikation in Proben, die für einen Zeitraum von Tagen in Formalin fixiert worden waren, um ~15 fach reduziert, während in jahrelang fixierten Proben eine ~200 fachen Reduktion der PPIA-Amplifikation beobachtet wurde (23). Auch in diesem Experiment hat sich die Amplifizierbarkeit der miRNAs 181a und 124 in denselben FFPE-Proben als enorm stabil erwiesen (23).

Basierend auf der stabilen Detektierbarkeit von miRNAs in FFPE-Gewebe, wurden 18 FFPE-Proben (MS n=13, gesunde Spender n=5) in eine Studie mit eingeschlossen, welche das miRNA-Expressionsmuster in MS-Läsionen im Vergleich zu gesundem Hirngewebe anhand einer qPCR-Analyse von 365 miRNAs untersucht hat (42).

Des Weiteren wurde ein Versuchsaufbau etabliert, der es ermöglicht, MS-Läsionsareale präzise aus der umgebenden normal erscheinenden weißen Substanz (normal appearing white matter, NAWM) auszuschneiden. Hierzu wurden mit Hilfe eines Mikrotomes Gewebeschnitte hergestellt, in einem heißen DEPC-Wasserbad geglättet, und auf PEN-Membran beschichtete Objektträger aufgezogen. Die RNA-Ausbeute und Amplifizierbarkeit von PPIA wurden durch diesen Ansatz nicht verändert. Parallelschnitte wurden mit Luxol Fast Blue (LFB) gefärbt und dienten als Schablone zur genauen Dissektion der MS Läsionen. Dieser Versuchsaufbau wurde auf 5 Gewebeproben angewandt (MS Läsionen n=3, gesunde Hirnproben n=2).

Aus den ausgeschnittenen Gewebeproben wurde RNA isoliert und die Expression von 84 Genen der extrazellulären Matrix anhand von TaqMan[®] Low Density Array

qPCR-Technologie untersucht. Die Ergebnisse in FFPE Gewebe wurden zu einem Datensatz aus Gefriergewebe verglichen, das auf ähnliche Weise prozessiert worden war. Die in FFPE-Gewebe gefundene Genregulation (MS vs. gesundes Gewebe) war dabei vergleichbar zu Gefriergewebe– vorausgesetzt, dass die Gene ausreichend abundant waren (23).

Die in dieser Untersuchung gefundene Hochregulierung der extrazellulären Matrix-Komponente Decorin konnte anhand von Immunhistochemie auf Proteinebene in denselben FFPE MS-Läsionen bestätigt werden. Dieses Ergebnis wurde als Teil einer Studie veröffentlicht, welche die Expression von verschiedenen extrazellulären Matrix-Genen in MS Läsionen anhand von Gefriergewebe untersucht hat, z. B. Kollagene und das Protein Biglycan (61). In dieser Studie konnte außerdem gezeigt werden, dass fibrilläre Kollagene zusammen mit Biglycan und Decorin eine perivaskuläre Fibrose bilden. Dort befinden sich die Immunzellinfiltrate in enger Assoziation mit diesen ECM Molekülen. Dies legt nahe, dass diese Proteine eine den Krankheitsprozess modifizierende Aufgabe haben (61).

Zusammenfassend präsentiert diese Arbeit ein detailliertes Protokoll wie autoptische FFPE-Gewebeproben verwendet werden können, um Expressionsprofile aus dissezierten MS Läsionen zu erhalten (23). Dieses Protokoll wurde mitverwendet, um die Veränderungen der ECM in MS Läsionen zu untersuchen (61) und das erste miRNA-Profil in MS Läsionen zu erhalten (42).

4 Publications

4.1 “Prospects of transcript profiling for mRNAs and microRNAs using formalin fixed and paraffin embedded dissected autoptic multiple sclerosis lesions”

Sylvia Eisele^{1,2}, Markus Krumbholz^{1,2}, Marie-Therese Fischer³, Hema Mohan², Andreas Junker^{1,2,5}, Thomas Arzberger⁴, Reinhard Hohlfeld^{1,2}, Monika Bradl³, Hans Lassmann³, Edgar Meinl^{1,2}

¹Institute of Clinical Neuroimmunology, University Hospital Großhadern, Ludwig-Maximilians-University, Marchioninstr. 15, 81377 Munich, Germany

²Department of Neuroimmunology, Max-Planck-Institute of Neurobiology, Am Klopferspitz 18, 82152 Martinsried, Germany

³Center for Brain Research, Medical University of Vienna, Spitalgasse 4, 1090 Vienna, Austria

⁴Center for Neuropathology and Prion Research, Ludwig-Maximilians-University, Feodor-Lynen-Str. 23, 81377 Munich, Germany

⁵Present address: Institute of Neuropathology, University Medical Center, Robert-Koch-Str. 40, 37099 Göttingen, Germany

Brain Pathology. 2012 Jan 10. doi: 10.1111/j.1750-3639.2012.00564.x.

[Epub ahead of print]

TECHNICAL ADVANCES

Prospects of Transcript Profiling for mRNAs and MicroRNAs Using Formalin-Fixed and Paraffin-Embedded Dissected Autoptic Multiple Sclerosis Lesions

Sylvia Eisele^{1,2}; Markus Krumbholz^{1,2}; Marie-Therese Fischer³; Hema Mohan²; Andreas Junker^{1,2*}; Thomas Arzberger⁴; Reinhard Hohlfeld^{1,2}; Monika Bradl³; Hans Lassmann³; Edgar Meinl^{1,2}

¹ Institute of Clinical Neuroimmunology, University Hospital Großhadern, Ludwig-Maximilians-University, Munich.

² Department of Neuroimmunology, Max-Planck-Institute of Neurobiology, Martinsried, Germany.

³ Center for Brain Research, Medical University of Vienna, Vienna, Austria.

⁴ Center for Neuropathology and Prion Research, Ludwig-Maximilians-University, Munich, Germany.

Keywords

FFPE, microRNA, molecular analysis, multiple sclerosis, quantitative PCR, transcriptome

Corresponding author:

Edgar Meinl, MD, Department of Neuroimmunology, Max-Planck-Institute of Neurobiology, Am Klopferspitz 18, 82152 Martinsried, Germany (E-mail: meinl@neuro.mpg.de)

Received 29 September 2011

Accepted 28 November 2011

Published Online Article Accepted 10 January 2012

* Present address: Institute of Neuropathology, University Medical Center, Robert-Koch-Str. 40, 37099 Göttingen, Germany.

Grants and Support: The Deutsche Forschungsgemeinschaft (SFB 571), Herrmann and Lilly Schilling Foundation, Verein zur Therapieforchung für Multiple-Sklerose-Kranke, the Bundesministerium für Bildung und Forschung ("Krankheitsbezogenes Kompetenznetz Multiple Sklerose"), the Excellency Initiative of the Ludwig Maximilians University Munich and the scholarship program "Förderung für Forschung und Lehre (FöFoLe)" of the Ludwig Maximilians University Munich, Germany.

doi:10.1111/j.1750-3639.2012.00564.x

INTRODUCTION

Recent advances in molecular biological techniques offer attractive tools to investigate pathogenetic mechanisms of multiple sclerosis (MS) or any other human disease. However, this requires that the appropriate tissue and analytical techniques can be brought

Abstract

The elaboration of novel pathogenic aspects of multiple sclerosis (MS) requires the analysis of well-defined stages of lesion development. However, specimens of certain stages and lesion types are either present in small brain biopsies, insufficient in size for further molecular studies or available as formalin-fixed and paraffin-embedded (FFPE) material only. Therefore, application of current molecular biology techniques to FFPE tissue is warranted. We compared FFPE and frozen tissue by using quantitative polymerase chain reaction and report: (1) FFPE material is highly heterogeneous regarding the utility for transcript profiling of mRNAs; well-preserved FFPE samples had about a 100-fold reduced sensitivity compared with frozen tissue, but gave similar results for genes of sufficient abundance; (2) FFPE samples not suitable for mRNA analysis are still highly valuable for miRNA quantification; (3) the length of tissue fixation greatly affects utility for mRNA but not for miRNA analysis; (4) FFPE samples can be processed via a hot water bath for dissection of defined lesion areas; and (5) *in situ* hybridization for proteolipid protein (PLP) helps to identify samples not suitable for mRNA amplification. In summary, we present a detailed protocol how to use autoptic FFPE tissue for transcript profiling in dissected tissue areas.

together (9, 17, 33, 35, 36). Particularly, the initial stages of MS are characterized by a focal pathology and pronounced temporal dynamic, and these are therefore of special interest. The majority of tissue specimens containing these lesion stages and types (eg, fulminant active MS lesions), are either available as small brain biopsies, where lesion size is often insufficient for further molecular

studies, or available as formalin-fixed and paraffin-embedded (FFPE) material only. Whereas good preservation of tissue structures in FFPE material allows for precise histopathological and immunohistochemical evaluation, investigation of RNA expression levels with modern techniques is challenging because of impaired RNA quality. Also, FFPE specimens could be useful for investigation of rare diseases, of which samples are difficult to obtain for prospective brain banks. Therefore it is interesting to see to which extent FFPE material can be used for such an approach and to provide a practical protocol for routine screening for the utility of FFPE material, in which conditions of tissue conservation are unknown.

Most of the previous studies on RNA expression analysis in FFPE tissue have used shortly fixed biopsy material (1, 10, 18, 25, 31, 34, 39, 40, 42). In contrast, archival brain tissues are obtained at autopsy and conditions of tissue conservation often variable and undefined. In these tissues RNA degradation by terminal hypoxia and post-mortem autolysis add to the inevitable RNA destruction and modification during tissue fixation and paraffin embedding (3, 6, 8, 20, 22, 26). However, studies using frozen specimens of brain tissue obtained by autopsy showed considerable stability of messenger RNA (mRNA) up to 48 h post-mortem (7, 12, 29, 43).

In addition to mRNA, non-coding RNA, for example, microRNAs (miRNAs), have increasingly been recognized as important players in physiology and pathology of many diseases including MS (14). Both microarray and quantitative polymerase chain reaction (qPCR) have been used to analyze miRNA expression in human tissue (34, 40, 42).

The purpose of this study was to elucidate to what extent FFPE MS tissue specimens of autptic origin can be used for reliable transcript profiling using qPCR technology and to present a detailed protocol how to do this. We specifically addressed the following issues: (i) RNA yield in FFPE compared with frozen brain tissue; (ii) ability to amplify transcripts coding for proteins and miRNAs in randomly selected archival brain specimens; (iii) effect of duration of tissue fixation on the amplification of protein coding mRNA and miRNAs in brain tissue; (iv) application of a more complex experimental setup including dissection of defined tissue areas from FFPE brain tissue sections and flattening in a hot water bath; (v) linkage of signal intensity of *in situ* hybridization to subsequent utility for qPCR amplification; (vi) comparison of FFPE vs. frozen tissue performance in analysis of gene expression profiles by TaqMan low density arrays (LDAs). For this purpose 84 genes coding for extracellular matrix (ECM)-related proteins were selected given their differential regulation in MS lesions and their wide spectrum of abundance in brain tissue (23).

MATERIALS AND METHODS

Analyzed tissue

In total, we analyzed 74 autptic tissue samples (frozen $n = 22$, FFPE $n = 52$) of 19 MS patients, one patient with Alzheimer's disease, one patient with meningitis tuberculosis and 12 healthy control donors by qPCR and *in situ* hybridization. Frozen samples were snap frozen in liquid nitrogen and then stored at -80°C . FFPE specimens had been formalin fixed under variable conditions over different time periods before paraffin embedding. Tissue samples were kindly provided by the Center for Brain Research in Vienna,

the Netherlands Brain Bank, the NeuroResource at UCL Institute of Neurology in London and the Neurobiobank Munich (Supporting Information Table S1).

Tissue conservation for experiments analyzing the effect of fixation time

To analyze the effect of fixation time on transcript amplification, 30 tissue specimens from six MS patients and three healthy donors were fixed in 4% paraformaldehyde (PFA) at 4°C for time periods ranging from 2 days to 3 years. After fixation, all samples were embedded in paraffin and stored at room temperature. One additional tissue specimen of each of these nine donors was snap frozen in liquid nitrogen and stored at -80°C . Three FFPE tissue specimens of three further MS patients were fixed in buffered formalin at room temperature for 1 month before paraffin embedding. From these three specimens also snap frozen mirror blocks were available.

Tissue processing and MS lesion dissection

FFPE tissue sections were obtained using a sliding microtome (SM 200R, Leica, Wetzlar, Germany). In one set of experiments the sections were directly collected in RNase free reaction tubes. Subsequently, the tissue was deparaffinized by incubation in xylol for 2×10 minutes followed by centrifugation (5 minutes at 12 000 rounds per minute). Supernatant was discarded before rehydration in descending dilutions of ethanol ($\sim 100\% \rightarrow 90\% \rightarrow 70\%$) for 7 minutes each followed by centrifugation (5 minutes at 12 000 rounds per minute) and discarding of the supernatant. To optimize RNA yield from FFPE tissue, we compared efficiency of RNA isolation in 4-, 6- and 8- μm sections and found 6- μm sections to give the most efficient RNA yield. Therefore, 6- μm

In another set of experiments, specific tissue areas were sections were used in subsequent experiments. dissection. For this purpose, 6- μm FFPE tissue sections were flattened in a 50°C DEPC water bath, taken onto polyethylene (PEN) membrane covered object slides (P.A.L.M Microsystems, Bernried, Germany) and air dried at 37°C overnight. Every 10th section underwent Luxol Fast Blue (LFB) staining and was used as a model for proper lesion dissection. All other sections were deparaffinized and rehydrated as described earlier. Then the MS lesion or the healthy white matter was excised with a scalpel and tissue was collected in RNase free reaction tubes for further processing. The total tissue amount ranged from 180 to 300 $\mu\text{m} \times 0.5 \text{ cm} \times 0.5 \text{ cm}$.

Of the frozen specimens, 10- to 20- μm -thick sections were obtained and mounted onto PEN membrane-coated object slides. Every 6th section was stained with LFB. Then MS lesions and healthy white matter were excised as described for FFPE tissue. The total tissue amount ranged from 200 to 300 $\mu\text{m} \times 0.5 \text{ cm} \times 0.5 \text{ cm}$.

This experimental setup was applied to 10 MS lesions (FFPE $n = 3$, frozen $n = 7$) and 8 white matter control samples (FFPE $n = 2$, frozen $n = 6$).

Tissue lysis and RNA isolation

For tissue lysis, 30 μL lysis buffer [50 mM Tris, 25 mM ethylenediaminetetraacetic acid (EDTA), 500 mM NaCl, 0.1% Nonidet[®]

P-40, 1% sodium dodecyl sulfate (SDS)] and 300 μ L Proteinase K (from *Tritirachium album*, $c = 20 \text{ mg/mL}$, molecular grade, RNase free, Sigma, Munich, Germany) were added per 1.5 mL reaction tube and incubated at 60°C for 14 h. To improve tissue lysis, reaction tubes were vortexed every 30 minutes at 1000 rpm for 5 minutes. RNA was isolated by: (i) adding 1 mL TRI[®]Reagent (Sigma) and 200 μ L chloroform; (ii) collecting the aqueous supernatant; and (iii) precipitating RNA with isopropanol. This was done twice to obtain high RNA purity. Finally, RNA was washed with 75% ethanol. RNA amount and purity [optical density (OD)_{260/280} ratio] were assessed with the Nanodrop[®] ND-1000 Spectrophotometer. For some samples, RNA was extracted using the Roche high pure FFPE RNA micro kit (Roche Diagnostics GmbH, Mannheim, Germany). To determine the RNA quality, one μ L of the test RNA (1–5 ng RNA/ μ L) was applied to an RNA Pico Chip (Agilent Technologies, Böblingen, Germany), which was then run on Agilent 2100 bioanalyzer.

Reverse Transcription, quantitative PCR, TaqMan[®] LDAs

For manually pipetted qPCR assays, cDNA from mRNA was synthesized using random hexamer primers (Roche Diagnostics GmbH) and Moloney Murine Leukemia Virus Reverse Transcriptase (Promega, Madison, WI, USA) or the ABI cDNA kit (Applied Biosystems, Darmstadt, Germany). MiRNAs were reversely transcribed with the TaqMan[®] MicroRNA Reverse Transcription Kit (Applied Biosystems) and miRNA specific RT primers (TaqMan[®] miRNA Assays, Applied Biosystems). Quantitative PCR for the housekeeping genes peptidyl-prolyl-isomerase A (PPIA) and glyceraldehyde-3-phosphate dehydrogenase (GAPDH) as well as miR-181a and miR-124 was performed using the qPCR Core Kit (RT-QP 73-05, Eurogentec, Seraing, Belgium) together with TaqMan[®] PCR Assays and TaqMan[®] miRNA Assays (both Applied Biosystems), respectively (Supporting Information Table S2). TaqMan[®] qPCR was performed on the 7900 HT Fast Real-Time PCR System (Applied Biosystems). The amount of cDNA used per manually pipetted qPCR reaction was usually 25 ng RNA equivalents for coding genes, but 9 ng in one case (MS 38). In this case, the Ct value for PPIA used in the analysis comparing qPCR and *in situ* hybridization results was corrected arithmetically according to the exponential nature of the amplification: $Ct_{\text{corr}} = Ct_{\text{measured}} + \log_2(\text{actually used ng}/25 \text{ ng})$. For miRNA analysis, 5 ng RNA equivalents were employed. Technical duplicates were measured and the standard deviation was calculated as $SD = 2^{-\Delta Ct} \cdot \sqrt{(\ln 2 \cdot SD_{\text{frozen}})^2 + (\ln 2 \cdot SD_{\text{FFPE}})^2}$ based on (16, 24).

For the TaqMan[®] LDA analysis, cDNA was synthesized using the High-Capacity cDNA Reverse Transcription Kit (Applied Biosystems). TaqMan[®] LDA reactions contained Gene Expression Mastermix (Applied Biosystems) and a RNA equivalent of 3–9.5 ng per reaction well. We conducted gene expression profiling in 18 tissue specimens (10 MS lesions (FFPE $n = 3$, frozen $n = 7$) and 8 healthy controls (FFPE $n = 2$, frozen $n = 6$) for 84 ECM-related genes (50 ECM components and 34 ECM modifying enzymes) on custom made TaqMan[®] LDAs (Applied Biosystems). PPIA and GAPDH were included as housekeeping genes (Supporting Information Table S2).

Data were analyzed with SDS 2.3 and RQ Manager 1.2 Software (Applied Biosystems). After comparing the ability to amplify

of GAPDH and PPIA in the five selected FFPE samples, PPIA was selected as the reference housekeeping gene because it was more abundant than GAPDH: mean Ct (PPIA, FFPE specimens) = 26.54; mean Ct (GAPDH, FFPE specimens) = 29.53. For normalization, relative gene expression with respect to the housekeeping gene PPIA was calculated and is shown as percent PPIA: $\% \text{ PPIA} = 2^{-\Delta Ct} \cdot 100$ with $\Delta Ct = Ct(\text{target gene}) - Ct(\text{PPIA})$.

In situ hybridization

In situ hybridization was performed essentially as described before (2): After deparaffinization and rehydration, RNA was fixed in 4% PFA for 20 minutes. Sections were rinsed with Tris buffered saline (TBS), followed by protein denaturation by incubation with 0.2 M HCl. Sections were again rinsed in TBS and then the tissue was partially digested with proteinase K (in TBS, supplemented with CaCl_2) to expose the RNA. Afterwards the slides were washed in TBS and left at 4°C for 5 minutes. To avoid non-specific binding, the slides were incubated with 0.5% acetic anhydride (in TBS, pH 8) for 10 minutes. Slices were dehydrated and put into a wet chamber (50°C, 30 minutes) to facilitate the dispersal of the hybridization mix containing the proteolipid protein 1 (PLP1) probe labeled with digoxigenin. The 1.4 kb RNA probe was constructed from a plasmid containing the DM20 variant of the mouse PLP1 sequence. Because of the high degree of sequence homology, this 1.4 kb RNA probe also binds to human PLP1/DM20. After application of the probe, a coverslip was put for protection and the slide was heated to 95°C for 4 minutes to linearize the RNA. Afterwards the hybridization was allowed to take place at 65°C over night. The coverslip was removed by incubation in 2× saline sodium citrate (SSC) followed by three highly stringent washing steps with 50% formamide in 1× SSC for 20 minutes each at 55°C. Sections were then washed thrice with 1× SSC (15 minutes per washing cycle), then rinsed with TBS and incubated with Boehringer Blocking Reagent containing 10% FCS for 15 minutes. Anti-digoxigenin antibodies, which were coupled to alkaline phosphatase (Roche) and dissolved in blocking reagent, were applied to the slices for 1 h. After five final washing steps with TBS, the development was performed with NBT/BCIP at 4°C, up to 140 h. For assessment of RNA quality, the signal appearance was controlled microscopically. Signal strength and distribution was evaluated semiquantitatively after 26 or 70 h of incubation as described detailed in the legend of Figure 4.

Statistical analysis

We tested the hypothesis that *in situ* hybridization signals and qPCR Ct values were negatively correlated (higher *in situ* hybridization signal ~ lower Ct value) using one-sided Spearman's rank correlation in R version 2.12.1 (R Development Core Team (2010). R: A language and environment for statistical computing (R Foundation for Statistical Computing, Vienna, Austria. ISBN 3-900051-07-0, URL <http://www.R-project.org/>) (28). `cor.test` Function was used with `option exact = F` as ties were present, resulting in $P = 0.008$ and $\sigma = -0.57$. To further address the extent of uncertainty introduced by ties, we applied a random tie breaking approach. In brief, ties were resolved by adding a random jitter that was smaller than the smallest non-zero difference between data

points, allowing us to apply cor.test function with option exact = TRUE in an iteration loop (i = 100 000). The median *P* (0.012) and σ (-0.55) values were only slightly different from the original ones, and 98.7% of all iterative *P*-values were <0.05. Therefore we concluded that the correlation between *in situ* hybridization signal and qPCR Ct value has to be regarded as significant with rounded *P* = 0.01 and rounded σ = -0.6 (Figure 4).

RESULTS

RNA yield from FFPE tissue is comparable with frozen tissue

In order to optimize the RNA yield from FFPE tissue blocks, we compared variations of section thickness and number of sections per reaction tube. Thereby we found that the RNA yield was optimal with 6- μ m sections at a maximum of 7 sections per 1.5 mL reaction tube. For average sized tissue blocks, a total tissue amount of 126 μ m \times 1–1.5 cm \times 1–1.5 cm, which was processed at a maximum of 7 \times 6- μ m sections per reaction tube was most efficient with respect to RNA yield and technical convenience. This was applied to 38 FFPE samples (nine MS and seven healthy donors) and the mean RNA yield was 5.8 μ g (range 1.5–15.5 μ g). This is comparable with the average RNA yield of 4.7 μ g (range 2.4–7.0 μ g) in 10 frozen samples (six MS and four healthy donors) of which similar total tissue amounts were used. RNA purity was acceptable for FFPE samples with a mean OD_{260/280} ratio of 1.82 (range 1.57–1.97) and for frozen specimens with a mean OD_{260/280} ratio of 1.91 (range 1.84–1.99).

We have evaluated RNA quality of three FFPE samples with the Agilent Bioanalyzer. Neither the 28S (4718 nucleotides) nor the 18S (1874 nucleotides) bands could be detected (data not shown), which is in harmony with previous observations (4, 5). The calculated RNA integrity numbers were 2.3–2.4. Nevertheless we were able to detect amplicons with a length <150 bp and all the more miRNAs in these samples. The Ct value of the housekeeping gene GAPDH was 30.3–30.7 in these samples.

Heterogenous (about 10⁵-fold different) amplifiability of coding RNA in various FFPE specimens

We evaluated utility of randomly selected FFPE samples for expression analysis by qPCR. To this end, we performed qPCR for the housekeeping gene PPIA in 27 FFPE specimens from 11 MS donors and compared results for each sample to mean expression level in frozen tissue (mean expression in six frozen samples from six MS donors). For this, an expression ratio $\frac{FFPE}{frozen}$ was calculated as $2^{-\Delta Ct}$. ΔCt was determined as difference between the Ct value for PPIA in each FFPE tissue specimen and the mean Ct for PPIA in six frozen samples [$\Delta Ct = Ct (FFPE) - \text{mean } Ct (frozen)$] (Figure 1).

In all FFPE samples, amplification of the housekeeping gene PPIA was considerably reduced compared with frozen tissue. However, the extent of reduced amplification was highly different between the randomly selected FFPE samples and ranged from 45-fold to more than 200 000-fold (Figure 1A).

The analysis of archival tissue specimens from healthy control donors yielded similar results: we analyzed eight FFPE specimens

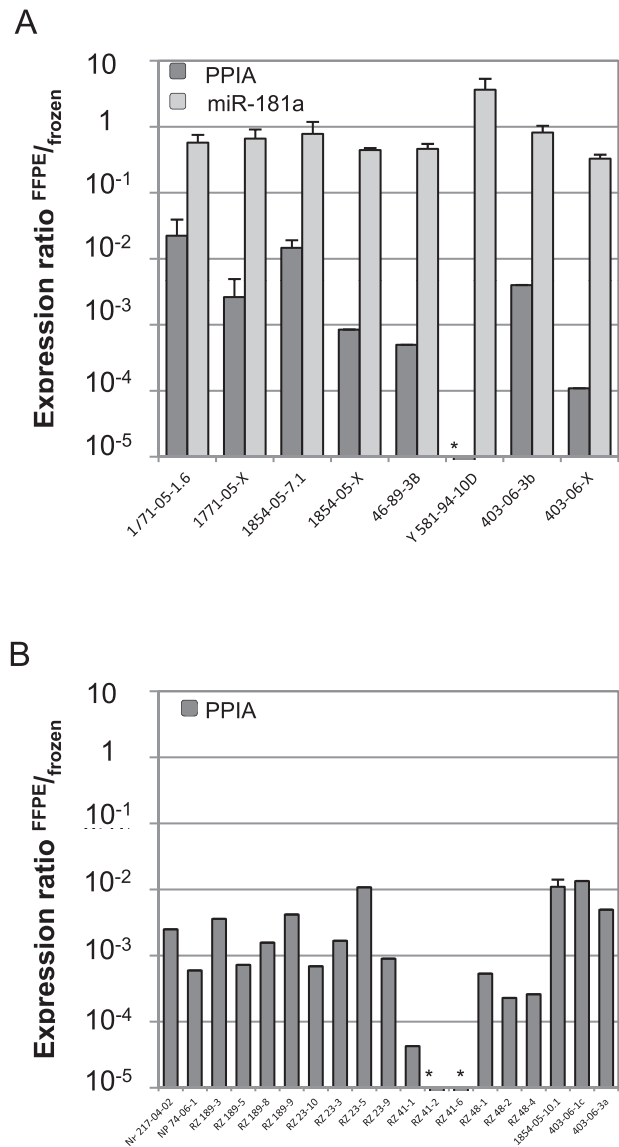


Figure 1. Amplification of peptidyl-prolyl-isomerase A (PPIA) and miR-181a in randomly selected archival multiple sclerosis (MS) tissue samples. **A.** Amplification of PPIA (dark gray columns) and miR-181a (light gray columns) was analyzed in eight formalin-fixed and paraffin-embedded (FFPE) specimens of five MS patients. Amplification in each FFPE specimen was compared with mean amplification in six frozen specimens (standard error of the mean <2%). The expression ratio $\frac{FFPE}{frozen}$ was calculated as $2^{-\Delta Ct}$ with $\Delta Ct = Ct (individual FFPE specimen) - \text{mean } Ct (n = 6 \text{ frozen})$. An expression ratio of 1 indicates comparable amplification in FFPE compared with frozen tissue. **B.** Similarly, PPIA was analyzed in 19 additional FFPE specimens of eight MS patients (dark gray columns). PPIA was not detected in samples marked with *. Error bars represent standard deviation for technical duplicates.

from seven donors and compared it with three frozen samples from three donors of whom also FFPE samples were obtained. The ability to amplify PPIA was reduced by a mean of 132-fold (data not shown).

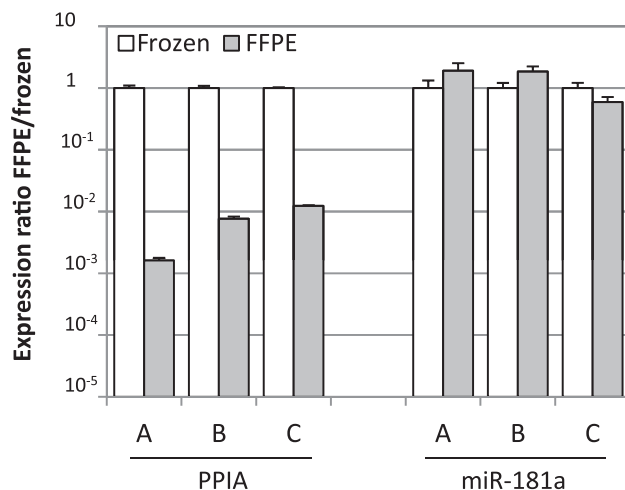


Figure 2. Comparative amplification of peptidyl-prolyl-isomerase A (PPIA) and miR-181a in formalin-fixed and paraffin-embedded (FFPE)-frozen mirror blocks. Each of three multiple sclerosis (MS) lesions (A = S06/126-11.3, B = S04/247-3 and C = S03/222-9.2) was represented by a FFPE (gray columns) and a frozen (white columns) tissue part. Transcript amplification of PPIA and miR-181a in the FFPE part was compared with the frozen part and is shown as expression ratio $^{FFPE/frozen}$, which was calculated as $2^{-\Delta Ct}$ with $\Delta Ct = Ct$ (individual FFPE specimen) – Ct (corresponding frozen sample). An expression ratio of 1 indicates comparable transcript amplification in FFPE compared with frozen tissue. Error bars represent standard deviation for technical duplicates.

We further had the chance to analyze three frozen MS tissue samples along with mirrored FFPE specimens reflecting the same tissue components. The ability to amplify the housekeeping gene PPIA was reduced by a mean of 277-fold (range 81- to 620-fold) (left part of Figure 2). This is in contrast to the largely unaltered amplification of miR-181a (right part of Figure 2).

We considered a FFPE specimen as suitable for further qPCR analysis, if the Ct value for PPIA was <30, because this allows detection of genes with an expression level of >3% PPIA if the detection limit is set as Ct = 35. Applying this, 31% (12/38) of the analyzed archival brain specimens were classified suitable.

Amplification of miRNAs in different FFPE specimens is remarkably stable

Analogous to PPIA, we also analyzed the ability to amplify miR-181a and miR-124 in a total of 36 samples (FFPE $n = 27$, frozen $n = 9$) from 14 MS and 7 healthy donors. We selected these two miRNAs because they are relatively abundant in the brain (13).

Amplification of miR-181a was analyzed in eight FFPE samples of five MS donors and compared with mean expression in six frozen samples of three overlapping MS donors. Again, the expression ratio $^{FFPE/frozen}$ was calculated as $2^{-\Delta Ct}$ for each analyzed sample (Figure 1). In contrast to PPIA, the ability to amplify of miR-181a in FFPE tissue compared with frozen tissue was found to be largely unaltered with a mean reduction by 1.7-fold only (range 0.3- to 3.1-fold, Figure 1A). Importantly, even in FFPE samples that are barely suitable for quantification of genes coding for proteins, the

miRNA can be quantified without evident loss of sensitivity (eg, samples Y581-94-10D and 403-06-X in Figure 1).

This is further supported by an only slightly reduced amplification of miR-181a in our mirrored FFPE-frozen MS lesions. In these samples, the ability to amplify miR-181a was reduced by a mean of 0.9-fold (range 0.5- to 1.7-fold) (Figure 2, right part). Similar results were obtained in healthy brain tissue (three FFPEs compared with three frozen samples of the same donors), where the ability to amplify of miR-181a was reduced by a mean of 1.6-fold (range 1- to 2.4-fold) (data not shown). Similarly, miR-124 was analyzed in 16 randomly selected archival brain samples of eight MS donors. Expression of miR-124 was considerably robust in all 16 samples with a mean Ct of 23.3 (SEM 0.32). This is in accordance with the stable ability to amplify of miR-181a ($n = 8$ FFPE samples, mean Ct 21.7, SEM 0.26).

Transcript amplification in FFPE tissue depends on duration of tissue fixation

To investigate the role of fixation time on amplification of gene transcripts we fixed tissue specimens for different periods of time before paraffin embedding and subsequent RNA analysis. For this purpose, we used 30 autoptic brain specimens (from three healthy donors and six MS patients). Of each donor one tissue sample was snap frozen in liquid nitrogen and 1–4 tissue samples were kept in 4% PFA over different time periods before embedding in paraffin. FFPE samples were grouped according to duration of formalin fixation: “days” ($n = 9$, fixation for 2–21 days), “months” ($n = 9$, fixation for 1–4 months) and “years” ($n = 3$, fixation for 2.5–3 years). Results in FFPE samples were compared with corresponding frozen specimens ($n = 9$). Expression of PPIA and miR-181a was measured in all 30 specimens. At first, the expression ratio $^{FFPE/frozen} = 2^{-\Delta Ct}$ was calculated for each FFPE-frozen pair. Then, the mean expression within each group was determined. Thereby we noted that the length of fixation has a strong impact on the ability to amplify of mRNAs, but had little effect on miRNAs. Fixation for days reduced amplifiable PPIA transcripts by a mean of 15-fold, fixation for months by 44-fold and fixation for years by about 600-fold. In contrast, amplification of miR-181a was largely unaltered by duration of fixation in 4% PFA (maximal 1.7-fold difference with year-long fixation (Figure 3). Although the fixation period did affect the ability to amplify RNA, it did not affect the RNA yield.

Unaltered RNA yield and transcript amplification after dissection from membrane-coated slides

We were looking for a suitable approach to dissect defined areas in FFPE tissue without impairment of subsequent RNA analysis. In this regard, we considered tissue flattening in a hot water bath and tissue dissection from membrane-coated slides as critical steps. In pilot experiments with human tonsils RNA yield and the ability to amplify GAPDH was remarkably reduced if the FFPE tissue had been exposed to tap water. In contrast, if exposed to DEPC treated water, RNA yield was comparable with tissue that had been processed without exposure to water at all. In following experiments, GAPDH amplification was unaltered in archival white matter specimens, of which sections were flattened in a 50°C water bath

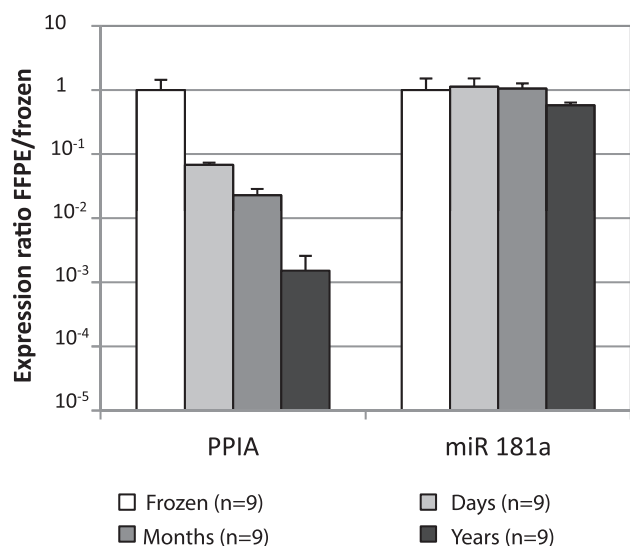


Figure 3. Effect of formalin fixation on amplification of PPIA and miR-181a. Thirty FFPE samples were grouped according to three time periods of fixation in 4% PFA: “days”: ($n = 9$, formalin fixed for 2–21 days), “months” ($n = 9$, formalin fixed for 2–4 months), “years” ($n = 3$, formalin fixed for 2–3 years) and transcript amplification was compared with “frozen” specimens of the same donors ($n = 9$). ΔCt was calculated for each FFPE and the corresponding frozen sample. Mean amplification in each of the three FFPE subgroups (columns in different shades of gray) is shown in relation to the mean amplification in the group “frozen” (white columns, SEM < 2%). The expression ratio $^{FFPE}_{frozen}$ was calculated as $2^{-\Delta Ct}$ with $\Delta Ct = \text{mean Ct of the FFPE subgroup} - \text{mean Ct of the frozen samples}$. An expression ratio of 1 indicates comparable transcript amplification in FFPE compared with frozen tissue. Error bars represent standard error of the mean (SEM).

and then dissected from PEN membrane-coated object slides as compared with directly processed white matter (data not shown).

In situ hybridization identifies tissue specimens not suitable for further PCR analysis

To determine whether *in situ* hybridization is a potential tool to identify archival specimens with good RNA quality we compared performance of 17 MS brain samples using an *in situ* hybridization for PLP and qPCR for PPIA. We found that specimens with low raw Ct values for PPIA (ie, better RNA quality) did also have stronger signals in the *in situ* hybridization for PLP (Figure 4). This inverse correlation between the signal strength of *in situ* hybridization and raw Ct values was statistically significant ($P = 0.01$, Spearman’s $\sigma = -0.6$). Statistical analysis was performed as described in materials and methods.

About 200 archival blocks from MS patients and control were examined by *in situ* hybridization in Vienna and classified for further molecular analysis based on the intensity of the *in situ* signal with the PLP probe after 70 h. From controls 30/47 blocks (22/27 cases) and from MS cases 45/152 blocks (27/57 cases) gave a high *in situ* signal. This means 50–60% of the MS blocks in a large archival collection have to be excluded from further molecular analysis. The ratios of controls and MS blocks are slightly

different, because all available MS cases were analyzed, whereas in controls mainly samples with a known short fixation period were included. In 33 cases, different blocks from the same donor could be analyzed. Typically, the RNA quality was similar in blocks from the same donor, but we also noted exceptions: The ratio of concordant/discordant was 8/2 in controls and 25/10 in MS cases.

Transcript profiling in FFPE compared with frozen tissue: similar pattern despite sensitivity loss

To define sensitivity and reliability of qPCR studies in FFPE compared with frozen tissue we quantified the expression of 84 ECM-related genes in five FFPE samples (three demyelinated MS lesions and two healthy white matter controls) which were selected based on good amplification of PPIA seen in previous experiments (Table 1). The ECM-related genes are particularly suitable in this regard, because the ECM is altered in MS lesions (23, 38) and they comprise a spectrum of genes ranging from high to low abundance. Results of FFPE samples were compared with values obtained with 13 frozen specimens (seven demyelinated MS lesions and six healthy white matter controls) (23).

We considered a gene reliably detected if the measured Ct value was <35. Using this as a detection limit, we noted a reduced sensitivity in FFPE material. Of all 84 ECM-related genes we were able to detect and quantify the expression of 68 of 84 genes (81%) in frozen tissue of both MS and controls (74/84 genes in the control and 68/84 genes in the MS group) and 36 genes (43%) in FFPE tissue (57/84 genes in the control group and 37/84 in the MS group). All the 36 genes detected in FFPE tissue were also detected in frozen tissue.

When evaluating the expression data of Table 1 in detail, we have to consider that in addition to the FFPE-frozen comparison, we have a biological variability of different samples. We compared the direction of the ratios MS/healthy and this showed that the analysis of FFPE tissue can give reliable results. To compare gene regulation results (in terms of up-, down- or no regulation) for the 36 genes detected in FFPE tissue, we calculated the gene expression ratio as $\% PPIA_{(MS)} / \% PPIA_{(healthy)}$. A gene was considered as up- or downregulated if the gene expression ratio was >2 or <0.5, respectively. This was done separately within FFPE and the frozen tissue before results were compared. The direction of the detected gene regulation (MS/healthy) in the frozen and the FFPE group were largely similar (Table 1): in the frozen MS lesions, 28 genes were up- and two were downregulated. Twenty-four of these 28 genes seen upregulated in frozen MS lesions were also classified as upregulated in FFPE MS lesions; the other four genes were also induced in the FFPE MS lesions but less than twofold. The two downregulated genes in frozen MS lesions (HAPLN2, ADAMTS4) were not regulated in FFPE MS lesions; of the six genes that were classified as not regulated in frozen tissue, four genes were not regulated in FFPE tissue and the other two genes (LAMA2, ADAMTS1) were considered as upregulated. In summary, 28 of these 36 genes were classified similarly in both, FFPE and frozen tissue (Table 1).

DISCUSSION

Here we present a detailed protocol describing how to use autoptic FFPE samples for mRNA and miRNA quantification and a quanti-

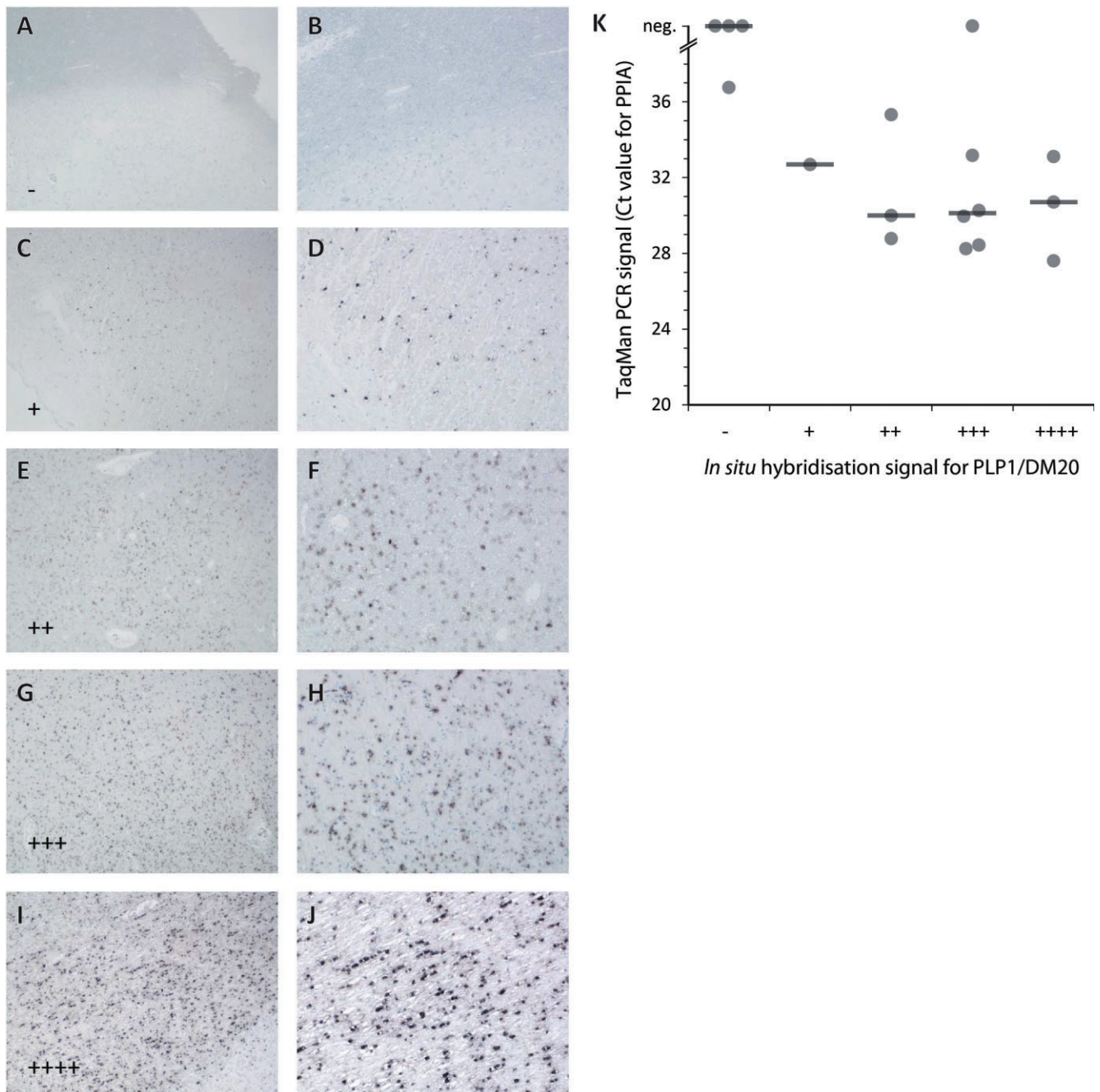


Figure 4. Comparison of *in situ* hybridization for PLP1/DM20 and quantitative polymerase chain reaction (qPCR) signal. Strength of the *in situ* hybridization signal of different tissue blocks was compared after 26 h of substrate reaction. Five different signal intensities were defined: (**A,B**) no signal (-); (**C,D**) weak signal in focal cells (+); (**E,F**) weak signal in most oligodendrocytes (++); (**G,H**) strong signal focally and moderate signal in most oligodendrocytes (+++); (**I,J**) strong signal in most/all oligodendro-

cytes (++++). Magnification: A, C, E, G, I: $\times 32$; B, D, F, H, J: 80. **K.** qPCR Ct values for PPIA were plotted against the PLP1/DM20 *in situ* hybridization signal. A negative qPCR signal ("neg.") was defined as no signal after 40 cycles. Horizontal lines indicate medians. The negative correlation between *in situ* hybridization signal and raw Ct value was statistically significant ($P = 0.01$, Spearman's $\sigma = -0.6$).

tative comparison of transcript amplification in FFPE and frozen tissue (Supporting Information Table S3). We found that the utility of FFPE material for the analysis of protein coding genes is highly heterogeneous and that the length of tissue fixation before embed-

ding in paraffin is a key factor in this regard. Remarkably, specimens that were poor candidates for mRNA analysis were still highly valuable for miRNA quantification. In an expression analysis of a larger set of ECM-related genes, FFPE tissue processing

Genes	FFPE			Frozen		
	% PPIA	% PPIA	Expression ratio	Expression ratio		
	Healthy	MS		$^{MS}/_{healthy}$	$^{MS}/_{healthy}$	
Fibrillar collagens						
COL1A1	0.10	10.62	104.69	↑	7.01	↑
COL1A2	0.09	3.10	34.27	↑	4.47	↑
COL3A1	0.16	1.33	8.43	↑	10.85	↑
COL5A1	0.04	1.55	34.72	↑	16.83	↑
COL5A2	nd	nd	*		6.51	↑
COL5A3	1.36	4.30	3.17	↑	6.64	↑
Basement membrane collagens						
COL4A1	0.33	14.89	45.32	↑	14.55	↑
COL4A2	nd	nd	*		5.49	↑
COL4A3	0.07	nd	*		1.21	↔
COL4A4	nd	nd	*		*	⋮
COL4A5	0.94	2.67	2.84	↑	2.67	↑
COL4A6	0.14	nd	*		2.22	↑
Anchoring collagen						
COL7A1	1.77	5.45	3.08	↑	3.63	↑
Nidogens						
NID1	0.64	4.68	7.28	↑	3.08	↑
NID2	0.38	6.89	18.04	↑	2.42	↑
Laminins						
LAMA1	0.66	1.37	2.09	↑	4.55	↑
LAMA2	0.28	2.13	7.51	↑	1.63	↔
LAMA3	0.29	nd	*		2.50	↑
LAMA4	1.48	4.19	2.84	↑	6.25	↑
LAMA5	0.04	nd	*		23.77	↑
LAMB1	0.06	nd	*		8.67	↑
LAMB2	3.71	40.61	10.93	↑	9.04	↑
LAMB3	0.52	nd	*		2.38	↑
LAMC1	0.32	2.68	8.35	↑	9.69	↑
LAMC2	nd	nd	*		*	⊖
Lecticans						
AGC1	0.06	nd	*		2.25	↑
BCAN	34.34	47.22	1.37	↔	2.43	↑
CSPG2	nd	nd	*		*	⋮
CSPG3	3.63	nd	*		0.87	↔
Small leucine rich proteoglycans (SLRPs)						
BGN	4.21	13.05	3.10	↑	9.41	↑
DCN	2.52	31.12	12.34	↑	3.56	↑
FMOD	nd	nd	*		10.37	↑
LUM	nd	nd	*		7.42	↑
Hyaluronan and proteoglycan link proteins (HAPLNs)						
HAPLN1	0.12	nd	*		*	⋮
HAPLN2	22.28	16.96	0.76	↔	0.15	↓
HAPLN3	0.28	9.46	33.66	↑	9.87	↑
HAPLN4	nd	nd	*		6.71	↑
Heparan sulfate proteoglycan (HSPG)						
HSPG2	0.71	11.81	16.69	↑	5.49	↑
Tenascins						
TNC	3.98	5.49	1.38	↔	2.14	↑
TNR	4.55	3.79	0.83	↔	0.93	↔
Thrombospondins						
THBS1	nd	22.28	*		11.90	↑
THBS2	1.29	4.19	3.25	↑	2.84	↑
THBS3	nd	nd	*		3.34	↑
THBS4	0.60	nd	*		2.71	↑

Table 1. Expression ratios $^{MS}/_{healthy}$ of 84 extracellular matrix (ECM)-related genes in formalin-fixed and paraffin-embedded (FFPE) tissue compared with frozen tissue. Abbreviations: ↑ = upregulated; ↓ = downregulated; ↔ = not regulated; nd = not detected; * = fold expression change not determinable; ⋮ = not detected in MS group; ⋮ = not detected in healthy group; ⊖ = not detected in MS and healthy group.

Table 1. Continued

Genes	FFPE			Frozen	
	% PPIA Healthy	% PPIA MS	Expression ratio	Expression ratio	
			$\frac{MS}{healthy}$	$\frac{MS}{healthy}$	
Fibrillins					
FBN1	4.92	4.52	0.92	↔	0.92 ↔
FBN2	0.06	nd	*		1.20 ↔
FBN3	0.25	nd	*		1.33 ↔
Others					
FN1	7.38	68.23	9.25	↑	3.36 ↑
RELN	0.28	nd	*		4.16 ↑
VTN	nd	nd	*		2.39 ↑
A disintegrin and metalloproteinase domains (ADAMs)					
ADAM8	0.24	nd	*		1.82 ↔
ADAM10	7.27	13.07	1.80	↔	1.52 ↔
ADAM12	0.26	nd	*		2.12 ↑
ADAM17	0.22	nd	*		1.76 ↔
A disintegrin-like and metalloproteinase with thrombospondin type 1 motifs (ADAMTS)					
ADAMTS1	2.29	21.03	9.19	↑	1.73 ↔
ADAMTS4	14.82	28.36	1.91	↔	0.22 ↓
ADAMTS5	0.09	nd	*		4.04 ↑
Matrix metalloproteinases (MMPs)					
MMP1	nd	nd	*		* ○
MMP2	0.73	8.37	11.51	↑	6.41 ↑
MMP3	nd	nd	*		* ○
MMP7	nd	nd	*		* ○
MMP8	nd	nd	*		* ○
MMP9	0.06	nd	*		12.46 ↑
MMP10	nd	nd	*		* ○
MMP11	nd	nd	*		6.43 ↑
MMP12	nd	nd	*		* ○
MMP13	nd	nd	*		* ○
MMP14	7.31	22.15	3.03	↑	11.59 ↑
MMP15	0.87	1.57	1.80	↔	1.93 ↔
MMP16	1.43	nd	*		2.14 ↑
MMP17	0.64	nd	*		11.64 ↑
MMP19	nd	nd	*		10.71 ↑
MMP20	nd	nd	*		* ○
MMP21	nd	nd	*		* ○
MMP23B	nd	nd	*		2.37 ↑
MMP24	0.45	nd	*		4.51 ↑
MMP25	nd	nd	*		* ○
MMP26	nd	nd	*		* ○
MMP27	nd	nd	*		* ○
MMP28	nd	nd	*		3.76 ↑
Tissue inhibitor of metalloproteinases (TIMPs)					
TIMP1	1.13	6.00	5.32	↑	11.94 ↑
TIMP2	34.80	35.65	1.02	↔	2.30 ↑
TIMP3	9.48	191.91	20.24	↑	4.83 ↑
TIMP4	2.65	4.37	1.65	↔	3.71 ↑

Data calculation: A Ct value < 35 was set as detection limit and the gene expression ratio $\frac{\% PPIA (MS)}{\% PPIA (healthy)}$ was determined. A total of five FFPE tissue specimens ($n = 3$ MS, $n = 2$ healthy) and 13 frozen tissue specimens ($n = 7$ MS, $n = 6$ healthy) were analyzed. Expression of the ECM-related genes in frozen tissue using glyceraldehyde-3-phosphate dehydrogenase (GAPDH) as a housekeeping gene were published in a different context (23).

including a hot water bath and subsequent dissection of MS lesion areas did not impair results. Compared with data obtained in frozen tissue, a similar pattern of gene expression was found in FFPE tissue—provided that the target genes were of sufficient abundance.

In our screening of archival MS brain samples for possible utility in coding gene expression analysis only about a third of all analyzed samples showed acceptable quality [defined as Ct (PPIA) < 30]. This is in concordance with a study in which utility of 157 archival tumor specimens for microarray analysis with respect to tumor classification was analyzed and in which only 25% of the performed arrays were informative (27).

In our autoptic FFPE brain specimens, the ability to amplify of PPIA was very heterogeneously distributed and ranged from very poor [$\Delta\text{Ct} (\text{Ct}_{\text{FFPE}} - \text{Ct}_{\text{frozen}}) > 15$] in some old archival tissue specimens to adequate ($\Delta\text{Ct} = 5$) in other specimens (eg, samples 1771-05-1.6, 1854-05-7.1, RZ 23-5, 1854-05-10.1 and mirror samples A, B, C in Figure 2). An average increase of Ct values by five cycles (which means a reduced sensitivity by a factor of $2^5 = 32$) has also been observed by different studies using bioptic FFPE specimens (10, 19). The decline of retrievable RNA copies in archival tissue has been explained in depth by: (i) chemical RNA destruction/modification by formalin fixation (8, 22, 26); (ii) variable conditions during tissue fixation such as pH (15), temperature (32) and length (3, 6, 22); (iii) level of tissue penetration by the fixative (31) and period of storage in paraffin (6, 20, 34).

Among these effects, we have analyzed the effect of fixation time in more detail. Under otherwise “standardized conditions” (PFA, 4°C) we found a progressive decline in the ability to amplify coding genes in correlation with progressive time of fixation leading to around 600-fold loss of amplifiable transcripts with tissue fixation over years (Figure 3). However, this loss in amplification is relatively moderate compared with the about 10^5 -fold loss of amplification in some other archival brain samples of which fixation conditions were unknown.

We further noticed that 15 of 18 of the specimens which had been fixed under these “standardized conditions” were suitable for subsequent gene expression analysis [Ct value (PPIA) < 30]. All of this suggests that utility of archival MS brain specimens depends on the overall quality of tissue preservation including length of tissue fixation.

Despite the heterogeneous utility of the FFPE samples for the analysis of mRNA expression levels, all of our archival brain specimens were found to be useful for subsequent miRNA quantification. In the present study we observed a mean Ct increase by 0.5 for FFPE samples analyzed for miR-181a compared with frozen tissue. We have already applied this observation to establish miRNA profiles of white matter lesions of MS patients (13). Our observation, that miRNAs can readily be quantified in FFPE tissue which is considered not useful for analysis of protein coding mRNA, does extend previous work on miRNA analysis in FFPE tissue (34, 40, 42). The small size (42) and protective miRNA–protein interactions (11, 21) might explain the enormous stability of miRNAs. All of this makes archival MS samples a valuable tissue resource for further investigation of the role of miRNAs in MS, for example, their impact on cortical demyelination (35) or the potential presence of viral agents (30, 41).

Five suitable FFPE specimens were used for gene expression analysis for a larger set of ECM related genes. This revealed an

expression pattern similar to 13 frozen specimens, where fibrillar collagens, decorin and biglycan were found to be associated with infiltrating immune cells (23). These genes were also found to be strongly induced in FFPE tissue along with basement membrane collagens and laminins, the induction of which was previously described using immunostaining (23, 37). However, we were not able to detect especially low abundant genes in FFPE tissue, for example, fibromodulin (FMOD), lumican (LUM), reelin (RELN) and most of the metalloproteinases (MMP9, MMP11, MMP17, MMP19, MMP24, MMP28) (Table 1).

Archival FFPE specimens are of great value for research on the pathogenesis of MS because certain lesion types are rarely encountered in biopsy specimens or in frozen material from human brain banks. The molecular analysis of some stages of MS lesion development therefore depends on FFPE tissue samples. In such precious FFPE samples, post-mortem time, pre-mortem conditions and duration of formalin fixation are often unknown and molecular research on such archival material is very challenging. Therefore, a simple and reliable method to pre-screen such material for its suitability for molecular studies is urgently required. Our present data show, that such a pre-screening can be performed by screening the ability to amplify a housekeeping gene by qPCR or *in situ* hybridization for an abundantly expressed mRNA, for example, PLP. In particular, a lack of signal in the *in situ* hybridization (“-” in Figure 4) identifies samples that are unlikely to perform well in qPCR studies of mRNA.

In summary, the present study shows that gene expression analysis for both mRNA and miRNA can be performed with FFPE specimens of good quality, even if a bioanalyzer indicates degraded RNA. Especially miRNA expression can be quantified in virtually all FFPE specimens with sensitivity that is comparable with frozen tissue, when amplification of mRNA is only possible in a subset of FFPE specimens. The mRNA analysis of FFPE material by qPCR is less sensitive than of frozen tissue but gives similar results for genes of sufficient abundance. The utility of archival MS tissue specimens for mRNA analysis can be evaluated by *in situ* hybridization with an abundant probe and by qPCR for a housekeeping gene. Furthermore, defined tissue areas can be dissected in FFPE specimens without impairment of subsequent qPCR analysis of mRNAs or miRNAs using the protocol described here.

ACKNOWLEDGMENTS

We are grateful to Heike Rübsamen, Angelika Henn and Ulrike Köck for technical advice and support. We are especially thankful to the Center for Brain Research in Vienna, the Netherlands Brain Bank, the NeuroResource at UCL Institute of Neurology in London, and the Neurobiobank Munich for providing valuable tissue specimens. We thank Drs. S. Rauskolb and G. Krishnamoorthy for helpful comments on the article. We are grateful to Prof. H. Wekerle for continuous support.

REFERENCES

1. Abrahamsen HN, Steiniche T, Nexø E, Hamilton-Dutoit SJ, Sørensen BS (2003) Towards quantitative mRNA analysis in paraffin-embedded tissues using real-time reverse transcriptase-polymerase chain reaction: a methodological study on lymph nodes from melanoma patients. *J Mol Diagn* 5:34–41.

2. Breitschopf H, Suchanek G, Gould RM, Colman DR, Lassmann H (1992) In situ hybridization with digoxigenin-labeled probes: sensitive and reliable detection method applied to myelinating rat brain. *Acta Neuropathol (Berl)* **84**:581–587.
3. Bresters D, Schipper ME, Reesink HW, Boeser-Nunnink BD, Cuypers HT (1994) The duration of fixation influences the yield of HCV cDNA-PCR products from formalin-fixed, paraffin-embedded liver tissue. *J Virol Methods* **48**:267–272.
4. Chung JY, Hewitt SM (2010) An optimized RNA extraction method from archival formalin-fixed paraffin-embedded tissue. *Methods Mol Biol* **611**:19–27.
5. Chung JY, Braunschweig T, Hewitt SM (2006) Optimization of recovery of RNA from formalin-fixed, paraffin-embedded tissue. *Diagn Mol Pathol* **15**:229–236.
6. Cronin M, Pho M, Dutta D, Stephans JC, Shak S, Kiefer MC *et al* (2004) Measurement of gene expression in archival paraffin-embedded tissues: development and performance of a 92-gene reverse transcriptase-polymerase chain reaction assay. *Am J Pathol* **164**:35–42.
7. Cummings TJ, Strum JC, Yoon LW, Szymanski MH, Hulette CM (2001) Recovery and expression of messenger RNA from postmortem human brain tissue. *Mod Pathol* **14**:1157–1161.
8. Finke J, Fritzen R, Ternes P, Lange W, Dolken G (1993) An improved strategy and a useful housekeeping gene for RNA analysis from formalin-fixed, paraffin-embedded tissues by PCR. *Biotechniques* **14**:448–453.
9. Fugger L, Friese MA, Bell JI (2009) From genes to function: the next challenge to understanding multiple sclerosis. *Nat Rev Immunol* **9**:408–417.
10. Godfrey TE, Kim SH, Chavira M, Ruff DW, Warren RS, Gray JW, Jensen RH (2000) Quantitative mRNA expression analysis from formalin-fixed, paraffin-embedded tissues using 5' nuclease quantitative reverse transcription-polymerase chain reaction. *J Mol Diagn* **2**:84–91.
11. Hui AB, Shi W, Boutros PC, Miller N, Pintilie M, Fyles T *et al* (2009) Robust global micro-RNA profiling with formalin-fixed paraffin-embedded breast cancer tissues. *Lab Invest* **89**:597–606.
12. Johnson SA, Morgan DG, Finch CE (1986) Extensive postmortem stability of RNA from rat and human brain. *J Neurosci Res* **16**:267–280.
13. Junker A, Krumbholz M, Eisele S, Mohan H, Augstein F, Bittner R *et al* (2009) MicroRNA profiling of multiple sclerosis lesions identifies modulators of the regulatory protein CD47. *Brain* **132**(Pt 12):3342–3352.
14. Junker A, Hohlfeld R, Meinl E (2011) Emerging role of miRNAs in multiple sclerosis. *Nat Rev Neurol* **7**:56–59.
15. Kingsbury AE, Foster OJ, Nisbet AP, Cairns N, Bray L, Eve DJ *et al* (1995) Tissue pH as an indicator of mRNA preservation in human post-mortem brain. *Brain Res Mol Brain Res* **28**:311–318.
16. Krumbholz M, Theil D, Cepok S, Hemmer B, Kivisakk P, Ransohoff RM *et al* (2006) Chemokines in multiple sclerosis: CXCL12 and CXCL13 up-regulation is differentially linked to CNS immune cell recruitment. *Brain* **129**(Pt 1):200–211.
17. Lassmann H (2011) The architecture of inflammatory demyelinating lesions: implications for studies on pathogenesis. *Neuropathol Appl Neurobiol* **37**:698–710.
18. Lehmann U, Glockner S, Kleeberger W, von Wasielewski HF, Kreipe H (2000) Detection of gene amplification in archival breast cancer specimens by laser-assisted microdissection and quantitative real-time polymerase chain reaction. *Am J Pathol* **156**:1855–1864.
19. Li J, Smyth P, Cahill S, Denning K, Flavin R, Aherne S *et al* (2008) Improved RNA quality and TaqMan Pre-amplification method (PreAmp) to enhance expression analysis from formalin fixed paraffin embedded (FFPE) materials. *BMC Biotechnol* **8**:10.
20. Lisowski AR, English ML, Opsahl AC, Bunch RT, Blomme EA (2001) Effect of the storage period of paraffin sections on the detection of mRNAs by in situ hybridization. *J Histochem Cytochem* **49**:927–928.
21. Lu J, Getz G, Miska EA, Alvarez-Saavedra E, Lamb J, Peck D *et al* (2005) MicroRNA expression profiles classify human cancers. *Nature* **435**:834–838.
22. Masuda N, Ohnishi T, Kawamoto S, Monden M, Okubo K (1999) Analysis of chemical modification of RNA from formalin-fixed samples and optimization of molecular biology applications for such samples. *Nucleic Acids Res* **27**:4436–4443.
23. Mohan H, Krumbholz M, Sharma R, Eisele S, Junker A, Sixt M *et al* (2010) Extracellular matrix in multiple sclerosis lesions: fibrillar collagens, biglycan and decorin are upregulated and associated with infiltrating immune cells. *Brain Pathol* **20**:966–975.
24. Muller PY, Janovjak H, Miserez AR, Dobbie Z (2002) Processing of gene expression data generated by quantitative real-time RT-PCR. *Biotechniques* **32**:1372–1379. Erratum in: *Biotechniques* 2002, **33**:514.
25. Nelson PT, Baldwin DA, Searce LM, Oberholtzer JC, Tobias JW, Mourelatos Z (2004) Microarray-based, high-throughput gene expression profiling of microRNAs. *Nat Methods* **1**:155–161.
26. Park YN, Abe K, Li H, Hsuih T, Thung SN, Zhang DY (1996) Detection of hepatitis C virus RNA using ligation-dependent polymerase chain reaction in formalin-fixed, paraffin-embedded liver tissues. *Am J Pathol* **149**:1485–1491.
27. Penland SK, Keku TO, Torrice C, He X, Krishnamurthy J, Hoadley KA *et al* (2007) RNA expression analysis of formalin-fixed paraffin-embedded tumors. *Lab Invest* **87**:383–391.
28. R Development Core Team (2010) R Foundation for Statistical Computing, Vienna, Austria. ISBN 3-900051-07-0. Available at: <http://www.R-project.org/> (accessed 6 February 2012).
29. Schramm M, Falkai P, Tepest R, Schneider-Axmann T, Przkora R, Waha A *et al* (1999) Stability of RNA transcripts in post-mortem psychiatric brains. *J Neural Transm* **106**:329–335.
30. Serafini B, Rosicarelli B, Franciotta D, Magliozzi R, Reynolds R, Cinque P *et al* (2007) Dysregulated Epstein-Barr virus infection in the multiple sclerosis brain. *J Exp Med* **204**:2899–2912.
31. Specht K, Richter T, Muller U, Walch A, Werner M, Hoffer H (2001) Quantitative gene expression analysis in microdissected archival formalin-fixed and paraffin-embedded tumor tissue. *Am J Pathol* **158**:419–429.
32. Srinivasan M, Sedmak D, Jewell S (2002) Effect of fixatives and tissue processing on the content and integrity of nucleic acids. *Am J Pathol* **161**:1961–1971.
33. Steinman L, Zamvil S (2003) Transcriptional analysis of targets in multiple sclerosis. *Nat Rev Immunol* **3**:483–492.
34. Szafranska AE, Davison TS, Shingara J, Doleshal M, Riggenbach JA, Morrison CD *et al* (2008) Accurate molecular characterization of formalin-fixed, paraffin-embedded tissues by microRNA expression profiling. *J Mol Diagn* **10**:415–423.
35. Torkildsen O, Stansberg C, Angelskar SM, Kooi EJ, Geurts JJ, Myhr KM *et al* (2010) Upregulation of immunoglobulin-related genes in cortical sections from multiple sclerosis patients. *Brain Pathol* **20**:720–729.
36. Trapp BD, Nave KA (2008) Multiple sclerosis: an immune or neurodegenerative disorder? *Annu Rev Neurosci* **31**:247–269.
37. van Horsen J, Bo L, Vos CM, Virtanen I, de Vries HE (2005) Basement membrane proteins in multiple sclerosis-associated inflammatory cuffs: potential role in influx and transport of leukocytes. *J Neuropathol Exp Neurol* **64**:722–729.
38. van Horsen J, Dijkstra CD, de Vries HE (2007) The extracellular matrix in multiple sclerosis pathology. *J Neurochem* **103**:1293–1301.

39. Waddell N, Cocciardi S, Johnson J, Healey S, Marsh A, Riley J *et al* (2010) Gene expression profiling of formalin-fixed, paraffin-embedded familial breast tumours using the whole genome-DASL assay. *J Pathol* **221**:452–461.
40. Weng L, Wu X, Gao H, Mu B, Li X, Wang JH *et al* (2010) MicroRNA profiling of clear cell renal cell carcinoma by whole-genome small RNA deep sequencing of paired frozen and formalin-fixed, paraffin-embedded tissue specimens. *J Pathol* **222**:41–51.
41. Willis SN, Stadelmann C, Rodig SJ, Caron T, Gattenloehner S, Mallozzi SS *et al* (2009) Epstein-Barr virus infection is not a characteristic feature of multiple sclerosis brain. *Brain* **132**:3318–3328.
42. Xi Y, Nakajima G, Gavin E, Morris CG, Kudo K, Hayashi K, Ju J (2007) Systematic analysis of microRNA expression of RNA extracted from fresh frozen and formalin-fixed paraffin-embedded samples. *RNA* **13**:1668–1674.
43. Yasojima K, McGeer EG, McGeer PL (2001) High stability of mRNAs postmortem and protocols for their assessment by RT-PCR. *Brain Res Brain Res Protoc* **8**:212–218.

SUPPORTING INFORMATION

Additional Supporting Information may be found in the online version of this article:

Table S1. Analyzed tissue specimens.

Table S2. Extracellular matrix and extracellular matrix related genes and corresponding TaqMan® PCR assays used for TaqMan® Low Density Array (LDA) analysis (Applied Biosystems, Darmstadt, Germany).

Table S3. Protocol for using archival FFPE specimen.

Please note: Wiley-Blackwell are not responsible for the content or functionality of any supporting materials supplied by the authors. Any queries (other than missing material) should be directed to the corresponding author for the article.

4.2 „Extracellular matrix in multiple sclerosis lesions: fibrillar collagens, biglycan and decorin are upregulated and associated with infiltrating immune cells“

Hema Mohan^{1,2}, Markus Krumbholz^{1,2}, Rakhi Sharma³, Sylvia Eisele^{1,2}, Andreas Junker^{1,2}, Michael Sixt⁴, Jia Newcombe⁵, Hartmut Wekerle², Reinhard Hohlfeld^{1,2}, Hans Lassmann³ and Edgar Meinl^{1,2}

¹Institute for Clinical Neuroimmunology, Ludwig Maximilians University, Munich, Germany

²Department of Neuroimmunology, Max-Planck-Institute of Neurobiology, Martinsried, Germany

³Center for Brain Research, Medical University of Vienna, Vienna, Austria

⁴Department of Molecular Medicine, Max-Planck-Institute of Biochemistry, Martinsried, Germany

⁵NeuroResource, U.C.L. Institute of Neurology, London, United Kingdom

Brain Pathology 2010 Sep; 20(5): 966-75

RESEARCH ARTICLE

Extracellular Matrix in Multiple Sclerosis Lesions: Fibrillar Collagens, Biglycan and Decorin are Upregulated and Associated with Infiltrating Immune Cells

Hema Mohan^{1,2}; Markus Krumbholz^{1,2}; Rakhi Sharma³; Sylvia Eisele^{1,2}; Andreas Junker^{1,2}; Michael Sixt⁴; Jia Newcombe⁵; Hartmut Wekerle²; Reinhard Hohlfeld^{1,2}; Hans Lassmann³; Edgar Meinl^{1,2}

¹ Institute for Clinical Neuroimmunology, Ludwig Maximilians University, Munich, Germany.

² Department of Neuroimmunology, Max-Planck-Institute of Neurobiology, Martinsried, Germany.

⁴ Department of Molecular Medicine, Max-Planck-Institute of Biochemistry, Martinsried, Germany.

³ Center for Brain Research, Medical University of Vienna, Vienna, Austria.

⁵ NeuroResource, U.C.L. Institute of Neurology, London, UK.

Keywords

extracellular matrix, inflammation, multiple sclerosis, neuroimmunology.

Corresponding author:

Dr. Edgar Meinl, MD, Department of Neuroimmunology, Max-Planck-Institute of Neurobiology, Am Klopferspitz 18, 82152 Martinsried, Germany (E-mail: meinl@neuro.mpg.de)

Received 3 February 2010; accepted 16 March 2010.

Grant support: Deutsche Forschungsgemeinschaft (SFB 571), Hermann and Lilly Schilling Foundation, Verein zur Therapieforschung für Multiple Sklerose-Kranke, BMBF (krankheitsbezogenes Kompetenznetz Multiple Sklerose), Excellency Initiative of the Ludwig Maximilians University Munich.

doi:10.1111/j.1750-3639.2010.00399.x

INTRODUCTION

The pathological hallmarks of active multiple sclerosis (MS) lesions are blood–brain barrier (BBB) disruption, inflammation and demyelination with axonal damage. The interactions between infiltrating immune cells and the central nervous system (CNS) environment, made up of both cellular surfaces and the extracellular matrix (ECM), contributes to control the progression of MS lesions.

ECM, the ground substance found in the interstitial spaces of all organs, provides support to cells. The ECM makes up about one-fifth of the normal brain (7, 38). Under normal conditions, the ECM, has a unique composition in the CNS as it contains relatively small amounts of fibrous proteins (collagens, laminins

Abstract

Extracellular matrix (ECM) proteins can modify immune reactions, e.g. by sequestering or displaying growth factors and by interacting with immune and glial cells. Here we quantified by quantitative polymerase chain reaction (qPCR) expression of 50 ECM components and 34 ECM degrading enzymes in multiple sclerosis (MS) active and inactive white matter lesions. *COL1A1*, *COL3A1*, *COL5A1* and *COL5A2* chains were induced strongly in active lesions and even more in inactive lesions. These chains interact to form collagen types I, III and V, which are fibrillar collagens. Biglycan and decorin, which can decorate fibrillar collagens, were also induced strongly. The fibrillar collagens, biglycan and decorin were largely found between the endothelium and astrocytic glia limitans in the perivascular space where they formed a meshwork which was closely associated with infiltrating immune cells. In active lesions collagen V was also seen in the heavily infiltrated parenchyma. Fibrillar collagens I and III inhibited *in vitro* human monocyte production of CCL2 (MCP-1), an inflammatory chemokine involved in recruitment of immune cells. Together, ECM changes in lesions with different activities were quantified and proteins forming a perivascular fibrosis were identified. Induced fibrillar collagens may contribute to limiting enlargement of MS lesions by inhibiting the production of CCL2 by monocytes.

and fibronectin), and high amounts of linear polysaccharides [glycosaminoglycans (GAGs) such as hyaluronan, chondroitin sulfate and heparan sulfate] (32, 36, 53). Endothelial cells, astrocytes, neurons, microglia and other CNS resident cells can synthesize and secrete ECM proteins (47, 48). The ECM has traditionally been considered to play predominantly a structural role, but recently additional features of the CNS ECM have emerged. During development the ECM is involved in migration, maturation, differentiation and survival of neurons (34). In adults the ECM not only provides physical support for CNS resident cells, but also regulates ionic and nutritional homeostasis (5, 36, 57). Furthermore, the ECM binds both growth promoting and growth inhibitory factors and acts as their reservoir (11, 12, 21, 22, 40).

Recent studies showed a complex alteration in the CNS ECM during the course of MS, including altered expression of both parenchymal and basement membrane related ECM proteins (50, 52). In particular, expression of chondroitin and dermatan sulphate proteoglycans in active MS lesions is changed and foamy macrophages accumulate these proteoglycans together with myelin breakdown products (43). Loss of tenascin-C and -R immunoreactivity is seen in acute MS lesions (15). The basement membrane protein vitronectin is enhanced in the blood vessel walls of active MS lesions, at the border of chronic active lesions and on some hypertrophic astrocytes (45). Finally, altered profiles of different laminin isoforms in the basement membrane of inflamed blood vessels and increased immunoreactivity for fibronectin, agrin and collagen IV have been observed around blood vessels (14, 44, 50).

Experimental autoimmune encephalomyelitis (EAE) studies have indicated decisive roles for basement membranes and their laminins for immune cell entry into the CNS (1, 35, 54). In addition, the ECM may cause the failure of MS lesions to remyelinate as hyaluronan, a major component of the ECM in demyelinated lesions, interferes with oligodendrocyte maturation (4, 42). Further understanding of the ECM changes in MS lesions and the impact of these changes on infiltrating immune cells and CNS resident cells is of importance in understanding the dynamics of MS lesion development. Therefore, we dissected active and inactive lesions as well as unaffected white matter from control brain and determined the expression of 50 ECM molecules and 34 ECM modifying enzymes by quantitative polymerase chain reaction (qPCR). Fibrillar collagens were the ECM molecules most strikingly induced in MS lesions. They localized to the perivascular space where they were closely associated with infiltrating immune cells. *In vitro* experiments revealed decreased production of monocytic CCL2 (MCP-1) in the presence of fibrillar collagens, which may inhibit further immune cell recruitment to MS lesions.

MATERIALS AND METHODS

Tissue samples

A total of 46 tissue blocks from 25 MS patients and six controls without clinical or histological evidence of CNS disease was analyzed (Supporting Information Table S1). The tissue blocks comprised 27 frozen specimens and 19 formalin-fixed, paraffin-embedded (FFPE) samples. Autopsy samples were obtained from the BrainNet Europe, the UK MS Brain Bank, the NeuroResource tissue bank at the UCL Institute of Neurology in London and the Center for Brain Research, Vienna. Some tissue samples were provided by the Netherlands Brain Bank (NBB), Netherlands Institute for Neuroscience, Amsterdam; all material has been collected from donors from whom a written informed consent for brain autopsy and the use of the material and clinical information for research purposes had been obtained by the NBB. The study was approved by the ethical committee of the Medical Faculty of Ludwig Maximilians University, Munich, Germany.

MS lesions were classified according to defined criteria: Active demyelinating lesions contained abundant macrophages with degraded myelin products [Luxol fast blue (LFB) or oil red O positive] either throughout the lesion (acute plaques) or as a broad rim around the lesion edge (chronic active plaques). Inactive demyelinated lesions were sharply demarcated from the normal appear-

ing white matter (NAWM) and without LFB or oil red O positive macrophages and a rim of microglial activation. Slowly expanding lesions revealed mild to moderate microglia activation at the lesion edge with few macrophages containing myelin debris.

Dissection of MS lesions

Seven demyelinated inactive and four demyelinated active white matter lesions were macrodissected manually. Cryosections (20 μ m) from the tissue samples were mounted on PEN slides (P.A.L.M. Microlaser, Bernried, Germany). Every sixth section (30 μ m) was stained with LFB to identify demyelinated areas and the unstained sections were superimposed on stained LFB sections. The lesion area was marked and manually macrodissected. In total, 200–300 μ m of each block was used. Macrodissected sections were then stained with LFB to check the dissected area. In addition, four blocks containing actively demyelinating lesions were used without macro dissection. Control tissue samples used for qPCR contained exclusively white matter.

RNA extraction, cDNA synthesis and qPCR

We used seven demyelinated inactive and eight demyelinated active lesions and six control white matter blocks. RNA was extracted twice with Trizol (TRI® Reagent, SIGMA, Munich, Germany), and cDNA was synthesized using random hexamers (High Capacity cDNA Reverse Transcription kit from Applied Biosystems (ABI; Darmstadt, Germany). qPCR was performed for 84 ECM-related genes (50 ECM components and 34 ECM modifying enzymes) using custom-made low-density arrays (LDA) (ABI). These genes are shown in Table 1 and Table 2. Data analysis was carried out using RQ Manager 1.2 software (ABI), taking *GAPDH*, *βactin* and *PPIA* as housekeeping genes.

RNA from cultured cells was isolated by lysing cells with Trizol and subsequently using RNeasy columns with DNase digestion step (Qiagen, Hilden, Germany). cDNA was synthesized using random hexamers (High Capacity cDNA Reverse Transcription kit, ABI). Genes selected for LDA for monocytic gene expression analysis included *CD80*, *PDL1-B7-H1*, *PDL2*, *CD69*, *CD200R*, *SIRPα*, *CD206*, *ADORA2A*, *IL-1R2*, *SLAM*, *IL-1*, *IL-6*, *IL-10*, *TNF*, *TGFβ*, *IL-12p40*, *CXCL10*, *CCL18*, *MPO*, *MMP9*, *CCR2*, *CX3CR1*, *CD62L*, *CD204*, *MT-2A*, *BDNF*, *NGF*, *NT-3*, *NT-4*, *NRTN*, *LIF*, *IGF-1*, *IL-4*, *IL-5*, *IFNγ*, *CD36*, *CD163*, *MFGE8*, *MERTK*, *CXCL8*, *CXCL2*, *CCL2*, *CCL5*, *CCL3*, *CCL4*, *BAFF*, *GAPDH*, *PPIA*.

Immunohistochemistry

Cryosections were fixed in 4% paraformaldehyde (PFA) and analyzed by LFB, H&E (hematoxylin and eosin), oil red O, and also CD68 immunohistochemistry (DAKO, Hamburg, Germany). Immunohistochemistry was performed using mouse peroxidase anti-peroxidase (PAP) or rabbit PAP system (DAKO). Cryosections were fixed with 4% PFA and endogenous peroxidase activity was blocked using 1.5% methanolic hydrogen peroxide. Primary antibodies were directed against collagen I (mAb, Abcam, Cambridge, UK), collagen III (mAb, Abcam), collagen V (pAb; AbD SeroTec, Düsseldorf, Germany), biglycan (rabbit serum, a kind gift from Prof Larry Fisher, NIH, USA) and decorin (mAb: R&D and rabbit

Table 1. Absolute expression and fold-change values of 50 extracellular matrix (ECM) genes. Abbreviations: NB = normal control brain; De.in = demyelinated inactive lesion; De.act = demyelinated active lesion; De.in : NB = ratio of expression level in demyelinated inactive lesion/control brain; De.act : NB = ratio of expression level in demyelinated active/control brain; ND = not detectable because of low expression level. In total six control white matter samples from four subjects, seven demyelinated inactive lesions from five subjects, and eight demyelinated active lesions from seven subjects were used for quantitative polymerase chain reaction analysis.

Genes	Absolute expression in % GAPDH			Fold change	
	NB	De.in	De.act	De.in : NB	De.act : NB
Fibrillar collagens (COL)					
<i>COL1A1</i>	0.08	0.87	0.45	10.86	5.63
<i>COL1A2</i>	0.34	0.40	0.74	1.18	2.18
<i>COL3A1</i>	0.06	0.72	0.32	12.00	5.33
<i>COL5A1</i>	0.06	1.57	0.15	26.17	2.50
<i>COL5A2</i>	0.05	0.10	0.15	2.00	3.00
<i>COL5A3</i>	0.44	0.79	0.68	1.80	1.55
Basement membrane collagens (COL)					
<i>COL4A1</i>	0.70	2.03	1.90	2.90	2.71
<i>COL4A2</i>	0.12	0.16	0.28	1.33	2.33
<i>COL4A3</i>	0.20	0.06	0.13	0.30	0.65
<i>COL4A4</i>	0.10	ND	0.11	*	1.10
<i>COL4A5</i>	0.65	1.07	0.84	1.65	1.30
<i>COL4A6</i>	0.15	0.12	0.20	0.80	1.33
Anchoring collagen (COL)					
<i>COL7A1</i>	0.51	0.60	0.71	1.18	1.39
Nidogens (NID)					
<i>NID1</i>	0.60	1.11	1.32	1.86	2.20
<i>NID2</i>	0.40	0.31	0.60	0.76	1.50
Laminins (LAMA)					
<i>LAMA1</i>	0.68	2.09	0.36	3.07	0.53
<i>LAMA2</i>	0.64	1.30	0.57	2.03	0.89
<i>LAMA3</i>	0.18	0.22	0.36	1.22	2.00
<i>LAMA4</i>	0.71	1.25	1.24	1.76	1.75
<i>LAMA5</i>	0.13	0.99	0.93	7.62	7.15
<i>LAMB1</i>	0.11	1.06	0.40	9.64	3.64
<i>LAMB2</i>	2.58	5.83	7.89	2.26	3.06
<i>LAMB3</i>	0.14	0.11	0.13	0.79	0.93
<i>LAMC1</i>	0.34	0.83	0.79	2.44	2.32
<i>LAMC2</i>	ND	ND	ND	*	*
Lecticans					
<i>AGC1</i> (Aggrecan)	0.05	0.03	0.41	0.60	8.20
<i>BCAN</i> (Brevican)	8.00	7.22	8.61	0.90	1.08
<i>CSPG3</i> (Neurocan)	13.89	7.40	8.80	0.53	0.63
<i>CSPG2</i> (Versican)	0.01	ND	0.01	*	1.00
Small leucine rich proteoglycans (SLRPs)					
<i>BGN</i> (Biglycan)	4.83	11.17	11.41	2.31	2.36
<i>DCN</i> (Decorin)	2.99	6.27	5.41	2.10	1.81
<i>FMOD</i> (Fibromodulin)	0.03	0.07	0.09	2.33	3.00
<i>LUM</i> (Lumican)	0.09	0.15	0.24	1.67	2.67
Hyaluronan and proteoglycan link proteins (HAPLNs)					
<i>HAPLN1</i>	0.09	ND	0.02	*	0.22
<i>HAPLN2</i>	29.85	5.08	25.74	0.17	0.86
<i>HAPLN3</i>	0.05	0.29	0.36	5.80	7.20
<i>HAPLN4</i>	0.03	0.17	0.03	5.67	1.00
Heparan sulphate proteoglycan (HSPG)					
<i>HSPG2</i> (Perlecan)	0.63	2.75	1.51	4.37	2.40
Tenascins (TNs)					
<i>TNC</i>	3.68	9.46	3.49	2.57	0.95
<i>TNR</i>	5.05	2.78	3.98	0.55	0.79

Table 1. *Continued*

Genes	Absolute expression in % GAPDH			Fold change	
	NB	De.in	De.act	De.in : NB	De.act : NB
Thrombospondins (THBSs)					
<i>THBS1</i>	0.12	0.98	0.41	8.17	3.42
<i>THBS2</i>	2.75	4.22	4.05	1.53	1.47
<i>THBS3</i>	0.01	0.02	0.03	2.00	3.00
<i>THBS4</i>	0.83	1.08	1.09	1.30	1.31
Fibrillins (FBNs)					
<i>FBN1</i>	2.59	3.12	1.46	1.20	0.56
<i>FBN2</i>	0.04	0.03	0.09	0.75	2.25
<i>FBN3</i>	0.11	0.10	0.13	0.91	1.18
Others					
<i>FN1</i> (Fibronectin)	2.60	4.86	3.94	1.87	1.52
<i>RELN</i> (Reelin)	0.08	0.63	0.04	7.86	0.50
<i>VTN</i> (Vitronectin)	0.03	0.03	0.03	1.00	1.00

*Calculation was not possible because at least one value was under the detection limit.

serum, also a kind gift from Prof Larry Fisher). Sections were incubated O/N at 4°C followed by secondary polyclonal rabbit anti-mouse (DAKO) or polyclonal swine anti-rabbit Ig (DAKO), for 1 h at room temperature and tertiary mouse PAP (mAb, DAKO) or rabbit PAP (pAb, DAKO), for 30 minutes at room temperature. Bound antibodies were detected with diaminobenzidine and sections were counterstained with hematoxylin. For immunofluorescence primary antibodies recognizing collagen V [pAb (rabbit), AbD SeroTec], CD31 (pAb, R&D, Wiesbaden, Germany), glial fibrillary acidic protein (GFAP; mAb, Molecular Probes, Karlsruhe, Germany, directly labeled with Alexa 488) were used. As secondary antibodies donkey anti-mouse Alexa 488, donkey anti-sheep Alexa 488 and donkey anti-rabbit Alexa 594 (all from Molecular Probes) were used. Confocal images were taken from Leica SP2UV microscope. Negative controls included omission of primary antibody. For FFPE tissue, antigen retrieval was performed by treatment with citrate buffer pH6 in a steaming water bath.

Cell culture

Peripheral blood mononuclear cells (PBMCs) were isolated from the blood of healthy donors by density gradient centrifugation. Monocytes were isolated by positive selection with immunomagnetic beads (CD14 MicroBeads, Miltenyi Biotech, Bergisch Gladbach, Germany) and were grown in the presence and absence of ECM proteins (coated culture plates) for 24 h.

Tissue culture plates were coated with collagen I at 2 µg/cm² (BD Biosciences, Heidelberg, Germany); collagen III, 2 µg/cm² (BD Biosciences); collagen V, 2 µg/cm² (BD Biosciences); biglycan, 10 µg/mL (R&D); decorin, 10 µg/mL (R&D). All ECM proteins were diluted to final concentration with Ca²⁺, Mg²⁺ free PBS (Gibco, Karlsruhe, Germany) and cell culture plates were incubated at RT for 2 h, and then washed with distilled water (Gibco) and air dried. All the ECM proteins were tested negative for presence of LPS (Biowhittaker™ LAL kit, Walkersville, MD, USA).

The myelin basic protein (MBP) specific T cell clone ES-BP8 (30) was stimulated with HLA-DR compatible PBMC and 20 µg/mL MBP (Biogenesis, Berlin, Germany) or 10 µg/mL MBP

29–48 peptide for 2 days. On the third day cultures were pulsed with 1 µCi/well of ³H-thymidine (Amersham Biosciences, Freiburg, Germany) for 24 h.

Enzyme-linked immunosorbent assays (ELISAs)

To detect CCL2, CCL4, IL10, IL1β in cell culture supernatants the Duoset ELISA system (R&D) was used. Assays were performed according to the manufacturer's instructions.

RESULTS

Altered expression of ECM components in MS lesions

In this study we quantified the expression of 50 genes coding for proteins forming the ECM (Table 1) and for 34 enzymes modifying the ECM (Table 2) in control brain, active and inactive MS lesions. Of the 50 ECM genes tested, 22 were upregulated more than two-fold in active lesions and 21 in inactive lesions (Table 1). Fifteen ECM components were induced in both active and chronic inactive lesions. Twenty-three genes in inactive and 25 in active lesions were considered unchanged, that is, they had a change between 0.51- and 1.99-fold.

Upregulated ECM components included fibrillar collagens, basement membrane collagen, laminins, SLRPs, hyaluronan link proteins, thrombospondins and perlecan (details in Table 1).

Fibrillar collagens and SLRPs form a perivascular fibrosis in MS lesions and are in close interaction with the infiltrating immune cells in the perivascular space

Our expression profiling identified a total of 22 components upregulated in active MS lesions and 21 in inactive MS lesions. Considering the relative induction in MS lesions and the absolute expression level of the ECM genes, our interest was directed to the fibrillar collagens and the SLRPs. We noted a strong induction of

Table 2. Absolute expression and fold-change values of 34 ECM modifying enzymes. Abbreviations: NB = normal control brain; De.in = demyelinated inactive lesion; De.act = demyelinated active lesion; De.in : NB = ratio of expression level in demyelinated inactive lesion/control brain; De.act : NB = ratio of expression level in demyelinated active/control brain; ND = not detectable because of low expression level. In total six control white matter samples from four subjects, seven demyelinated inactive lesions from five subjects, and eight demyelinated active lesions from seven subjects were used for quantitative polymerase chain reaction analysis.

Genes	Absolute expression in % GAPDH			Fold change	
	NB	De.in	De.act	De.in : NB	De.act : NB
A disintegrin and metalloproteinase domains (ADAMs)					
<i>ADAM8</i>	0.11	0.05	0.31	0.45	2.82
<i>ADAM10</i>	16.40	13.58	13.23	0.83	0.81
<i>ADAM12</i>	0.30	0.29	0.40	0.97	1.33
<i>ADAM17</i>	1.29	0.85	1.32	0.66	1.02
A disintegrin like and metalloproteinase with thrombospondin type 1 motifs (ADAMTs)					
<i>ADAMTS1</i>	7.38	7.88	3.92	1.07	0.53
<i>ADAMTS4</i>	16.04	3.24	15.15	0.20	0.94
<i>ADAMTS5</i>	0.04	0.17	0.06	4.25	1.50
Matrix metalloproteinases (MMPs)					
<i>MMP1</i>	ND	ND	ND	*	*
<i>MMP2</i>	0.61	1.09	3.36	1.79	5.50
<i>MMP3</i>	ND	ND	ND	*	*
<i>MMP7</i>	ND	ND	0.03	*	*
<i>MMP8</i>	ND	ND	ND	*	*
<i>MMP9</i>	0.01	0.05	0.13	5.00	13.00
<i>MMP10</i>	ND	ND	ND	*	*
<i>MMP11</i>	0.05	0.30	0.30	6.00	6.00
<i>MMP12</i>	ND	ND	ND	*	*
<i>MMP13</i>	ND	ND	ND	*	*
<i>MMP14</i>	1.00	5.71	4.61	5.71	4.61
<i>MMP15</i>	0.71	0.83	0.36	1.17	0.51
<i>MMP16</i>	0.75	0.97	1.03	1.29	1.37
<i>MMP17</i>	0.39	5.05	0.36	12.95	0.92
<i>MMP19</i>	0.01	0.04	0.08	4.00	8.00
<i>MMP20</i>	ND	ND	ND	*	*
<i>MMP21</i>	0.07	ND	0.07	*	1.00
<i>MMP23</i>	0.02	0.01	0.01	0.50	0.50
<i>MMP24</i>	0.37	1.21	0.34	3.27	0.92
<i>MMP25</i>	ND	ND	0.01	*	*
<i>MMP26</i>	ND	ND	ND	*	*
<i>MMP27</i>	ND	ND	ND	*	*
<i>MMP28</i>	0.24	0.75	0.08	3.13	0.33
Tissue inhibitor of metalloproteinases (TIMPs)					
<i>TIMP1</i>	0.97	5.96	7.00	6.14	7.22
<i>TIMP2</i>	13.78	9.56	13.82	0.69	1.00
<i>TIMP3</i>	9.21	22.98	15.51	2.50	1.68
<i>TIMP4</i>	0.88	0.69	0.98	0.78	1.11

*Calculation was not possible because the values were under the detection limit.

COL1A1, *COL3A1*, *COL5A1*, *COL5A2* chains, both in active and inactive demyelinated lesions (Table 1). These collagens interact to form collagen types I, III and V, which are grouped as fibrillar collagens, known to act as structural proteins (20). Biglycan and decorin, both classified as SLRPs, were also strongly induced in active and inactive demyelinated lesions (Table 1).

The ECM molecules identified by the transcript analysis were then localized by immunostaining. In control brain tissue we saw faint staining around blood vessels with antibodies to the three

fibrillar collagens, decorin and biglycan (Figure 2E, H and data not shown). Similar stainings were observed in the NAWM (Figure 1C, and data not shown). In contrast, in both active and inactive MS lesions staining of fibrillar collagens, decorin, and biglycan was more intense (Figure 2A–D, F, G) and localized around small, medium and large blood vessels (Figure 1A).

In the larger blood vessels in MS lesions the extended perivascular (Virchow Robin) space was filled by a meshwork of fibrillar collagen, biglycan and decorin (Figure 2). In chronic active and



Figure 1. Overview of the extent of induction of fibrillar collagens in multiple sclerosis (MS) lesions. Immunostaining for collagen V is shown in **A–C**. Collagen V is deposited around small and large blood vessels in a chronic inactive MS lesion. The strong expression of collagen V in the

lesion core decreases towards the lesion edge and in the normal appearing white matter (NAWM) it becomes similar to that of control brain. 3,3'-Diaminobenzidine (DAB) was used as a substrate for immunostaining and hematoxylin for counterstain. Original magnifications: **A–C** ×100.

also in acute lesions the infiltrating immune cells in the perivascular space were in close contact with fibrillar collagens, biglycan and decorin (Figure 2). Upregulation of these ECM molecules decreased with the distance from the lesion core and ultimately came close to the expression seen in the control brain (Figure 1A–C). The differences in the expression level of these ECM molecules in the lesion core compared to the surrounding NAWM shows

that the observed induction of fibrillar collagens, biglycan and decorin is not an age-related phenomenon, but a disease-related phenomenon.

Double staining of lesions with the endothelial cell marker CD31 plus collagen V and GFAP plus collagen V located the collagens between the endothelial cells and the astrocytic glial limitans (Figure 3).

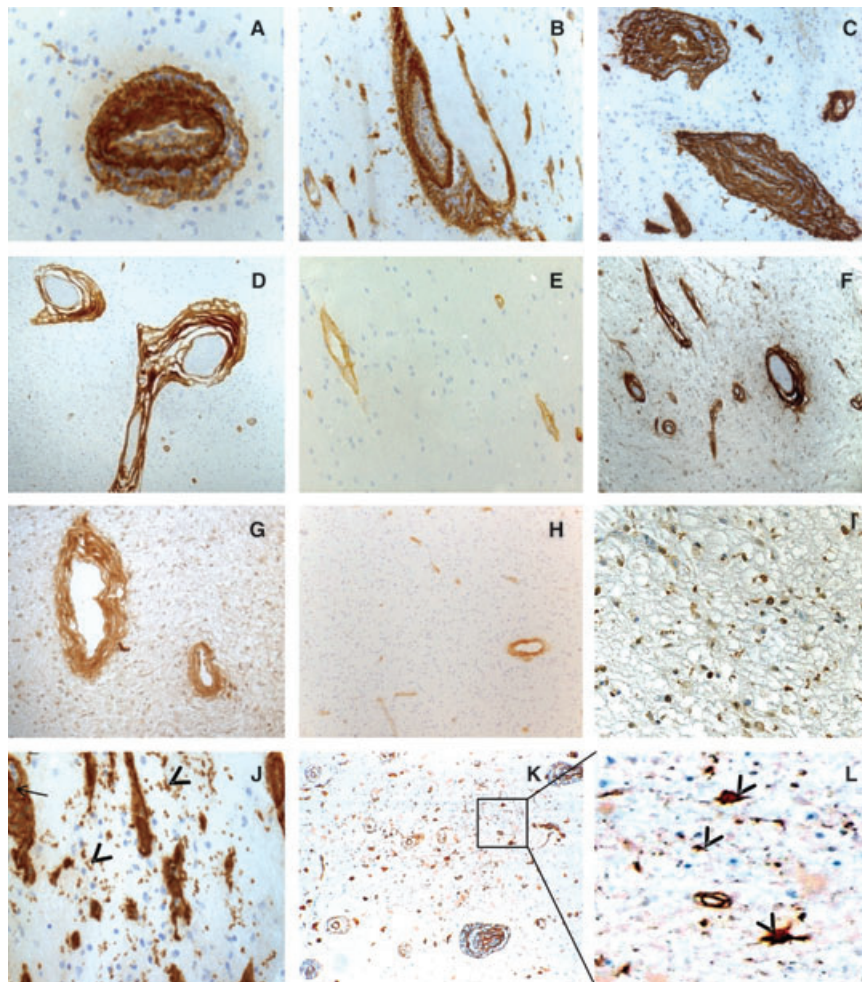


Figure 2. Localization of upregulated extracellular matrix (ECM) components in multiple sclerosis (MS) lesions. (**A–C, I–L**) Chronic active lesions; (**D, F, G**) chronic inactive lesions; (**E, H**) control white matter. The fibrillar collagens collagen I (**A**); collagen III (**B, D**); collagen V (**C**) form a meshwork in the perivascular space in MS lesions. In the control brain, fibrillar collagens are detected at lower levels around blood vessels than in chronic plaques (Collagen I in **E**). In active lesions (**J–L**) collagen V was found around blood vessels and in close interaction with the infiltrating immune cells in the PVS (arrow in **J**) and also outside the PVS (arrowhead in **J** and **L**; in **L** a higher magnification of the boxed area in **K** is shown). Biglycan is detected in infiltrating immune cells in active lesions (**I**) and in inactive lesions the fibrotic meshwork in the PVS also contains biglycan (**G**) and decorin (**F**). In control brain lower levels of biglycan (**H**) and decorin (not shown) are seen around blood vessels. DAB was used as a substrate for immunostaining and hematoxylin for counter stain. Original magnifications: **A, E, I, J**: ×400; **B, C, D**: ×200; **F–H**: ×100; **K**: ×250; and **L** is a sevenfold magnification of **K**.

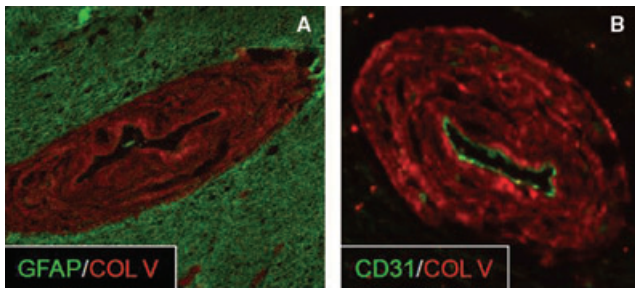


Figure 3. Fibrillar collagens in the PVS. The meshwork formed by fibrillar collagens is strictly limited to the PVS between endothelial cells (CD31 positive) and the astrocytic scar [glial fibrillary acidic protein (GFAP)-positive] in the parenchyma. Double staining of collagen V (red) and GFAP (green) in **A** and collagen V (red) and CD31 (green) in **B**. Original magnifications: **A,B**: $\times 200$.

Collagen V deposits were also observed in the parenchyma of 6/8 acute lesions, probably related to astrocytes (Figure 2J–L). Infiltrating immune cells in the parenchyma of active lesions stained positive for biglycan (Figure 2I).

ECM modifying enzymes in control brain and MS lesions

We quantified the expression of 34 enzymes that can, among other features, modulate ECM composition (Table 2). In control white matter, 7 out of 26 matrix metalloproteinases (MMPs), namely, MMP2, MMP14–17, MMP24 and MMP28 were expressed ($>0.1\%$ GAPDH). Ten of these enzymes were upregulated in active lesions and seven in inactive lesions (more than twofold; Table 2). Five of these, namely MMP9, MMP11, MMP14, MMP19 and tissue inhibitor of matrix metalloproteinase (TIMP) 1 were induced in both chronic inactive and active lesions. We also noted that additional ECM modulating enzymes were differentially regulated: MMP2, MMP9 and MMP19 were stronger induced in active lesions, whereas MMP17, MMP24 and MMP28 were stronger upregulated in inactive lesions. Among the four TIMPs analyzed, TIMP1 was most strongly enhanced. It was induced about six- to sevenfold in both active and inactive lesions, whilst TIMP3 was upregulated in inactive lesions and just slightly in active lesions (Table 2).

Fibrillar collagens upregulated in MS lesions modulate chemokine production by monocytes

Having noted a close association of infiltrating immune cells with fibrillar collagens, decorin, and biglycan in MS lesions, we tested the effect of these upregulated ECM proteins on the activation of MBP-specific T cells and cytokine/chemokine production by monocytes. We activated MBP specific T cells in the presence of fibrillar collagens (I, III, V) with MBP and PBMC as antigen-presenting cells. The stimulated antigen-specific proliferation was unchanged in the presence of either collagen I, III or V (data not shown).

Then, purified monocytes were cultured in the presence or absence of the fibrillar collagens, decorin and biglycan, and

46 immune-related genes (for gene list refer to Materials and Methods) were quantified by qPCR. Collagen I reduced the expression level of CCL2, CCL4, IL-10 and IL-1 β in monocytes by about 50%, whereas collagen III reduced it by 20%–40% (Figure 4A and data not shown). In contrast, biglycan, decorin and collagen V did not modulate the production of any of the 46 genes tested.

We went on to test whether the reduced transcript levels detected in our qPCR screening were mirrored at the protein level. CCL2, CCL4, IL-10 and IL-1 β were detected by ELISA in the supernatant of monocytes in three individual experiments. Although CCL4, IL-10 and IL-1 β were not significantly changed in these experiments, we noted a reduction of CCL2 that mirrored the transcript

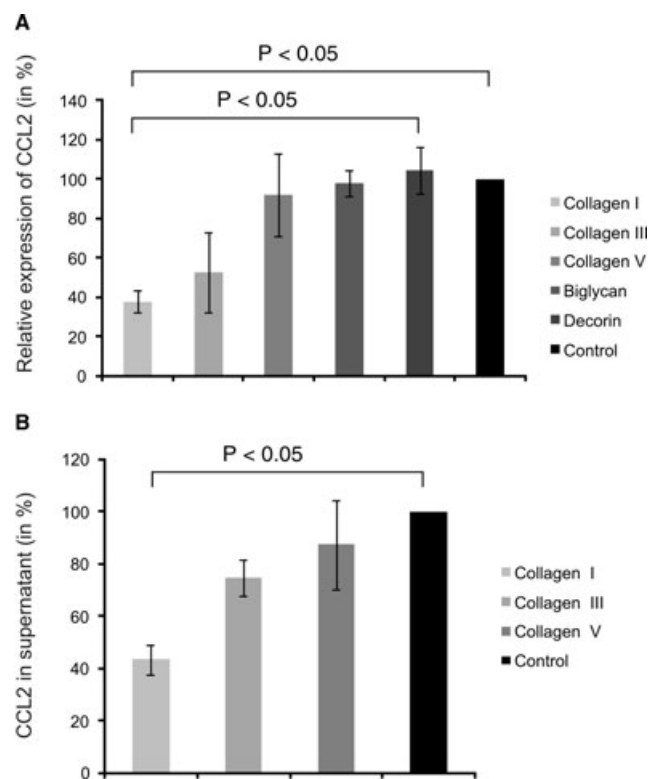


Figure 4. Collagen I decreases CCL2 production by monocytes. Human monocytes purified from peripheral blood mononuclear cell (PBMC) were cultured for 24 h on tissue culture plates coated with the indicated extracellular matrix (ECM) components. **(A)** The transcript level of CCL2 was determined by quantitative polymerase chain reaction using GAPDH as housekeeping gene. Expression of CCL2 in the control wells was set as 100% and the expression level in the presence of the indicated ECM components was calculated. The values given are mean \pm standard error of the mean (SEM) of 3 (collagen I, III, biglycan and decorin) and \pm SEM of 2 (collagen V) independent experiments. **(B)** The amount of CCL2 in the culture supernatant was measured by enzyme-linked immunosorbent assay and is given as percent of that in control dish without ECM component. The mean \pm SEM of three experiments is given. The experiments in A and B were independently performed. Differences in diagrams derived from several independent experiments and more than two groups were analyzed by one-way repeated measures analysis of variance, followed by post hoc test (Holm–Sidak method). Normality and equal variance assumptions were fulfilled. Calculations were done using Sigma Plot.

levels. Collagen I reduced the production of CCL2 protein by 60% and collagen III by 25% (Figure 4B). This decrease in the production of CCL2 by monocytes was not explained by absorption of CCL2 on the collagens: In a parallel experiment, 1730 pg/mL of CCL2, the spontaneous level produced by unstimulated monocytes, was added to the medium in the collagen coated culture plates and >95% of CCL2 could be recovered from the supernatant after 24 h.

DISCUSSION

In this study we have quantified the transcript levels of ECM components in MS lesions, identified components of the perivascular fibrosis and studied their interaction with human immune cells *in vitro*. The most strongly altered ECM components were the chains forming the fibrillar collagens, namely *COL1A1*, *COL3A1*, *COL5A1*, *COL5A2* and the SLRPs biglycan and decorin. Decorin and biglycan can interact with and decorate fibrillar collagens (10).

Although the most prominent function of collagens is to maintain the structure of different tissues, they also have various other functions. The collagen types I, III, and V form collagen fibrils that provide many tissues such as tendon, ligament, cartilage, skin and cornea with firm but flexible characteristics (33, 49). The structure of collagens is characterized by triple helices formed by the homotrimeric or heterotrimeric interaction of three individual collagen polypeptide chains (49).

We have shown in this study that these fibrillar collagens, biglycan and decorin are molecular components of the perivascular fibrosis in MS lesions. The presence of fibrous structures around blood vessels in chronic CNS inflammation has been noted historically by neuropathologists (24, 46), and modern imaging techniques combining three MRI sequence modalities suggest that the perivascular space regulates inflammation in the brain of MS patients (56). Perivascular deposits are a feature of chronicity as fibrillar collagens were more prominent in chronic inactive lesions than in active lesions. Perivascular fibrosis is not unique to MS, it is also observed in liver cirrhosis, hypertensive heart failure and atherosclerosis (25), where collagens I and III form the perivascular deposits, which is similar to that observed in chronic MS lesions. Perivascular fibrosis is also found in HTLV-1 associated myelopathy, where the perivascular deposits consisting mainly of elastin and collagen fibers are found both in the spinal cord and in the brain (3, 55). The upregulation of some of these fibrillar collagen chains and of biglycan we observed is in harmony with previous proteomic studies on chronic active MS lesions (supporting information Table S1 in Ref. 16).

The balance of synthesis and degradation determines the final protein levels. Therefore we quantified not only the ECM components, but also the potential degrading enzymes. Among these are MMP1, -2, -3, -8, -9, -10, -13, -14 and -16 (37, 39, 58), the important collagenases degrading fibrillar collagens. MMP1, -3, -8, -10 and -13 were not detected in MS lesions. Instead, we observed strong induction of MMP2, -9, -11, -14 and -19 in the active lesions. MMP2 and -9 are involved in the BBB leakage (2, 9, 27). MMP19 may participate in the pathogenesis of MS by remodeling the ECM (51). We observed strong induction of MMP11, -14, -17, -24, and -28 in inactive lesions and this is the first study to show the involvement of these MMPs in MS. Our

immunostaining showed a strong deposition of fibrillar collagens. This indicates that the synthesis of fibrillar collagens superseded its degradation by collagenases such as MMP2, -9 and -14, which were induced in the same lesions. In addition, the inhibitor TIMP1 was induced in both active and inactive lesions that might also contribute in shifting the balance towards synthesis and deposition of collagens.

The cellular source of these upregulated ECM components is not known. In our studies we saw induction of TGF β 1 in inactive and active MS lesions in parallel with the previously published data (6). TGF β 1 stimulates production of numerous ECM genes/proteins (23), the increase in TGF β 1 levels in MS lesions might trigger the expression of ECM components accumulated in perivascular fibrosis. In chronic lesions the fibrillar collagens were deposited in the PVS between endothelial cells and the astrocytic glia limitans. Candidates for the production of fibrillar collagens are, besides fibroblasts, astrocytes, which at least *in vitro* synthesize fibrillar collagens (17). In our *in vitro* studies human fibroblasts were much stronger producers of fibrillar collagens than astrocytes, in particular with regard to *COL1A1* and *COL3A1* (data not shown), which we found to be induced in MS lesions. Endothelial cells can produce decorin (31), and thus qualify as a source of decorin in the PVS. The upregulated biglycan in the perivascular space and also within infiltrating cells in the parenchyma of active lesions could also be derived from macrophages (41).

The close interaction between components of the perivascular fibrosis and the infiltrating immune cells was indicated by immunostaining and further studied *in vitro*. We found that fibrillar collagens reduced the production of CCL2 by monocytes. CCL2, a potent attractant for monocytes, dendritic cells, memory T-cells and basophils, is considered to be a major inflammatory chemokine in autoimmune CNS inflammation (8, 18, 28). The inhibition of CCL2 production by monocytes might limit lesion growth. This interpretation is supported by transfer EAE experiments (24) suggesting that reticulin fibers in the perivascular space contribute to vascular blockade and thereby limiting infiltration and lesion development.

CCL2 has been reported to be cleaved *in vitro* by MMP1, 2, 3, -8 and -9 (13, 29). The cleavage products have reduced chemotactic activity (13) or function even as an antagonist (29). In MS lesions we detected MMP2 and -9, but not MMP1, 3 and -8. Further studies are required to identify how CCL2 is processed *in vivo* in MS lesions. Additional effects of the altered ECM on immune cells could be mediated by biglycan, which has been reported to be a ligand for TLR2 and TLR4 in the mouse (41). However, in our study biglycan did not stimulate cytokine production by human monocytes. Furthermore, decorin absorbs and neutralizes TGF β (19), a major modulator of autoimmune CNS inflammation (26). Thus the induction of decorin in MS might also contribute to lesion dynamics.

In summary, we have quantified changes in the ECM in MS lesions at different stages of development, identified the components of the perivascular fibrosis occurring in chronic MS lesions, and shown that the fibrillar collagens I and III inhibit the production of CCL2 by human monocytes. The perivascular fibrosis is a typical feature of chronic lesions and might function as both a physical and a biological barrier that limits immune cell recruitment and the expansion of MS lesions.

ACKNOWLEDGMENTS

We are grateful to Prof Larry Fisher, NIH, USA, for providing antibodies to biglycan and decorin. We thank Drs. N. Kawakami and M. Kerschensteiner for carefully reviewing our manuscript.

REFERENCES

- Agrawal S, Anderson P, Durbeej M, van RN, Ivars F, Opdenakker G *et al* (2006) Dystroglycan is selectively cleaved at the parenchymal basement membrane at sites of leukocyte extravasation in experimental autoimmune encephalomyelitis. *J Exp Med* **203**:1007–1019.
- Anthony DC, Ferguson B, Matyzak MK, Miller KM, Esiri MM, Perry VH (1997) Differential matrix metalloproteinase expression in cases of multiple sclerosis and stroke. *Neuropathol Appl Neurobiol* **23**:406–415.
- Aye MM, Matsuoka E, Moritoyo T, Umehara F, Suehara M, Hokezu Y *et al* (2000) Histopathological analysis of four autopsy cases of HTLV-I-associated myelopathy/tropical spastic paraparesis: inflammatory changes occur simultaneously in the entire central nervous system. *Acta Neuropathol* **100**:245–252.
- Back SA, Tuohy TM, Chen H, Wallingford N, Craig A, Struve J *et al* (2005) Hyaluronan accumulates in demyelinated lesions and inhibits oligodendrocyte progenitor maturation. *Nat Med* **11**:966–972.
- Bandtlow CE, Zimmermann DR (2000) Proteoglycans in the developing brain: new conceptual insights for old proteins. *Physiol Rev* **80**:1267–1290.
- Baranzini SE, Elfstrom C, Chang SY, Butunoi C, Murray R, Higuchi R *et al* (2000) Transcriptional analysis of multiple sclerosis brain lesions reveals a complex pattern of cytokine expression. *J Immunol* **165**:6576–6582.
- Bignami A, Hosley M, Dahl D (1993) Hyaluronic acid and hyaluronic acid-binding proteins in brain extracellular matrix. *Anat Embryol (Berl)* **188**:419–433.
- Charo IF, Ransohoff RM (2006) The many roles of chemokines and chemokine receptors in inflammation. *N Engl J Med* **354**:610–621.
- Cuzner ML, Gveric D, Strand C, Loughlin AJ, Paemen L, Opdenakker G *et al* (1996) The expression of tissue-type plasminogen activator, matrix metalloproteinases and endogenous inhibitors in the central nervous system in multiple sclerosis: comparison of stages in lesion evolution. *J Neuropathol Exp Neurol* **55**:1194–1204.
- Danielson KG, Baribault H, Holmes DF, Graham H, Kadler KE, Iozzo RV (1997) Targeted disruption of decorin leads to abnormal collagen fibril morphology and skin fragility. *J Cell Biol* **136**:729–743.
- Deepa SS, Umehara Y, Higashiyama S, Itoh N, Sugahara K (2002) Specific molecular interactions of oversulfated chondroitin sulfate E with various heparin-binding growth factors. Implications as a physiological binding partner in the brain and other tissues. *J Biol Chem* **277**:43707–43716.
- Deepa SS, Yamada S, Zako M, Goldberger O, Sugahara K (2004) Chondroitin sulfate chains on syndecan-1 and syndecan-4 from normal murine mammary gland epithelial cells are structurally and functionally distinct and cooperate with heparan sulfate chains to bind growth factors. A novel function to control binding of midkine, pleiotrophin, and basic fibroblast growth factor. *J Biol Chem* **279**:37368–37376.
- Denney H, Clench MR, Woodroffe MN (2009) Cleavage of chemokines CCL2 and CXCL10 by matrix metalloproteinases-2 and -9: implications for chemotaxis. *Biochem Biophys Res Commun* **382**:341–347.
- Esiri MM, Morris CS (1991) Immunocytochemical study of macrophages and microglial cells and extracellular matrix components in human CNS disease. 2. Non-neoplastic diseases. *J Neurol Sci* **101**:59–72.
- Gutowski NJ, Newcombe J, Cuzner ML (1999) Tenascin-R and C in multiple sclerosis lesions: relevance to extracellular matrix remodelling. *Neuropathol Appl Neurobiol* **25**:207–214.
- Han MH, Hwang SI, Roy DB, Lundgren DH, Price JV, Ousman SS *et al* (2008) Proteomic analysis of active multiple sclerosis lesions reveals therapeutic targets. *Nature* **451**:1076–1081.
- Heck N, Garwood J, Schutte K, Fawcett J, Faissner A (2003) Astrocytes in culture express fibrillar collagen. *Glia* **41**:382–392.
- Huang DR, Wang J, Kivisakk P, Rollins BJ, Ransohoff RM (2001) Absence of monocyte chemoattractant protein 1 in mice leads to decreased local macrophage recruitment and antigen-specific T helper cell type 1 immune response in experimental autoimmune encephalomyelitis. *J Exp Med* **19**:713–726.
- Iozzo RV (1999) The biology of the small leucine-rich proteoglycans. Functional network of interactive proteins. *J Biol Chem* **274**:18843–18846.
- Kadler KE, Baldock C, Bella J, Boot-Handford RP (2007) Collagens at a glance. *J Cell Sci* **120**:1955–1958.
- Kantor DB, Chivatakarn O, Peer KL, Oster SF, Inatani M, Hansen MJ *et al* (2004) Semaphorin 5A is a bifunctional axon guidance cue regulated by heparan and chondroitin sulfate proteoglycans. *Neuron* **44**:961–975.
- Kawashima H, Atarashi K, Hirose M, Hirose J, Yamada S, Sugahara K *et al* (2002) Oversulfated chondroitin/dermatan sulfates containing GlcAβ61/IdoAα1-3GalNAc(4,6-O-disulfate) interact with L- and P-selectin and chemokines. *J Biol Chem* **277**:12921–12930.
- Leask A, Abraham DJ (2004) TGF-beta signaling and the fibrotic response. *FASEB J* **18**:816–827.
- Levine S (1970) Allergic encephalomyelitis: cellular transformation and vascular blockade. *J Neuropathol Exp Neurol* **29**:6–20.
- Lopez SB, Ravassa AS, Arias GT, Gonzalez MA, Querejeta R, Diez MJ (2006) Altered fibrillar collagen metabolism in hypertensive heart failure. Current understanding and future prospects. *Rev Esp Cardiol* **59**:1047–1057.
- Luo J, Ho PP, Buckwalter MS, Hsu T, Lee LY, Zhang H *et al* (2007) Glia-dependent TGF-beta signaling, acting independently of the TH17 pathway, is critical for initiation of murine autoimmune encephalomyelitis. *J Clin Invest* **117**:3306–3315.
- Maeda A, Sobel RA (1996) Matrix metalloproteinases in the normal human central nervous system, microglial nodules, and multiple sclerosis lesions. *J Neuropathol Exp Neurol* **55**:300–309.
- Mahad DJ, Ransohoff RM (2003) The role of MCP-1 (CCL2) and CCR2 in multiple sclerosis and experimental autoimmune encephalomyelitis (EAE). *Semin Immunol* **15**:23–32.
- McQuibban GA, Gong JH, Wong JP, Wallace JL, Clark-Lewis I, Overall CM (2002) Matrix metalloproteinase processing of monocyte chemoattractant proteins generates CC chemokine receptor antagonists with anti-inflammatory properties *in vivo*. *Blood* **100**:1160–1167.
- Meinl E, Hart BA, Bontrop RE, Hoch RM, Iglesias A, de Waal MR *et al* (1995) Activation of a myelin basic protein-specific human T cell clone by antigen-presenting cells from rhesus monkeys. *Int Immunol* **7**:1489–1495.
- Nelimarkka L, Salminen H, Kuopio T, Nikkari S, Ekfors T, Laine J *et al* (2001) Decorin is produced by capillary endothelial cells in inflammation-associated angiogenesis. *Am J Pathol* **158**:345–353.
- Novak U, Kaye AH (2000) Extracellular matrix and the brain: components and function. *J Clin Neurosci* **7**:280–290.

33. Okada M, Miyamoto O, Shibuya S, Zhang X, Yamamoto T, Itano T (2007) Expression and role of type I collagen in a rat spinal cord contusion injury model. *Neurosci Res* **58**:371–377.
34. Oohira A, Matsui F, Tokita Y, Yamauchi S, Aono S (2000) Molecular interactions of neural chondroitin sulfate proteoglycans in the brain development. *Arch Biochem Biophys* **374**:24–34.
35. Owens T, Bechmann I, Engelhardt B (2008) Perivascular spaces and the two steps to neuroinflammation. *J Neuropathol Exp Neurol* **67**:1113–1121.
36. Rauch U (2004) Extracellular matrix components associated with remodeling processes in brain. *Cell Mol Life Sci* **61**:2031–2045.
37. Rowe RG, Weiss SJ (2008) Breaching the basement membrane: who, when and how? *Trends Cell Biol* **18**:560–574.
38. Rutka JT, Apodaca G, Stern R, Rosenblum M (1988) The extracellular matrix of the central and peripheral nervous systems: structure and function. *J Neurosurg* **69**:155–170.
39. Sabeh F, Li XY, Saunders TL, Rowe RG, Weiss SJ (2009) Secreted versus membrane-anchored collagenases: relative roles in fibroblast-dependent collagenolysis and invasion. *J Biol Chem* **284**:23001–23011.
40. Saksela O, Rifkin DB (1990) Release of basic fibroblast growth factor-heparan sulfate complexes from endothelial cells by plasminogen activator-mediated proteolytic activity. *J Cell Biol* **110**:767–775.
41. Schaefer L, Babelova A, Kiss E, Hausser HJ, Baliova M, Krzyzankova M *et al* (2005) The matrix component biglycan is proinflammatory and signals through Toll-like receptors 4 and 2 in macrophages. *J Clin Invest* **115**:2223–2233.
42. Sherman LS, Back SA (2008) A “GAG” reflex prevents repair of the damaged CNS. *Trends Neurosci* **31**:44–52.
43. Sobel RA, Ahmed AS (2001) White matter extracellular matrix chondroitin sulfate/dermatan sulfate proteoglycans in multiple sclerosis. *J Neuropathol Exp Neurol* **60**:1198–1207.
44. Sobel RA, Mitchell ME (1989) Fibronectin in multiple sclerosis lesions. *Am J Pathol* **135**:161–168.
45. Sobel RA, Chen M, Maeda A, Hinojoza JR (1995) Vitronectin and integrin vitronectin receptor localization in multiple sclerosis lesions. *J Neuropathol Exp Neurol* **54**:202–213.
46. Spielmeyer W (1922) *Histopathologie des Nervensystems*. Verlag von Julius Springer: Berlin.
47. Tilling T, Engelbertz C, Decker S, Korte D, Huwel S, Galla HJ (2002) Expression and adhesive properties of basement membrane proteins in cerebral capillary endothelial cell cultures. *Cell Tissue Res* **310**:19–29.
48. Van der Laan LJ, De Groot CJ, Elices MJ, Dijkstra CD (1997) Extracellular matrix proteins expressed by human adult astrocytes *in vivo* and *in vitro*: an astrocyte surface protein containing the CS1 domain contributes to binding of lymphoblasts. *J Neurosci Res* **50**:539–548.
49. Van der Rest M, Garrone R (1991) Collagen family of proteins. *FASEB J* **5**:2814–2823.
50. Van Horsen J, Bo L, Vos CM, Virtanen I, de Vries HE (2005) Basement membrane proteins in multiple sclerosis-associated inflammatory cuffs: potential role in influx and transport of leukocytes. *J Neuropathol Exp Neurol* **64**:722–729.
51. Van Horsen J, Vos CM, Admiraal L, van Haastert ES, Montagne L, van d V *et al* (2006) Matrix metalloproteinase-19 is highly expressed in active multiple sclerosis lesions. *Neuropathol Appl Neurobiol* **32**:585–593.
52. Van Horsen J, Dijkstra CD, de Vries HE (2007) The extracellular matrix in multiple sclerosis pathology. *J Neurochem* **103**:1293–1301.
53. Viapiano MS, Matthews RT (2006) From barriers to bridges: chondroitin sulfate proteoglycans in neuropathology. *Trends Mol Med* **12**:488–496.
54. Wu C, Ivars F, Anderson P, Hallmann R, Vestweber D, Nilsson P *et al* (2009) Endothelial basement membrane laminin alpha5 selectively inhibits T lymphocyte extravasation into the brain. *Nat Med* **15**:519–527.
55. Wu E, Dickson DW, Jacobson S, Raine CS (1993) Neuroaxonal dystrophy in HTLV-1-associated myelopathy/tropical spastic paraparesis: neuropathologic and neuroimmunologic correlations. *Acta Neuropathol* **86**:224–235.
56. Wuerfel J, Haertle M, Waiczies H, Tysiak E, Bechmann I, Wernecke KD *et al* (2008) Perivascular spaces—MRI marker of inflammatory activity in the brain? *Brain* **131**:2332–2340.
57. Yamaguchi Y (2000) Lecticans: organizers of the brain extracellular matrix. *Cell Mol Life Sci* **57**:276–289.
58. Yong VW, Power C, Forsyth P, Edwards DR (2001) Metalloproteinases in biology and pathology of the nervous system. *Nat Rev Neurosci* **2**:502–511.

SUPPORTING INFORMATION

Additional Supporting Information may be found in the online version of this article:

Table S1. Tissue samples of patients and controls.

Please note: Wiley-Blackwell are not responsible for the content or functionality of any supporting materials supplied by the authors. Any queries (other than missing material) should be directed to the corresponding author for the article.

4.3 „Micro RNA profiling of multiple sclerosis lesions identifies modulators of the regulatory protein CD47”

Andreas Junker^{1,2}, Markus Krumbholz^{1,2}, Sylvia Eisele^{1,2}, Hema Mohan², Florian Augstein^{1,2}, Robert Bittner^{1,2}, Hans Lassmann³, Hartmut Wekerle², Reinhard Hohlfeld^{1,2} and Edgar Meinl^{1,2}

¹Institute for Clinical Neuroimmunology, Ludwig Maximilians University, Munich, Germany

²Department of Neuroimmunology, Max-Planck-Institute of Neurobiology, Martinsried, Germany

³Center for Brain Research, Medical University of Vienna, Vienna, Austria

Brain. 2009 Dec; 132(Pt 12): 3342-52

MicroRNA profiling of multiple sclerosis lesions identifies modulators of the regulatory protein CD47

Andreas Junker,^{1,2} Markus Krumbholz,^{1,2} Sylvia Eisele,^{1,2} Hema Mohan,² Florian Augstein,^{1,2} Robert Bittner,^{1,2} Hans Lassmann,³ Hartmut Wekerle,² Reinhard Hohlfeld^{1,2} and Edgar Meinl^{1,2}

1 Institute for Clinical Neuroimmunology, Ludwig Maximilians University, Munich, Germany

2 Department of Neuroimmunology, Max-Planck-Institute of Neurobiology, Martinsried, Germany

3 Centre for Brain Research, Medical University of Vienna, Vienna, Austria

Correspondence to: Dr Edgar Meinl,
Department of Neuroimmunology,
Max-Planck-Institute of Neurobiology,
Am Klopferspitz 18,
82152 Martinsried, Germany
E-mail: meinl@neuro.mpg.de

We established microRNA profiles from active and inactive multiple sclerosis lesions. Using laser capture microdissection from multiple sclerosis lesions to pool single cells and *in vitro* cultures, we assigned differentially expressed microRNA to specific cell types. Astrocytes contained all 10 microRNA that were most strongly upregulated in active multiple sclerosis lesions, including microRNA-155, which is known to modulate immune responses in different ways but so far had not been assigned to central nervous system resident cells. MicroRNA-155 was expressed in human astrocytes *in situ*, and further induced with cytokines in human astrocytes *in vitro*. This was confirmed with astrocyte cultures from microRNA-155-lacZ mice. We matched microRNA upregulated in phagocytically active multiple sclerosis lesions with downregulated protein coding transcripts. This converged on CD47, which functions as a 'don't eat me' signal inhibiting macrophage activity. Three microRNA upregulated in active multiple sclerosis lesions (microRNA-34a, microRNA-155 and microRNA-326) targeted the 3'-untranslated region of CD47 in reporter assays, with microRNA-155 even at two distinct sites. Our findings suggest that microRNA dysregulated in multiple sclerosis lesions reduce CD47 in brain resident cells, releasing macrophages from inhibitory control, thereby promoting phagocytosis of myelin. This mechanism may have broad implications for microRNA-regulated macrophage activation in inflammatory diseases.

Keywords: multiple sclerosis; microRNAs; CD47; autoimmunity; inflammation

Abbreviations: CT = cycle threshold; GFAP = glial fibrillary acidic protein; LCM = laser capture microdissection; miRNA = micro-ribonucleic acid; qPCR = quantitative polymerase chain reaction; SIRP- α = signal regulatory protein; UTR = untranslated region

Introduction

A few hundred microRNAs (miRNAs) post-transcriptionally regulate the expression of about one-third of all protein-coding genes (Lewis *et al.*, 2005). miRNAs recognize partially complementary target

sequences in cognate mRNAs and either destabilize their mRNA targets or inhibit protein translation. A single miRNA can regulate the expression of hundreds of target genes (Baek *et al.*, 2008; Selbach *et al.*, 2008). miRNA-mediated gene regulation is critical during development and adulthood, e.g. by regulating and

maintaining functions of the immune (Taganov *et al.*, 2007; Lodish *et al.*, 2008) and nervous (Kosik, 2006) systems. Although the quantitative impact of miRNA 'fine tuning' on gene expression levels is relatively small, miRNAs are nevertheless implicated in the pathogenesis of different diseases, including cancer, cardiac failure and neurodegenerative diseases (Papagiannakopoulos and Kosik, 2008; Thum *et al.*, 2008; Hebert and De, 2009; Visone and Croce, 2009). Moreover, miRNAs represent promising novel targets for therapy (Krutzfeldt *et al.*, 2005; Czech, 2006; Elmen *et al.*, 2008).

In this study, we set out to identify miRNA profiles of multiple sclerosis lesions. Multiple sclerosis is a chronic disease of the CNS, characterized by inflammation and demyelination. A complex interplay between brain-invading immune cells and CNS resident cells determines lesion development (Fugger *et al.*, 2009; Goverman, 2009; Steinman, 2009). Activation of macrophages/microglia plays a central role in the effector phase of myelin breakdown (Sospedra and Martin, 2005; Trapp and Nave, 2008; Steinman, 2009). In previous investigations, unbiased approaches starting from the transcriptome (Lock *et al.*, 2002) or proteome (Han *et al.*, 2008) of multiple sclerosis lesions provided important new insights into the pathogenesis and yielded potential targets for therapy. Here we asked whether analysis of miRNA profiles in active and chronic inactive multiple sclerosis lesions could (i) link miRNAs to specific genes that are dysregulated in multiple sclerosis lesions; (ii) identify novel miRNA targets; and (iii) provide new mechanisms regarding the contribution of tissue-resident cells in the disease process.

Materials and methods

Tissue specimens

Twenty-one tissue blocks from 20 different multiple sclerosis patients and nine tissue blocks from nine subjects without any known neurological disease were used for miRNA analyses (Supplementary Table S1). These samples included four frozen active, 12 formalin-fixed, paraffin embedded active, one formalin-fixed, paraffin embedded inactive and four frozen inactive multiple sclerosis lesions. From control subjects, four frozen white matter and five formalin-fixed, paraffin embedded white matter specimens were used (Supplementary Table S1). Additionally, RNA from four active lesions was used for profiling of protein-coding transcripts. The study was approved by the Institutional Review Board of the Ludwig-Maximilians University, Munich.

Histology

Sections were stained with haematoxylin and eosin, luxol fast blue for myelin and Oil Red O for neutral lipids (frozen sections only). Antibodies against CD4, CD8, CD20, CD47, CD68 and glial fibrillary acidic protein (GFAP) (Supplementary Table S2) were used for immune staining, along with standard peroxidase procedures (DAKO, Hamburg, Germany) using diaminobenzidine as substrate. Double staining for proteolipoprotein and CD47 or GFAP and CD47 were performed with polyclonal rabbit antibodies to proteolipoprotein or GFAP and the mouse monoclonal antibody to CD47 LS-B1959

(Supplementary Table S2). Confocal microscopy was done with a Leica SP-2 microscope.

Tissue blocks were classified according to defined criteria: active lesions contained abundant macrophages with early (luxol fast blue and Oil Red O positive) myelin degradation products, either throughout the whole lesion or in a broad rim at the lesion edge. Inactive demyelinated lesions were sharply demarcated from the periplaque white matter, lacked a rim of microglia activation and were devoid of luxol fast blue- or Oil Red O-reactive myelin degradation products in immune cells.

Dissection of multiple sclerosis lesions, laser capture microdissection, RNA extraction and quantitative PCR

Frozen and paraffin sections were mounted on membrane-covered polyethylene naphthalate slides (Zeiss, Jena, Germany). Parallel sections were stained with luxol fast blue to allow identification of the lesions. For the analysis of miRNA profiles, white matter multiple sclerosis lesions or control white matter specimens were dissected from the slides with a scalpel and 10–15 sections were pooled for RNA extraction. This miRNA analysis was restricted to white matter tissue samples to limit possible confounding effects of neuronal miRNAs. Formalin-fixed, paraffin embedded tissue was deparaffinized and digested with proteinase K (Sigma-Aldrich, Steinheim, Germany) before RNA extraction.

Laser capture microdissection (LCM) was used to assign miRNAs to certain cell types using quick immunofluorescence staining as described previously (Junker *et al.*, 2007; for antibodies see Supplementary Table S2). RNA from 100 pooled LCM cells per sample was prepared from eight different sections. The miRNeasy Mini Kit (Qiagen, Hilden, Germany) was used for macrodissected lesions and the RNeasy Micro Kit (Qiagen) for LCM cells. miRNAs were transcribed using the TaqMan[®] miRNA Reverse Transcription Kit and miRNA-specific stem-looped primers (Applied Biosystems, Darmstadt, Germany). These stem-looped primers bind to the miRNAs and generate a longer cDNA transcript in the RT reaction, which then can easily be amplified in a normal quantitative (q) PCR reaction. For analysis of RNA representing protein coding transcripts, random hexamer primers (High-Capacity cDNA Reverse Transcription Kit, Applied Biosystems) were used for cDNA synthesis.

The qPCR was performed on the ABI 7900 (Applied Biosystems) using the qPCR Core Kit and uracyl *N*-glycosylase (both from Eurogentec, Cologne, Germany). miRNAs were detected with single TaqMan[®] miRNA Assays (Applied Biosystems) and with Taqman Low Density miRNA Arrays (TaqMan[®] Human MiRNA Array v1.0; Early Access; Applied Biosystems), which contains 365 different human miRNA assays. The total amount of transcribed RNA equivalent used per PCR reaction was 0.2–1 ng for miRNAs. Different methods were used for normalization of the measurements. For analysis of Low Density miRNA Arrays (Applied Biosystems), the median of the most abundant 43 miRNAs (43 miRNAs could be detected with a raw cycle threshold (CT) <30 in all samples) was used as a surrogate house-keeping gene. The relative expression of miRNAs in multiple sclerosis lesions versus control tissue was calculated with the $\Delta\Delta\text{CT}$ method [$\Delta\Delta\text{CT} = (\text{median of CT miRNA multiple sclerosis lesions} - \text{median of most abundant 43 miRNAs in the group of multiple sclerosis lesions}) - (\text{CT miRNA control} - \text{median of most abundant 43 miRNAs of group of controls})$]. For the analysis of LCM material and cultured cells, single miRNA Taqman Assays (Applied Biosystems) were used,

and the small nuclear RNA RNU6B was used for normalization in the $\Delta\Delta\text{CT}$ method (Ng *et al.*, 2009).

Both frozen and formalin-fixed, paraffin embedded tissue specimens were used to quantify miRNAs by qPCR. We noted that the miRNA transcripts could be amplified with a comparable level from frozen and formalin-fixed, paraffin embedded tissue: the median of the most abundant (CT < 30) 43 miRNAs was 24.0 in the frozen and 25.4 in the formalin-fixed, paraffin embedded tissue specimens, and the calculated $\Delta\Delta\text{CT}$ was very similar in frozen and formalin-fixed, paraffin embedded tissue, which is in agreement with Doleshal *et al.* (2008). Therefore miRNA levels obtained from formalin-fixed, paraffin embedded and frozen tissue samples of the same lesion type or control tissue were placed into one group for statistical analyses.

The expression levels of 528 genes (519 genes of interest and nine slots for housekeeping genes) were determined by qPCR (custom-made low density arrays; Applied Biosystems). The 519 selected genes were related to immune function, myelin biology, extracellular matrix and neurotrophic factors.

Cell culture

Monocytes and T cells were isolated from peripheral blood mononuclear cells by negative isolation (MACS, Miltenyi, Bergisch Gladbach, Germany). Human astrocytes of embryonic origin (Krumbholz *et al.*, 2005) were used after the third or fourth passage. Owing to their embryonic origin, these astrocyte cultures are devoid of microglial cells or macrophages (Aloisi *et al.*, 1992; Krumbholz *et al.*, 2005). All cells were cultured in Roswell Park Memorial Institute medium supplemented with 5–20% foetal calf serum (PAN Biotech, Aidenbach and Biochrom, Berlin, Germany). In some experiments, human cells were stimulated overnight with gamma-interferon (0.1 U/ μl ; Roche, Diagnostics GmbH, Mannheim, Germany), interleukin-1 β (0.05 $\mu\text{g}/\text{ml}$; R&D, Minneapolis, MN, USA), transforming growth factor- β 1 (1 ng/ml; R&D) or tumour necrosis factor- α (0.01 $\mu\text{g}/\text{ml}$; R&D).

Luciferase assays for analysing miRNA targeting

Oligonucleotides of 50 base pair length (Metabion, Martinsried, Germany) containing specific miRNA binding sites (sequences shown in Supplementary Table S3) were cloned into the 3' untranslated region (UTR) of luciferase in a reporter plasmid (pMIR-REPORTTM miRNA Expression Reporter Vector System Ambion/Applied Biosystems).

Pre-miRsTM or anti-miRsTM (Ambion/Applied Biosystems) were transfected into HeLa cells with Lipofectamin[®] 2000 (Invitrogen, Karlsruhe, Germany) along with the luciferase plasmid containing the predicted binding site of the respective miRNA. A control plasmid coding for β -galactosidase without any known miRNA binding site in its 3' UTR was used for normalization of the luciferase signal; 200 ng of each plasmid and 25 nmol pre- or anti-miR were applied to transfect 8×10^4 HeLa cells. Pre-miR control-1 (Ambion/Applied Biosystems) with a scrambled nucleotide sequence was used as a control.

Luciferase and β -galactosidase were measured 24 h after triple transfection (see above) using the Dual Light Luciferase Assay from Applied Biosystems and the Victor Luminometer from Perkin Elmer.

miRNA-155-deficient astrocytes

B6.Cg-Mirm155tm1.1Rsky/J mice (Thai *et al.*, 2007) were purchased from the Jackson Laboratory (Bar Harbor, ME, USA). In these miR-155

knockout mice, the *lacZ* reporter allows detection of bic/miR-155 promoter transcriptional activity. Astrocyte cultures from these mice were established essentially as described (Sasaki *et al.*, 1989). These astrocyte cultures were stimulated with murine tumour necrosis factor- α (10 ng/ml, PeProtech, Hamburg, Germany) for 24 h and bic/miR-155 promoter activity was detected with a β -galactosidase staining kit (Active Motif, Rixensart, Belgium). GFAP staining of cultured astrocytes was performed with GFAP antibody Z0334 (DAKO), which had been previously labelled with the Cy3-mAb Labelling Kit (GE, Amersham).

All animal procedures used in this report were in accordance with guidelines of the committee on animals of the Max Planck Institute for Neurobiology and with the license of the Regierung von Oberbayern (Munich, Germany).

Statistical analyses

For statistical analysis, we used the Mann–Whitney U-test. The significance levels are indicated in the individual figures and tables.

Results

miRNA pattern in different multiple sclerosis lesions

To identify miRNA profiles of multiple sclerosis lesions we quantified the expression level of 365 different mature miRNAs by qPCR in 16 active and 5 inactive white matter multiple sclerosis brain lesions and in 9 control white matter specimens. One hundred and sixty-seven miRNAs were detectable in all groups of examined specimens with a raw CT-value < 35.

We considered abundance (CT < 35), amount of regulation (at least 2-fold) and significance ($P < 0.01$; U-test) to establish miRNA signatures of the different types of multiple sclerosis lesions. Using these criteria, in active lesions 20 miRNAs were at least twice more abundant and 8 miRNAs at least twice less abundant than in normal white matter (Table 1). In inactive lesions, 22 miRNAs were at least twice more abundant and 13 miRNAs at least twice less abundant than in normal white matter (Table 1). The complete data set of all miRNAs expressed in the examined brain specimens is given in Supplementary Table S4.

Eight of our active multiple sclerosis brain specimens derive from multiple sclerosis cases with a very fulminant disease course called Marburg's variant. We analysed the group of Marburg's and non-Marburg's variant separately (Supplementary Table S5). We noted that the 28 most prominently regulated miRNAs ($P < 0.01$ in the entire group) were regulated in the same direction in both groups of active lesions. Eight of the 10 miRNAs upregulated the most in the entire group of active lesions were significantly upregulated in both Marburg and non-Marburg cases. Some miRNAs were more prominently regulated in the Marburg variant than in the other active lesions. This probably reflects the more intense tissue destruction in the Marburg variant.

Among the significantly altered miRNAs, some showed a differential regulation in active versus inactive lesions, whereas others were modified in the same direction (details in Fig. 1A and Table 1). As one example, details of the expression of miRNA-155, which we further analysed in detail (see below), are shown in Fig. 1B.

Table 1 miRNA profiles in active and inactive multiple sclerosis lesions

miRNAs upregulated in lesions ^a	Percent surrogate housekeeping gene ^b in lesions	Fold regulation in lesions compared to normal brain white matter ^c	miRNAs downregulated in lesions ^a	Percent surrogate housekeeping gene ^b in lesions	Fold regulation in lesions compared to normal brain white matter ^c
miRNA profiles in active multiple sclerosis lesions					
miR-650	5.7	15.1**	miR-656	0.2	0.15**
miR-155	37.1	11.9**	miR-184	0.9	0.21**
miR-326	1.5	8.9**	miR-139	1.1	0.36**
miR-142-3p	68.5	7.7**	miR-23b	16.9	0.37**
miR-146a	73.7	6.4**	miR-328	34.1	0.46**
miR-146b	50.4	5.1**	miR-487b	4.7	0.46**
miR-34a	9.3	4.9**	miR-181c	2.1	0.48**
miR-21	82.7	3.9**	miR-340	7.2	0.50**
miR-23a	1.4	3.9**			
miR-199a	1.2	3.3**			
miR-27a	88.3	3.1**			
miR-142-5p	8.3	3.0**			
miR-193a	10.5	2.9**			
miR-15a	12.3	2.8**			
miR-200c	2.3	2.8**			
miR-130a	9.8	2.6**			
miR-223	167.9	2.4**			
miR-22	25.1	2.4**			
miR-320	49.2	2.2**			
miR-214	2.5	2.1**			
miRNA profiles in inactive multiple sclerosis lesions					
miR-629	1.4	10.1**	miR-219	0.9	0.02**
miR-148a	16.1	9.8**	miR-338	1.1	0.04**
miR-23a	2.9	8.8**	miR-642	0.3	0.06**
miR-28	15.4	6.9**	miR-181b	55.0	0.13**
miR-195	214.9	5.0**	miR-18a	0.7	0.14**
miR-497	11.2	4.8**	miR-340	3.9	0.15**
miR-214	4.5	4.3**	miR-190	0.5	0.16**
miR-130a	16.0	4.2**	miR-213	1.4	0.22**
miR-135a	37.8	3.7**	miR-330	3.5	0.24**
miR-204	127.0	3.2**	miR-181d	22.0	0.32**
miR-200c	2.7	3.1**	miR-151	20.7	0.37**
miR-660	32.5	3.1**	miR-23b	15.4	0.37**
miR-152	54.4	3.1**	miR-140	52.6	0.50**
miR-30a-5p	424.8	3.0**			
miR-30a-3p	73.7	3.0**			
miR-365	37.0	2.9**			
miR-532	16.2	2.9**			
miR-126	288.0	2.4**			
let7c	136.2	2.4**			
miR-20b	7.0	2.4**			
miR-30d	67.0	2.3**			
miR-9	239.8	2.2**			

a Those miRNAs are listed, which were at least 2-fold and significantly (** $P < 0.01$; U-test) regulated in active or inactive lesions in comparison to normal brain.

b Surrogate housekeeping gene: the median of the 43 most abundant miRNAs (CT < 30).

c Sixteen active lesions, five inactive lesions and nine control white matter specimens were examined.

Assignment of regulated miRNAs to specific cell types

In principle, these altered miRNA profiles might reflect the presence of infiltrating immune cells, changes in brain resident cells, or both.

To assign the differentially expressed miRNAs to specific cell types, we performed three types of experiments. First, we analysed cultured human astrocytes, T cells and monocytes *in vitro*. Second, we used LCM to isolate CD68⁺ macrophages/microglia, CD8⁺ T cells, CD20⁺ B cells and GFAP⁺ astrocytes from human brain tissue. And

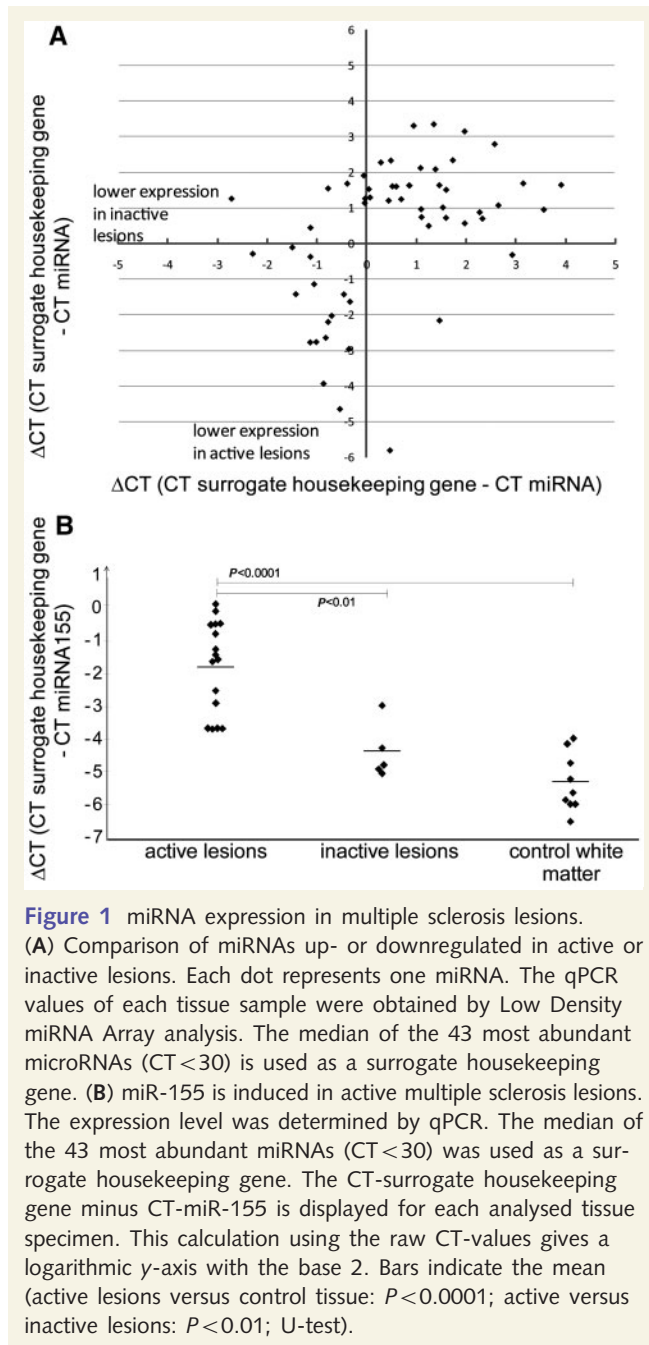


Figure 1 miRNA expression in multiple sclerosis lesions. (A) Comparison of miRNAs up- or downregulated in active or inactive lesions. Each dot represents one miRNA. The qPCR values of each tissue sample were obtained by Low Density miRNA Array analysis. The median of the 43 most abundant microRNAs (CT < 30) is used as a surrogate housekeeping gene. (B) miR-155 is induced in active multiple sclerosis lesions. The expression level was determined by qPCR. The median of the 43 most abundant miRNAs (CT < 30) was used as a surrogate housekeeping gene. The CT-surrogate housekeeping gene minus CT-miR-155 is displayed for each analysed tissue specimen. This calculation using the raw CT-values gives a logarithmic y -axis with the base 2. Bars indicate the mean (active lesions versus control tissue: $P < 0.0001$; active versus inactive lesions: $P < 0.01$; U-test).

third, we investigated the expression of miR-155, which we found to be particularly relevant for this study, in brain-derived cells from miR-155 deficient mice, which have the *lacZ* reporter instead of miR-155 (Thai *et al.*, 2007).

Based on the miRNA profiling of multiple sclerosis lesions (Table 1), we selected 21 miRNAs, including the 10 miRNAs most strongly upregulated in active lesions, for expression analysis in cultured cells. The majority of the 21 miRNAs analysed were expressed in T cells, monocytes and astrocytes (Supplementary Table S6). Some miRNAs, however, were differentially expressed in the studied cell types; miR-130a and miR-30a-3p were most abundant in astrocytes, miR-23a, miR-199a# and miR-152 in monocytes, and miR-146b in T cells and cytokine-stimulated astrocytes. Notably, 18 out of 21 miRNAs, selected because

they were induced in multiple sclerosis lesions, were detectable in cultured astrocytes (Supplementary Table S6).

We analysed how miRNA expression levels were regulated in astrocytes by inflammatory cytokines. We stimulated human astrocytes with interleukin- 1β , tumour necrosis factor- α , gamma-interferon and transforming growth factor- β , and investigated the expression of 19 miRNAs. These included the 10 miRNAs most upregulated in active multiple sclerosis lesions and the miRNAs predicted to target CD47 (which were also upregulated in active lesions). In particular, miR-23a, miR-146a and miR-155 were strongly induced by the applied cytokines (Fig. 2).

We applied LCM to assign selected miRNAs to specific cell types that are prominent in active and inactive multiple sclerosis lesions. We dissected CD8 $^+$, GFAP $^+$, CD20 $^+$ and CD68 $^+$ cells from multiple sclerosis tissue (four active and four inactive lesions). Eight cell pools, each consisting of 100 individually microdissected cells, were compiled from astrocytes, monocytes, CD8 $^+$ cells and four pools of CD20 $^+$ B cells. Using this material, we found that the two miRNAs most prominently upregulated in active multiple sclerosis lesions, miR-155 and miR-650, were present in microdissected astrocytes (miR-155 in Fig. 3a; data for miR-650 not shown), and CD8 $^+$ T cells, B cells and CD68 $^+$ macrophages (raw CT < 33 in microdissected cells; data not shown); miR-34a and miR-326, other regulators of CD47 (see below), were detected both in astrocytes and infiltrating immune cells, with a CT-value between 33 and 37 (data not shown).

Because miR-155 has been described so far in different immune cells (Rodriguez *et al.*, 2007; Thai *et al.*, 2007), but not in brain resident cells, we elaborated this point using mice expressing *lacZ* instead of miR-155 (Thai *et al.*, 2007). We established astrocyte cultures from these mice and observed co-localization of *lacZ* encoded β -galactosidase and GFAP, in particular after cytokine stimulation of the astrocytes (Fig. 3B and C).

CD47 as a shared target of miRNAs upregulated in multiple sclerosis lesions

Having identified several miRNAs that are upregulated in multiple sclerosis lesions, we examined whether the *in silico* predicted target transcripts of these miRNAs are actually downregulated in the lesions. Using qPCR we determined the expression levels of 519 selected targets, including immune- and myelin-related genes from eight active multiple sclerosis lesions (four of which had also been used for miRNA analysis), four inactive lesions and control white matter. We detected around 40 genes that were downregulated in the active lesions; among them was CD47.

Transcripts of CD47 were downregulated by $\sim 50\%$ in active lesions compared to control white matter (data not shown), which is consistent with a previous report (Koning *et al.*, 2007). In contrast, in inactive lesions, the CD47 expression level was similar to normal white matter as seen by qPCR (data not shown). Immunohistochemistry with three different monoclonal antibodies specific for CD47 showed a reduced expression in active multiple sclerosis lesions (Supplementary Fig. S1; data not shown). Chronic inactive lesions showed CD47 expression in their

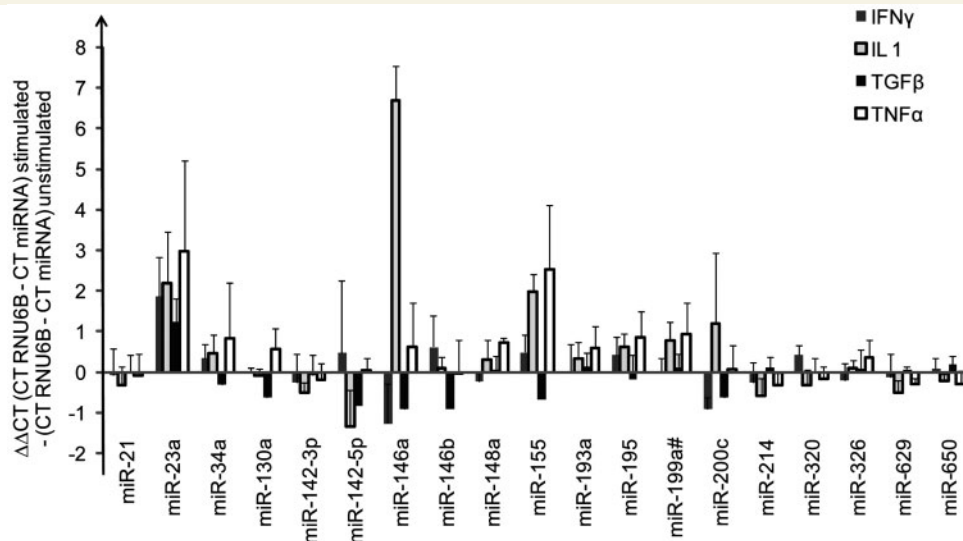


Figure 2 miRNA expression is regulated in astrocytes. Cultured human astrocytes were stimulated with interleukin (IL)-1, tumour necrosis factor (TNF)- α , gamma-interferon (IFN)- γ and transforming growth factor (TGF)- β for 24 h or left untreated. Subsequently the expression levels of the indicated microRNAs were determined by qPCR. The small nuclear RNA RNU6B was used as a housekeeping gene (Ng *et al.*, 2009) and the cytokine-induced regulation was calculated as $\Delta\Delta\text{CT}$ -value [$\Delta\Delta\text{CT} = (\text{CT RNU6B} - \text{CT miRNA})_{\text{stimulated}} - (\text{CT RNU6B} - \text{CT miRNA})_{\text{unstimulated}}$]. This calculation using the raw CT-values gives a logarithmic y-axis with the base 2. The mean \pm SEM of 2–6 experiments is shown.

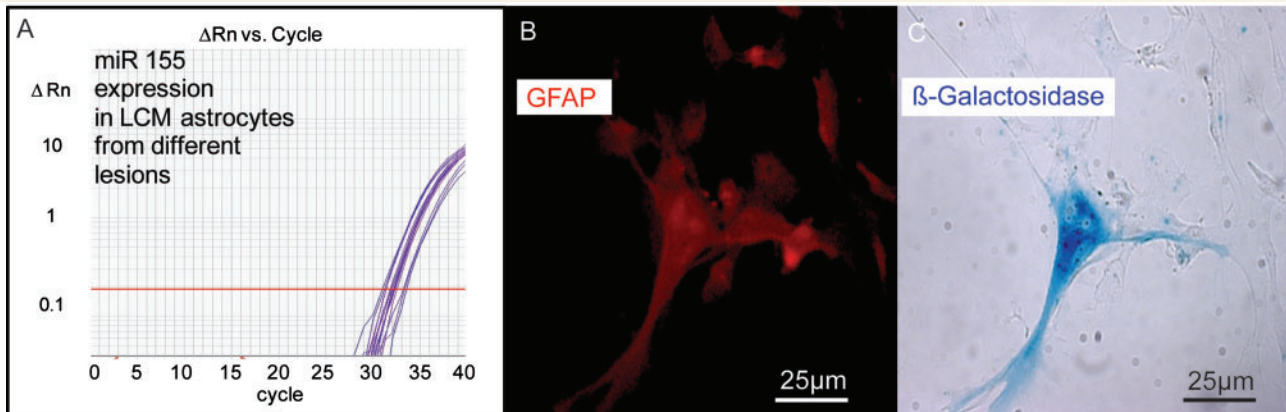


Figure 3 Astrocytes express miR-155. (A) GFAP+ astrocytes from multiple sclerosis lesions were obtained by LCM, 100 dissected cells from one lesion were pooled and analysed for miR-155 expression by qPCR. Depicted are the amplification curves in duplicates of dissected astrocyte samples from eight different multiple sclerosis lesions. (B, C) Cultured astrocytes from mice expressing the reporter *LacZ* instead of miR-155 (Thai *et al.*, 2007) were stimulated with tumour necrosis factor- α for 24 h. The *LacZ* expression (C) co-localized with GFAP (B).

demyelinated lesion core (Supplementary Fig. S1). CD47 co-localized with both GFAP and proteolipoprotein (Supplementary Fig. S1), indicating that this broadly expressed protein is displayed by both astrocytes and oligodendrocytes.

We then searched the miRNAs induced in active lesions (Table 1) using Targetscan 5.0 (Lewis *et al.*, 2005; Grimson *et al.*, 2007) for highly conserved binding sites in the 3'UTR of these transcripts that were downregulated in active lesions. CD47 appeared to be most promising because Targetscan 5.0 detected two potential conserved and several unconserved

miRNA binding sites in its 3'UTR assigned to those miRNAs that were most strongly upregulated in the active multiple sclerosis lesions (Supplementary Table S3).

Eight of the 20 miRNAs most upregulated in active multiple sclerosis lesions (Table 1) are predicted to target CD47 as assessed by Targetscan 5.0 (Lewis *et al.*, 2005; Grimson *et al.*, 2007), namely miR-155, miR-214, miR-34a, miR-21, miR-142-5p, miR-193a, miR-320 and miR-326. These eight miRNAs were tested in luciferase assays for targeting of the 3'UTR of CD47 (Fig. 4A and B). We found that miR-155 targeted both its highly conserved

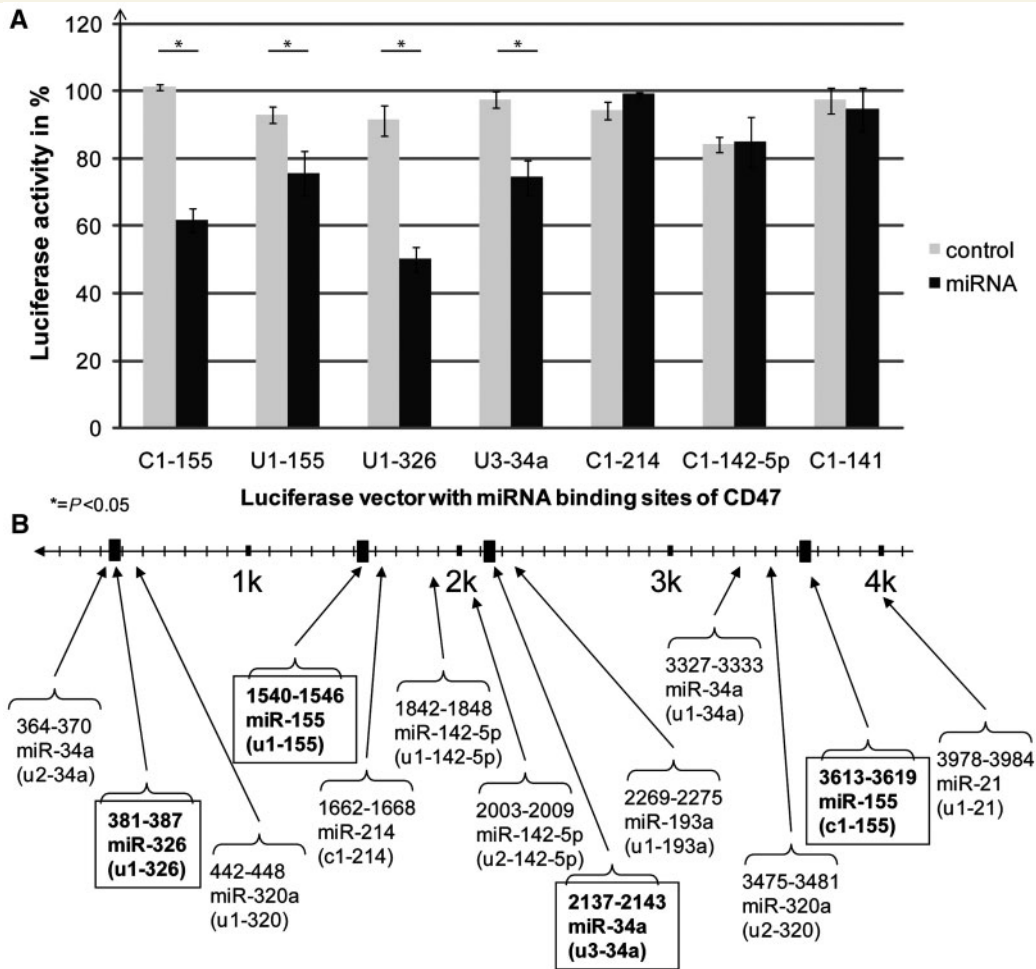


Figure 4 miRNAs target the 3'UTR of CD47. (A) The luciferase activity in HeLa cells transfected with the indicated luciferase vectors and the corresponding premiR or control miR (premiR with a scrambled RNA sequence) is shown. Details of the applied luciferase reporter vectors are in Supplementary Table S3. A control vector with β -galactosidase was used for normalization. Luciferase activity was divided by β -galactosidase activity and then normalized on a mock-transfected control. Luciferase measurements were done in quadruplicates in each individual experiment. The SEM of three to four experiments is shown. Significant differences between the scrambled control premiR and the premiRs predicted to target CD47 are indicated (U-test, $P < 0.05$). (B) 3'UTR of CD47 with predicted and proven binding sites of microRNAs upregulated in active multiple sclerosis lesions. MicroRNA target sites of human CD47 3'UTR NM_001025079 (length 4189) were predicted with Targetscan human (release 5.0: December 2008). Interaction of miR-34a, miR-155, miR-326 with their predicted target sites u1-326, c1-155, u1-155, u3-34a could be confirmed by luciferase assays (A) and are indicated with their position in CD47 3'UTR in the figure (B). Of each predicted binding site the first line indicates the position in 3'UTR of CD47. Thereby 'c' indicates a highly conserved binding site and 'u' indicates a less conserved binding site. The second line names the miRNA predicted to bind, and the third line is the designation of the luciferase vector that includes the binding site. Binding sites functional in the luciferase assay (A) are boxed.

and less conserved binding site in the 3'UTR of CD47 (Fig. 4A). Furthermore, miR-34a and miR-326 also targeted the 3'UTR of CD47. Nine additional potential miRNA binding sites were analysed in the same way, but the corresponding miRNAs did not significantly reduce the luciferase activity in our assay (Fig. 4A and B; data not shown).

Discussion

Establishing miRNA signatures of active and inactive multiple sclerosis lesions led us to identify the 'don't eat me' signal

CD47 as a target of miRNA-mediated regulation. This extends the current concepts of multiple sclerosis lesion activity to the level of miRNA mediated gene regulation. Our observations may have broad implications for the regulation of macrophage activation in autoimmune and inflammatory diseases in general.

When we matched the miRNAs that are upregulated in active multiple sclerosis lesions with the pattern of transcripts that are downregulated in active multiple sclerosis lesions (own data), we noted that eight miRNAs found to be upregulated in active multiple sclerosis lesions are predicted to target CD47, which was one of the down-regulated transcripts in the active lesions in

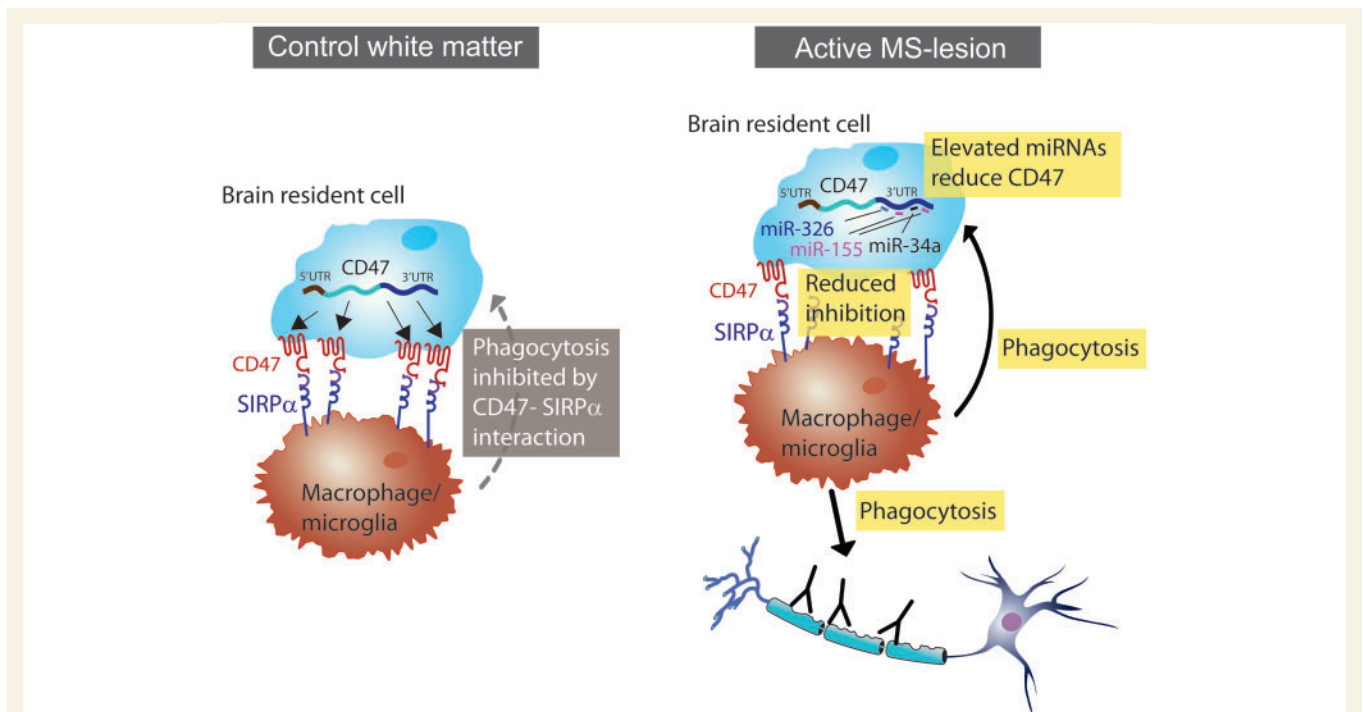


Figure 5 Hypothetical model of miRNA-regulated macrophage activity in multiple sclerosis lesions. In active multiple sclerosis (MS) lesions miRNA-155, miRNA-34a and miRNA-326 are upregulated in comparison with control white matter. These miRNAs target the 3'UTR of CD47 and might thereby reduce CD47 expression. These CD47-regulating miRNAs were found in astrocytes. Their expression in other brain resident cells needs to be explored. Reduced expression of CD47 might release macrophages/microglia from inhibitory control normally mediated by interaction of signal regulatory protein (SIRP)- α on macrophages/microglia with CD47 on potential targets. Reduced signalling via signal regulatory protein- α might then promote phagocytosis of CD47^{low} target cells, and possibly also of susceptible bystander cells, e.g. oligodendrocytes. 'Unleashed' phagocytosis will be directed particularly against opsonized (e.g. antibody-coated) targets, because reduced CD47 is known to promote phagocytosis of antibody-coated cells.

comparison to normal brain white matter. *In vitro* testing of these predicted binding sites revealed that miR-34a, miR-155 and miR-326 indeed target the 3'UTR of CD47, with miR-155 even at two sites. Notably, these three identified miRNA regulators of CD47 were among the 10 most strongly induced miRNAs in active multiple sclerosis lesions.

CD47 is ubiquitously expressed and can mediate multiple functions (Barclay, 2009; Matozaki *et al.*, 2009). It interacts in *cis* with integrins (hence its previous name, integrin activating protein, IAP) and in *trans* with the extracellular matrix molecule thrombospondin-1 and signal regulatory protein- α (CD172a), which is found on macrophages and dendritic cells. CD47 inhibits the phagocytic activity of macrophages (Oldenburg *et al.*, 2000; Yamao *et al.*, 2002; Ishikawa-Sekigami *et al.*, 2006) and cytokine production of dendritic cells via signal regulatory protein- α (Latour *et al.*, 2001). Owing to its inhibitory effect on macrophages, CD47 has been considered as a 'don't eat me signal' and as a 'marker of self' (Oldenburg *et al.*, 2000; Yamao *et al.*, 2002). In some apoptotic cells, CD47 is lost and the reduced level of this 'don't eat me' signal entitles macrophages to engulf these apoptotic cells (Gardai *et al.*, 2005). The importance of CD47 as a marker of self is also supported by the observation that interspecies incompatibilities of CD47 contribute to the rejection of xenogeneic grafts by macrophages (Ide *et al.*, 2007). The biological importance of

macrophage inhibition by CD47 is further highlighted by the fact that most poxviruses encode a CD47 homologue. In the case of myxomavirus, it was shown that the viral CD47 homologue is a virulence factor acting by inhibition of macrophages (Cameron *et al.*, 2005).

The interaction of CD47 with signal regulatory protein- α on macrophages blocks Immunoglobulin G or complement-induced phagocytosis indicating a protective role of CD47 in immunopathology (Oldenburg *et al.*, 2001). Beyond this, expression of CD47 on haematopoietic stem cells, leukaemia cells or other tumour cells leads to prevention of phagocytosis (Blazar *et al.*, 2001; Chan *et al.*, 2009; Jaiswal *et al.*, 2009; Majeti *et al.*, 2009). CD47 expression is reduced in active multiple sclerosis lesions as shown in this study and by Koning *et al.* (2007). Active lesions are defined by the presence of myelin degradation products in macrophages, and phagocytosis of myelin by activated macrophages/microglia is a crucial step in tissue destruction in multiple sclerosis (Ozawa *et al.*, 1994).

We propose that the local up-regulation of the three miRNAs miR-34a, miR-155 and miR-326 in active multiple sclerosis lesions is linked to the local down-regulation of CD47 on brain resident cells, thereby unleashing macrophages for tissue destruction (Fig. 5). As shown here, CD47 is expressed by both astrocytes and myelin. The expression of CD47 on myelin indeed suggests

that this directly regulates phagocytosis. Typically macrophages specifically select their target (frequently opsonized by complement or Ig). CD47 also regulates the phagocytosis of opsonized cells (Oldenborg *et al.*, 2002). Our work warrants further analysis of the local regulation of miRNAs in oligodendrocytes in active and newly forming multiple sclerosis lesions. The activation of phagocytosis by a disturbed CD47–signal regulatory protein- α interaction is not necessarily limited to a direct interaction of the phagocytes with their CD47 bearing target cells, but might also have an effect on bystander phagocytosis, since soluble CD47 reduces the phagocytosis of colloidal carriers (Hsu *et al.*, 2003). So it is also plausible that specific phagocytosis in multiple sclerosis lesions is enhanced by a reduced CD47 on bystander cells, e.g. astrocytes.

Owing to the multiple biological effects of CD47, including inhibition of macrophage activation (Oldenborg *et al.*, 2000, 2001; Yamao *et al.*, 2002; Gardai *et al.*, 2005; Ide *et al.*, 2007), extravasation (de Vries *et al.*, 2002) and T cell co-stimulation (Vallejo *et al.*, 2003; Piccio *et al.*, 2005), a simple CD47-deficient experimental autoimmune encephalomyelitis mouse model would not allow detailed conclusions. Cell-type-specific and/or conditional knockout mice could be used for experimental autoimmune encephalomyelitis models, but it is unclear whether this would reflect the human multiple sclerosis lesion environment. Additional mechanisms of CD47 regulation may add to the complexity. Surprisingly, despite the enormous biological importance of CD47 (Jaiswal *et al.*, 2009; Majeti *et al.*, 2009), details of its regulation are largely unknown. The three miRNAs we identify here provide some insight into the regulation of CD47 expression.

miRNAs typically repress target protein expression by less than 2-fold. It is therefore usually assumed that miRNA-mediated regulation is biologically relevant only if a 2-fold (down) regulation of the corresponding protein translates into biologically meaningful effects (Seitz, 2009). Indeed, CD47-dependent processes are sensitive to around 2-fold regulation, as seen by the dose dependency of macrophage uptake of immunoglobulin G-sensitized targets (Olsson *et al.*, 2007). CD47^{+/-} platelets and erythrocytes were more prone to phagocytosis than their wild-type counterparts (Olsson *et al.*, 2006, 2007). A recent paper (Jaiswal *et al.*, 2009) has shown that haematopoietic stem cells of such CD47^{+/-} mice express just half the amount of CD47 and are more prone to phagocytosis. This lends support to our model.

Our present findings demonstrate that miRNA levels in astrocytes are highly regulated in response to inflammatory cytokines. We could assign miRNAs that are induced in multiple sclerosis lesions to astrocytes: the 10 most strongly induced miRNAs in active lesions were expressed by astrocytes and three miRNAs could be induced in astrocytes by *in vitro* stimulation with inflammatory cytokines. Our study provides further evidence for an involvement of astrocytes in shaping the environment in multiple sclerosis lesions.

Considering that post-transcriptional regulation by miRNAs affects approximately one-third of all genes, one has to assume that many of the already published downregulated proteins or transcripts observed in multiple sclerosis lesions are actually regulated, or at least 'fine-tuned', by miRNAs. We would therefore expect that beyond our observations on CD47, several additional differentially regulated miRNAs identified in this work may explain

some other previous observations regarding transcript or protein regulation in multiple sclerosis lesions.

Therefore, we compared our miRNA profiles with previous microarray (Lock *et al.*, 2002) or proteome analyses (Han *et al.*, 2008) of multiple sclerosis tissue using Targetscan 5.0 for *in silico* searches (Lewis *et al.*, 2005; Grimson *et al.*, 2007). This revealed several interesting connections. For example, myocyte enhancer factor-2c, which is downregulated in multiple sclerosis lesions (Lock *et al.*, 2002), is a predicted target of three miRNAs (miR-23a, miR-223 and miR-27) that we found to be upregulated in active multiple sclerosis lesions. Myocyte enhancer factor-2c, a transcription factor that promotes (among other features) myeloid progenitor proliferation, is a proven target of miR-223 (Johnnidis *et al.*, 2008). Furthermore, microtubule-associated protein 1b is downregulated in active multiple sclerosis lesions (Han *et al.*, 2008) and is a predicted target of miR-130a and miR-27a, which are identified here in our miRNA signature. Microtubule-associated protein 1b is one of the major growth-associated and cytoskeletal proteins in neuronal and glial cells (Riederer, 2007).

While the implications of these proven or predicted interactions for multiple sclerosis lesion development need to be established, our miRNA profiles might explain another earlier observation related to macrophage activation: using *in situ* hybridization it has been noted that colony-stimulating factor receptor 1 was downregulated in macrophages/microglia in active multiple sclerosis lesions as compared to adjacent normal white matter (Werner *et al.*, 2002). Our finding that miR-155 is upregulated in active multiple sclerosis lesions, along with the previous finding that colony-stimulating factor receptor 1 is a proven target of miR-155 (O'Connell *et al.*, 2008), now suggests a mechanism that might at least contribute to the loss of colony-stimulating factor receptor 1 in active multiple sclerosis lesions.

In conclusion, we present miRNA signatures of active and inactive brain lesions of patients with multiple sclerosis. Our finding that three of the most upregulated miRNAs in multiple sclerosis lesions target CD47 extends the concept of tissue destruction in multiple sclerosis lesions to the level of miRNA-regulated gene expression. We postulate that downregulation of CD47 by miR-34a, miR-155 and miR-326 in the lesion environment releases macrophages/microglia from inhibitory control. This promotes myelin phagocytosis, the pathological hallmark of active multiple sclerosis lesions. Targeting these miRNAs might represent a promising therapeutic strategy to calm down lesion activity. Because of the ubiquitous expression of CD47 and its critical role in self-recognition and macrophage activation, our results may have implications for other immunopathological conditions.

Note added in proof

After this paper was accepted, miR-326 was reported to be higher in peripheral blood leukocytes of MS patients and to regulate TH-17 differentiation (Du *et al.* 2009). We found that this miRNA was one of the three most up-regulated miRNAs in active MS lesions (Table 1) lending further support to the relevance of this miRNA for MS pathogenesis.

Acknowledgements

We thank Drs Inga Sinicina, Wolfgang Eisenmenger and Kerstin Berer for valuable support, and Drs Dieter Jenne and Martin Kerschensteiner for helpful comments on the manuscript. We are grateful to Nancy Meyer for useful discussions and help with molecular cloning techniques. We thank Dr Francesca Aloisi for providing primary human astrocyte cultures and Robert Schorner for assistance with Figure 5. We thank the Netherlands Brain Bank and the UK MS Tissue Bank for providing tissue samples. The authors have no conflicting financial interests.

Funding

Deutsche Forschungsgemeinschaft (grants SFB 571-A1 and -C3); Verein zur Therapieforchung für Multiple Sclerosis –Kranke; Friedrich Baur Stiftung; and the Hermann und Lilly Schilling Foundation.

Supplementary material

Supplementary material is available at *Brain* online.

References

- Aloisi F, Borsellino G, Samoggia P, Testa U, Chelucci C, Russo G, et al. Astrocyte cultures from human embryonic brain: characterization and modulation of surface molecules by inflammatory cytokines. *J Neurosci Res* 1992; 32: 494–506.
- Baek D, Villen J, Shin C, Camargo FD, Gygi SP, Bartel DP. The impact of microRNAs on protein output. *Nature* 2008; 455: 64–71.
- Barclay AN. Signal regulatory protein alpha (SIRPalpha)/CD47 interaction and function. *Curr Opin Immunol* 2009; 21: 47–52.
- Blazar BR, Lindberg FP, Ingulli E, Panoskaltis-Mortari A, Oldenborg PA, Iizuka K, et al. CD47 (integrin-associated protein) engagement of dendritic cell and macrophage counterreceptors is required to prevent the clearance of donor lymphohematopoietic cells. *J Exp Med* 2001; 194: 541–9.
- Cameron CM, Barrett JW, Mann M, Lucas A, McFadden G. Myxoma virus M128L is expressed as a cell surface CD47-like virulence factor that contributes to the downregulation of macrophage activation in vivo. *Virology* 2005; 337: 55–67.
- Chan KS, Espinosa I, Chao M, Wong D, Ailles L, Diehn M, et al. Identification, molecular characterization, clinical prognosis, and therapeutic targeting of human bladder tumor-initiating cells. *Proc Natl Acad Sci USA* 2009; 106: 14016–21.
- Czech MP. MicroRNAs as therapeutic targets. *N Engl J Med* 2006; 354: 1194–5.
- de Vries HE, Hendriks JJ, Honing H, De Lavalette CR, van der Pol SM, Hooijberg E, et al. Signal-regulatory protein alpha-CD47 interactions are required for the transmigration of monocytes across cerebral endothelium. *J Immunol* 2002; 168: 5832–9.
- Doleshal M, Magotra AA, Choudhury B, Cannon BD, Labourier E, Szafranska AE. Evaluation and validation of total RNA extraction methods for microRNA expression analyses in formalin-fixed, paraffin-embedded tissues. *J Mol Diagn* 2008; 10: 203–11.
- Du C, Liu C, Kang J, Zhao G, Ye Z, Huang S, et al. MicroRNA miR-326 regulates T(H)-17 differentiation and is associated with the pathogenesis of multiple sclerosis. *Nat Immunol* 2009, publisher online 18 October 2009; doi:10.1038/ni.1798 [Epub ahead of print].
- Elmen J, Lindow M, Schutz S, Lawrence M, Petri A, Obad S, et al. LNA-mediated microRNA silencing in non-human primates. *Nature* 2008; 452: 896–9.
- Fugger L, Friese MA, Bell JI. From genes to function: the next challenge to understanding multiple sclerosis. *Nat Rev Immunol* 2009; 9: 408–417.
- Gardai SJ, McPhillips KA, Frasch SC, Janssen WJ, Starefeldt A, Murphy-Ullrich JE, et al. Cell-surface calreticulin initiates clearance of viable or apoptotic cells through trans-activation of LRP on the phagocyte. *Cell* 2005; 123: 321–34.
- Goverman J. Autoimmune T cell responses in the central nervous system. *Nat Rev Immunol* 2009; 9: 393–407.
- Grimson A, Farh KK, Johnston WK, Garrett-Engele P, Lim LP, Bartel DP. MicroRNA targeting specificity in mammals: determinants beyond seed pairing. *Mol Cell* 2007; 27: 91–105.
- Han MH, Hwang SI, Roy DB, Lundgren DH, Price JV, Ousman SS, et al. Proteomic analysis of active multiple sclerosis lesions reveals therapeutic targets. *Nature* 2008; 451: 1076–81.
- Hebert SS, De SB. Alterations of the microRNA network cause neurodegenerative disease. *Trends Neurosci* 2009; 32: 199–206.
- Hsu YC, Acuna M, Tahara SM, Peng CA. Reduced phagocytosis of colloidal carriers using soluble CD47. *Pharm Res* 2003; 20: 1539–42.
- Ide K, Wang H, Tahara H, Liu J, Wang X, Asahara T, et al. Role for CD47-SIRPalpha signaling in xenograft rejection by macrophages. *Proc Natl Acad Sci U S A* 2007; 20:104: 5062–6.
- Ishikawa-Sekigami T, Kaneko Y, Okazawa H, Tomizawa T, Okajo J, Saito Y, et al. SHPS-1 promotes the survival of circulating erythrocytes through inhibition of phagocytosis by splenic macrophages. *Blood* 2006; 107: 341–8.
- Jaiswal S, Jamieson CH, Pang WW, Park CY, Chao MP, Majeti R, et al. CD47 is upregulated on circulating hematopoietic stem cells and leukemia cells to avoid phagocytosis. *Cell* 2009; 138: 271–85.
- Johnnidis JB, Harris MH, Wheeler RT, Stehling-Sun S, Lam MH, Kirak O, et al. Regulation of progenitor cell proliferation and granulocyte function by microRNA-223. *Nature* 2008; 451: 1125–9.
- Junker A, Ivanidze J, Malotka J, Eiglmeier I, Lassmann H, Wekerle H, et al. Multiple sclerosis: T-cell receptor expression in distinct brain regions. *Brain* 2007; 130: 2789–99.
- Koning N, Bo L, Hoek RM, Huitinga I. Downregulation of macrophage inhibitory molecules in multiple sclerosis lesions. *Ann Neurol* 2007; 62: 504–14.
- Kosik KS. The neuronal microRNA system. *Nat Rev Neurosci* 2006; 7: 911–20.
- Krumbholz M, Theil D, Derfuss T, Rosenwald A, Schrader F, Monoranu CM, et al. BAFF is produced by astrocytes and up-regulated in multiple sclerosis lesions and primary central nervous system lymphoma. *J Exp Med* 2005; 201: 195–200.
- Krutzfeldt J, Rajewsky N, Braich R, Rajeev KG, Tuschl T, Manoharan M, et al. Silencing of microRNAs in vivo with 'antagomirs'. *Nature* 2005; 438: 685–9.
- Latour S, Tanaka H, Demeure C, Mateo V, Rubio M, Brown EJ, et al. Bidirectional negative regulation of human T and dendritic cells by CD47 and its cognate receptor signal-regulator protein-alpha: down-regulation of IL-12 responsiveness and inhibition of dendritic cell activation. *J Immunol* 2001; 167: 2547–54.
- Lewis BP, Burge CB, Bartel DP. Conserved seed pairing, often flanked by adenosines, indicates that thousands of human genes are microRNA targets. *Cell* 2005; 120: 15–20.
- Lock C, Hermans G, Pedotti R, Brendolan A, Schadt E, Garren H, et al. Gene-microarray analysis of multiple sclerosis lesions yields new targets validated in autoimmune encephalomyelitis. *Nat Med* 2002; 8: 500–8.
- Lodish HF, Zhou B, Liu G, Chen CZ. Micromanagement of the immune system by microRNAs. *Nat Rev Immunol* 2008; 8: 120–30.
- Majeti R, Chao MP, Alizadeh AA, Pang WW, Jaiswal S, Gibbs KD Jr, et al. CD47 is an adverse prognostic factor and therapeutic antibody target on human acute myeloid leukemia stem cells. *Cell* 2009; 138: 286–99.

- Matozaki T, Murata Y, Okazawa H, Ohnishi H. Functions and molecular mechanisms of the CD47-SIRPalpha signalling pathway. *Trends Cell Biol* 2009; 19: 72–80.
- Ng EK, Chong WW, Jin H, Lam EK, Shin VY, Yu J, et al. Differential expression of microRNAs in plasma of patients with colorectal cancer: A potential marker for colorectal cancer screening. *Gut* 2009; 58: 1375–81.
- O'Connell RM, Rao DS, Chaudhuri AA, Boldin MP, Taganov KD, Nicoll J, et al. Sustained expression of microRNA-155 in hematopoietic stem cells causes a myeloproliferative disorder. *J Exp Med* 2008; 205: 585–94.
- Oldenberg PA, Gresham HD, Chen Y, Izui S, Lindberg FP. Lethal autoimmune hemolytic anemia in CD47-deficient nonobese diabetic (NOD) mice. *Blood* 2002; 99: 3500–4.
- Oldenberg PA, Gresham HD, Lindberg FP. CD47-signal regulatory protein alpha (SIRPalpha) regulates Fcgamma and complement receptor-mediated phagocytosis. *J Exp Med* 2001; 193: 855–62.
- Oldenberg PA, Zheleznyak A, Fang YF, Lagenaur CF, Gresham HD, Lindberg FP. Role of CD47 as a marker of self on red blood cells. *Science* 2000; 288: 2051–4.
- Olsson M, Nilsson A, Oldenberg PA. Dose-dependent inhibitory effect of CD47 in macrophage uptake of IgG-opsonized murine erythrocytes. *Biochem Biophys Res Commun* 2007; 352: 193–7.
- Ozawa K, Suchanek G, Breitschopf H, Bruck W, Budka H, Jellinger K, et al. Patterns of oligodendroglia pathology in multiple sclerosis. *Brain* 1994; 117: 1311–22.
- Papagiannakopoulos T, Kosik KS. MicroRNAs: regulators of oncogenesis and stemness. *BMC Med* 2008; 6: 15.
- Piccio L, Vermi W, Boles KS, Fuchs A, Strader CA, Facchetti F, et al. Adhesion of human T cells to antigen-presenting cells through SIRPbeta2-CD47 interaction costimulates T-cell proliferation. *Blood* 2005; 105: 2421–7.
- Riederer BM. Microtubule-associated protein 1B, a growth-associated and phosphorylated scaffold protein. *Brain Res Bull* 2007; 71: 541–58.
- Rodriguez A, Vigorito E, Clare S, Warren MV, Couttet P, Soond DR, et al. Requirement of bic/microRNA-155 for normal immune function. *Science* 2007; 316: 608–11.
- Sasaki A, Levison SW, Ting JP. Comparison and quantitation of Ia antigen expression on cultured macroglia and amoeboid microglia from Lewis rat cerebral cortex: analyses and implications. *J Neuroimmunol* 1989; 25: 63–74.
- Seitz H. Redefining microRNA targets. *Curr Biol* 2009; 19: 870–3.
- Selbach M, Schwanhauser B, Thierfelder N, Fang Z, Khanin R, Rajewsky N. Widespread changes in protein synthesis induced by microRNAs. *Nature* 2008; 455: 58–63.
- Sospedra M, Martin R. Immunology of multiple sclerosis. *Annu Rev Immunol* 2005; 23: 683–747.
- Steinman L. A molecular trio in relapse and remission in multiple sclerosis. *Nat Rev Immunol* 2009; 9: 440–7.
- Taganov KD, Boldin MP, Baltimore D. MicroRNAs and immunity: tiny players in a big field. *Immunity* 2007; 26: 133–7.
- Thai TH, Calado DP, Casola S, Ansel KM, Xiao C, Xue Y, et al. Regulation of the germinal center response by microRNA-155. *Science* 2007; 316: 604–8.
- Thum T, Gross C, Fiedler J, Fischer T, Kissler S, Bussen M, et al. MicroRNA-21 contributes to myocardial disease by stimulating MAP kinase signalling in fibroblasts. *Nature* 2008; 456: 980–4.
- Trapp BD, Nave KA. Multiple sclerosis: an immune or neurodegenerative disorder? *Annu Rev Neurosci* 2008; 31: 247–69.
- Vallejo AN, Yang H, Klimiuk PA, Weyand CM, Goronzy JJ. Synovium-mediated expansion of inflammatory T cells in rheumatoid synovitis is dependent on CD47-thrombospondin 1 interaction. *J Immunol* 2003; 171: 1732–40.
- Visone R, Croce CM. MiRNAs and cancer. *Am J Pathol* 2009; 174: 1131–8.
- Werner K, Bitsch A, Bunkowski S, Hemmerlein B, Bruck W. The relative number of macrophages/microglia expressing macrophage colony-stimulating factor and its receptor decreases in multiple sclerosis lesions. *Glia* 2002; 40: 121–9.
- Yamao T, Noguchi T, Takeuchi O, Nishiyama U, Morita H, Hagiwara T, et al. Negative regulation of platelet clearance and of the macrophage phagocytic response by the transmembrane glycoprotein SHPS-1. *J Biol Chem* 2002; 277: 39833–9.

5 Abbreviations

AGC1	Aggrecan
BCAN	Brevican
BGN	Biglycan
COL	Collagen
CSPG	Chondroitin sulfate proteoglycan
DCN	Decorin
ECM	Extracellular matrix
FFPE	Formalin fixed and paraffin embedded
FMOD	Fibromodulin
FN1	Fibronectin
GAPDH	Glyceraldehydes 3-phosphate dehydrogenase
GM	Grey matter
HAPLN	Hyaluronan and proteoglycan link protein
HSPG	Heparin sulfate proteoglycan
LAM	Laminin
LDA	Low density array
MiRNA	micro ribonucleic acid
MMP	Matrix metalloproteinase
MS	Multiple sclerosis
NAWM	Normal appearing white matter
PPIA	Peptidyl-prolyl isomerase A (=cyclophilin A)
QPCR	Quantitative polymerase chain reaction
RELN	Reelin
RNA	Ribonucleic Acid
RT	Reverse transcription
SLRP	Small leucine rich proteoglycan
WM	White matter

6 References

1. Abrahamsen HN, Steiniche T, Nexø E, Hamilton-Dutoit SJ, Sørensen BS (2003) Towards quantitative mRNA analysis in paraffin-embedded tissues using real-time reverse transcriptase-polymerase chain reaction: a methodological study on lymph nodes from melanoma patients. *J Mol Diagn.*5(1):34-41.
2. Allen IV, McKeown SR (1979) A histological, histochemical and biochemical study of the macroscopically normal white matter in multiple sclerosis. *J Neurol Sci.*41(1):81-91.
3. Avolio C, Ruggieri M, Giuliani F, Liuzzi GM, Leante R, Riccio P, Livrea P, Trojano M (2003) Serum MMP-2 and MMP-9 are elevated in different multiple sclerosis subtypes. *J Neuroimmunol.*136(1-2):46-53.
4. Babinski J (1885) *Etude anatomique et clinique sur la sclérose en plaques*, A. Parent: Paris.
5. Bitsch A, Schuchardt J, Bunkowski S, Kuhlmann T, Brück W (2000) Acute axonal injury in multiple sclerosis. Correlation with demyelination and inflammation. *Brain.*123 (Pt 6):1174-1183.
6. Bo L, Vedeler CA, Nyland H, Trapp BD, Mork SJ (2003) Intracortical multiple sclerosis lesions are not associated with increased lymphocyte infiltration. *Mult Scler.*9(4):323-331.
7. Bo L, Vedeler CA, Nyland HI, Trapp BD, Mork SJ (2003) Subpial demyelination in the cerebral cortex of multiple sclerosis patients. *J Neuropathol Exp Neurol.*62(7):723-732.
8. Booss J, Esiri MM, Tourtellotte WW, Mason DY (1983) Immunohistological analysis of T lymphocyte subsets in the central nervous system in chronic progressive multiple sclerosis. *J Neurol Sci.*62(1-3):219-232.
9. Bourneville DaG, L. (1869) *De la sclérose en plaques disséminées: Nouvelles études sur quelques points de la sclérose en plaques disséminées* par Bourneville, A. Delahaye: Paris.
10. Breij EC, Brink BP, Veerhuis R, van den Berg C, Vloet R, Yan R, Dijkstra CD, van der Valk P, Bo L (2008) Homogeneity of active demyelinating lesions in established multiple sclerosis. *Ann Neurol.*63(1):16-25.
11. Bresters D, Cuypers HT, Reesink HW, Chamuleau RA, Schipper ME, Boeser-Nunnink BD, Lelie PN, Jansen PL (1992) Detection of hepatitis C viral RNA sequences in fresh and paraffin-embedded liver biopsy specimens of non-A, non-B hepatitis patients. *J Hepatol.*15(3):391-395.
12. Brownell B, Hughes JT (1962) The distribution of plaques in the cerebrum in multiple sclerosis. *J Neurol Neurosurg Psychiatry.*25:315-320.

13. Cannella B, Raine CS (1995) The adhesion molecule and cytokine profile of multiple sclerosis lesions. *Ann Neurol.*37(4):424-435.
14. Chabas D, Baranzini SE, Mitchell D, Bernard CC, Rittling SR, Denhardt DT, Sobel RA, Lock C, Karpuj M, Pedotti R, Heller R, Oksenberg JR, Steinman L (2001) The influence of the proinflammatory cytokine, osteopontin, on autoimmune demyelinating disease. *Science.*294(5547):1731-1735.
15. Charcot JM (1868) *Histologie de la sclérose en plaques.* Gazette des Hopitaux.
16. Charcot JM (1877) *Lectures on the diseases of the nervous system delivered at La Sâlpêtrière (translated from French),* The New Sydenham Society: London.
17. Cronin M, Pho M, Dutta D, Stephans JC, Shak S, Kiefer MC, Esteban JM, Baker JB (2004) Measurement of gene expression in archival paraffin-embedded tissues: development and performance of a 92-gene reverse transcriptase-polymerase chain reaction assay. *Am J Pathol.*164(1):35-42.
18. Cruveilhier J (1829-1842) *L'Anatomie pathologique du corps humain; descriptions avec figures lithographiées et coloriées: diverses alterations morbides dont le corps humain est susceptible,* J.B. Bailliere, Paris (two volume folio).
19. Cummings TJ, Strum JC, Yoon LW, Szymanski MH, Hulette CM (2001) Recovery and expression of messenger RNA from postmortem human brain tissue. *Mod Pathol.*14(11):1157-1161.
20. Cuzner ML, Opdenakker G (1999) Plasminogen activators and matrix metalloproteases, mediators of extracellular proteolysis in inflammatory demyelination of the central nervous system. *J Neuroimmunol.*94(1-2):1-14.
21. De Santis G, Ferracin M, Biondani A, Caniatti L, Rosaria Tola M, Castellazzi M, Zagatti B, Battistini L, Borsellino G, Fainardi E, Gavioli R, Negrini M, Furlan R, Granieri E (2010) Altered miRNA expression in T regulatory cells in course of multiple sclerosis. *J Neuroimmunol.*226(1-2):165-171.
22. Du C, Liu C, Kang J, Zhao G, Ye Z, Huang S, Li Z, Wu Z, Pei G (2009) MicroRNA miR-326 regulates TH-17 differentiation and is associated with the pathogenesis of multiple sclerosis. *Nat Immunol.*10(12):1252-1259.
23. Eisele S, Krumbholz M, Fischer MT, Mohan H, Junker A, Arzberger T, Hohlfeld R, Bradl M, Lassmann H, Meinl E (2012) Prospects of Transcript Profiling for mRNAs and MicroRNAs Using Formalin-Fixed and Paraffin-Embedded Dissected Optic Multiple Sclerosis Lesions. *Brain Pathol.* 10.1111/j.1750-3639.2012.00564.x epub ahead of print
24. Esiri MM (1977) Immunoglobulin-containing cells in multiple-sclerosis plaques. *Lancet.*2(8036):478.

25. Evangelou N, Konz D, Esiri MM, Smith S, Palace J, Matthews PM (2000) Regional axonal loss in the corpus callosum correlates with cerebral white matter lesion volume and distribution in multiple sclerosis. *Brain*.123 (Pt 9):1845-1849.
26. Ferguson B, Matyszak MK, Esiri MM, Perry VH (1997) Axonal damage in acute multiple sclerosis lesions. *Brain*.120 (Pt 3):393-399.
27. Filippi M, Bozzali M, Rovaris M, Gonen O, Kesavadas C, Ghezzi A, Martinelli V, Grossman RI, Scotti G, Comi G, Falini A (2003) Evidence for widespread axonal damage at the earliest clinical stage of multiple sclerosis. *Brain*.126(Pt 2):433-437.
28. Filippi M, Rocca MA, Martino G, Horsfield MA, Comi G (1998) Magnetization transfer changes in the normal appearing white matter precede the appearance of enhancing lesions in patients with multiple sclerosis. *Ann Neurol*.43(6):809-814.
29. Finke J, Fritzen R, Ternes P, Lange W, Dolken G (1993) An improved strategy and a useful housekeeping gene for RNA analysis from formalin-fixed, paraffin-embedded tissues by PCR. *Biotechniques*.14(3):448-453.
30. Fraenkel M. JA (1913) Zur Pathologie der multiplen Sklerose mit besonderer Berücksichtigung der akuten Formen. *Z Neurol.* (14):565-603.
31. Ganter P, Prince C, Esiri MM (1999) Spinal cord axonal loss in multiple sclerosis: a post-mortem study. *Neuropathol Appl Neurobiol*.25(6):459-467.
32. Gay FW, Drye TJ, Dick GW, Esiri MM (1997) The application of multifactorial cluster analysis in the staging of plaques in early multiple sclerosis. Identification and characterization of the primary demyelinating lesion. *Brain*.120 (Pt 8):1461-1483.
33. Godfrey TE, Kim SH, Chavira M, Ruff DW, Warren RS, Gray JW, Jensen RH (2000) Quantitative mRNA expression analysis from formalin-fixed, paraffin-embedded tissues using 5' nuclease quantitative reverse transcription-polymerase chain reaction. *J Mol Diagn*.2(2):84-91.
34. Gruber AD, Greiser-Wilke IM, Haas L, Hewicker-Trautwein M, Moennig V (1993) Detection of bovine viral diarrhea virus RNA in formalin-fixed, paraffin-embedded brain tissue by nested polymerase chain reaction. *J Virol Methods*.43(3):309-319.
35. Gutowski NJ, Newcombe J, Cuzner ML (1999) Tenascin-R and C in multiple sclerosis lesions: relevance to extracellular matrix remodelling. *Neuropathol Appl Neurobiol*.25(3):207-214.
36. Han MH, Hwang SI, Roy DB, Lundgren DH, Price JV, Ousman SS, Fernald GH, Gerlitz B, Robinson WH, Baranzini SE, Grinnell BW, Raine CS, Sobel RA, Han DK, Steinman L (2008) Proteomic analysis of active multiple sclerosis lesions reveals therapeutic targets. *Nature*.451(7182):1076-1081.

37. Hirsch CS, Ellner JJ, Blinkhorn R, Toossi Z (1997) In vitro restoration of T cell responses in tuberculosis and augmentation of monocyte effector function against *Mycobacterium tuberculosis* by natural inhibitors of transforming growth factor beta. *Proc Natl Acad Sci U S A*.94(8):3926-3931.
38. Huang D, Han Y, Rani MR, Glabinski A, Trebst C, Sorensen T, Tani M, Wang J, Chien P, O'Bryan S, Bielecki B, Zhou ZL, Majumder S, Ransohoff RM (2000) Chemokines and chemokine receptors in inflammation of the nervous system: manifold roles and exquisite regulation. *Immunol Rev*.177:52-67.
39. Iozzo RV (1997) The family of the small leucine-rich proteoglycans: key regulators of matrix assembly and cellular growth. *Crit Rev Biochem Mol Biol*.32(2):141-174.
40. Jackson DP, Quirke P, Lewis F, Boylston AW, Sloan JM, Robertson D, Taylor GR (1989) Detection of measles virus RNA in paraffin-embedded tissue. *Lancet*.1(8651):1391.
41. Johnson SA, Morgan DG, Finch CE (1986) Extensive postmortem stability of RNA from rat and human brain. *J Neurosci Res*.16(1):267-280.
42. Junker A, Krumbholz M, Eisele S, Mohan H, Augstein F, Bittner R, Lassmann H, Wekerle H, Hohlfeld R, Meinl E (2009) MicroRNA profiling of multiple sclerosis lesions identifies modulators of the regulatory protein CD47. *Brain*.132(Pt 12):3342-3352.
43. Kidd D, Barkhof F, McConnell R, Algra PR, Allen IV, Revesz T (1999) Cortical lesions in multiple sclerosis. *Brain*.122 (Pt 1):17-26.
44. Kingsbury AE, Foster OJ, Nisbet AP, Cairns N, Bray L, Eve DJ, Lees AJ, Marsden CD (1995) Tissue pH as an indicator of mRNA preservation in human post-mortem brain. *Brain Res Mol Brain Res*.28(2):311-318.
45. Kornek B, Storch MK, Weissert R, Wallstroem E, Stefferl A, Olsson T, Linington C, Schmidbauer M, Lassmann H (2000) Multiple sclerosis and chronic autoimmune encephalomyelitis: a comparative quantitative study of axonal injury in active, inactive, and remyelinated lesions. *Am J Pathol*.157(1):267-276.
46. Krumbholz M, Theil D, Derfuss T, Rosenwald A, Schrader F, Monoranu CM, Kalled SL, Hess DM, Serafini B, Aloisi F, Wekerle H, Hohlfeld R, Meinl E (2005) BAFF is produced by astrocytes and up-regulated in multiple sclerosis lesions and primary central nervous system lymphoma. *J Exp Med*.201(2):195-200.
47. Kuhlmann T, Lingfeld G, Bitsch A, Schuchardt J, Bruck W (2002) Acute axonal damage in multiple sclerosis is most extensive in early disease stages and decreases over time. *Brain*.125(Pt 10):2202-2212.
48. Kutzelnigg A, Lassmann H (2005) Cortical lesions and brain atrophy in MS. *J Neurol Sci*.233(1-2):55-59.

49. Kutzelnigg A, Lucchinetti CF, Stadelmann C, Bruck W, Rauschka H, Bergmann M, Schmidbauer M, Parisi JE, Lassmann H (2005) Cortical demyelination and diffuse white matter injury in multiple sclerosis. *Brain*.128(Pt 11):2705-2712.
50. Lassmann H (1983) Comparative neuropathology of chronic experimental allergic encephalomyelitis and multiple sclerosis. *Schriftenr Neurol*.25:1-135.
51. Lehmann U, Glockner S, Kleeberger W, von Wasielewski HF, Kreipe H (2000) Detection of gene amplification in archival breast cancer specimens by laser-assisted microdissection and quantitative real-time polymerase chain reaction. *Am J Pathol*.156(6):1855-1864.
52. Li J, Smyth P, Cahill S, Denning K, Flavin R, Aherne S, Pirotta M, Guenther SM, O'Leary JJ, Sheils O (2008) Improved RNA quality and TaqMan Pre-amplification method (PreAmp) to enhance expression analysis from formalin fixed paraffin embedded (FFPE) materials. *BMC Biotechnol*.8:10.
53. Lindberg RL, Hoffmann F, Mehling M, Kuhle J, Kappos L (2010) Altered expression of miR-17-5p in CD4+ lymphocytes of relapsing-remitting multiple sclerosis patients. *Eur J Immunol*.40(3):888-898.
54. Lisowski AR, English ML, Opsahl AC, Bunch RT, Blomme EA (2001) Effect of the storage period of paraffin sections on the detection of mRNAs by in situ hybridization. *J Histochem Cytochem*.49(7):927-928.
55. Lock C, Hermans G, Pedotti R, Brendolan A, Schadt E, Garren H, Langer-Gould A, Strober S, Cannella B, Allard J, Klonowski P, Austin A, Lad N, Kaminski N, Galli SJ, Oksenberg JR, Raine CS, Heller R, Steinman L (2002) Gene-microarray analysis of multiple sclerosis lesions yields new targets validated in autoimmune encephalomyelitis. *Nat Med*.8(5):500-508.
56. Lucchinetti C, Bruck W, Parisi J, Scheithauer B, Rodriguez M, Lassmann H (2000) Heterogeneity of multiple sclerosis lesions: implications for the pathogenesis of demyelination. *Ann Neurol*.47(6):707-717.
57. Lucchinetti CF, Popescu BF, Bunyan RF, Moll NM, Roemer SF, Lassmann H, Bruck W, Parisi JE, Scheithauer BW, Giannini C, Weigand SD, Mandrekar J, Ransohoff RM (2011) Inflammatory cortical demyelination in early multiple sclerosis. *N Engl J Med*.365(23):2188-2197.
58. Luster AD (1998) Chemokines--chemotactic cytokines that mediate inflammation. *N Engl J Med*.338(7):436-445.
59. Margolis RU, Margolis RK (1994) Aggrecan-versican-neurocan family proteoglycans. *Methods Enzymol*.245:105-126.
60. Masuda N, Ohnishi T, Kawamoto S, Monden M, Okubo K (1999) Analysis of chemical modification of RNA from formalin-fixed samples and optimization of molecular biology applications for such samples. *Nucleic Acids Res*.27(22):4436-4443.

61. Mohan H, Krumbholz M, Sharma R, Eisele S, Junker A, Sixt M, Newcombe J, Wekerle H, Hohlfeld R, Lassmann H, Meinl E (2010) Extracellular matrix in multiple sclerosis lesions: Fibrillar collagens, biglycan and decorin are upregulated and associated with infiltrating immune cells. *Brain Pathol.*20(5):966-975.
62. Nelson PT, Baldwin DA, Scarce LM, Oberholtzer JC, Tobias JW, Mourelatos Z (2004) Microarray-based, high-throughput gene expression profiling of microRNAs. *Nat Methods.*1(2):155-161.
63. Novak U, Kaye AH (2000) Extracellular matrix and the brain: components and function. *J Clin Neurosci.*7(4):280-290.
64. Nyland H, Mork S, Matre R (1982) In-situ characterization of mononuclear cell infiltrates in lesions of multiple sclerosis. *Neuropathol Appl Neurobiol.*8(5):403-411.
65. Marburg O. (1906) Die sogenannte "akute Multiple Sklerose". *Jahrbücher für Psychiatrie* 2:211-312.
66. Oleszewski M, Beer S, Katich S, Geiger C, Zeller Y, Rauch U, Altevogt P (1999) Integrin and neurocan binding to L1 involves distinct Ig domains. *J Biol Chem.*274(35):24602-24610.
67. Park YN, Abe K, Li H, Hsuih T, Thung SN, Zhang DY (1996) Detection of hepatitis C virus RNA using ligation-dependent polymerase chain reaction in formalin-fixed, paraffin-embedded liver tissues. *Am J Pathol.*149(5):1485-1491.
68. Penland SK, Keku TO, Torrice C, He X, Krishnamurthy J, Hoadley KA, Woosley JT, Thomas NE, Perou CM, Sandler RS, Sharpless NE (2007) RNA expression analysis of formalin-fixed paraffin-embedded tumors. *Lab Invest.*87(4):383-391.
69. Peterson JW, Bo L, Mork S, Chang A, Trapp BD (2001) Transected neurites, apoptotic neurons, and reduced inflammation in cortical multiple sclerosis lesions. *Ann Neurol.*50(3):389-400.
70. Prineas JW, Kwon EE, Cho ES, Sharer LR (1984) Continual breakdown and regeneration of myelin in progressive multiple sclerosis plaques. *Ann N Y Acad Sci.*436:11-32.
71. Rauch U (2004) Extracellular matrix components associated with remodeling processes in brain. *Cell Mol Life Sci.*61(16):2031-2045.
72. Robinson WH, DiGennaro C, Hueber W, Haab BB, Kamachi M, Dean EJ, Fournel S, Fong D, Genovese MC, de Vegvar HE, Skriner K, Hirschberg DL, Morris RI, Muller S, Pruijn GJ, van Venrooij WJ, Smolen JS, Brown PO, Steinman L, Utz PJ (2002) Autoantigen microarrays for multiplex characterization of autoantibody responses. *Nat Med.*8(3):295-301.

73. Ruoslahti E (1996) Brain extracellular matrix. *Glycobiol.*6(5):489-492.
74. Schaefer L, Iozzo RV (2008) Biological functions of the small leucine-rich proteoglycans: from genetics to signal transduction. *J Biol Chem.*283(31):21305-21309.
75. Schramm M, Falkai P, Tepest R, Schneider-Axmann T, Przkora R, Waha A, Pietsch T, Bonte W, Bayer TA (1999) Stability of RNA transcripts in post-mortem psychiatric brains. *J Neural Transm.*106(3-4):329-335.
76. Sobel RA (2001) The extracellular matrix in multiple sclerosis: an update. *Braz J Med Biol Res.*34(5):603-609.
77. Specht K, Richter T, Muller U, Walch A, Werner M, Hofler H (2001) Quantitative gene expression analysis in microdissected archival formalin-fixed and paraffin-embedded tumor tissue. *Am J Pathol.*158(2):419-429.
78. Szafranska AE, Davison TS, Shingara J, Doleshal M, Riggenschach JA, Morrison CD, Jewell S, Labourier E (2008) Accurate molecular characterization of formalin-fixed, paraffin-embedded tissues by microRNA expression profiling. *J Mol Diagn.*10(5):415-423.
79. Trapp BD, Peterson J, Ransohoff RM, Rudick R, Mork S, Bo L (1998) Axonal transection in the lesions of multiple sclerosis. *N Engl J Med.*338(5):278-285.
80. Traugott U, Reinherz EL, Raine CS (1983) Multiple sclerosis: distribution of T cell subsets within active chronic lesions. *Science.*219(4582):308-310.
81. Viapiano MS, Matthews RT (2006) From barriers to bridges: chondroitin sulfate proteoglycans in neuropathology. *Trends Mol Med.*12(10):488-496.
82. von Weizsacker F, Labeit S, Koch HK, Oehlert W, Gerok W, Blum HE (1991) A simple and rapid method for the detection of RNA in formalin-fixed, paraffin-embedded tissues by PCR amplification. *Biochem Biophys Res Commun.*174(1):176-180.
83. Waddell N, Cocciardi S, Johnson J, Healey S, Marsh A, Riley J, da Silva L, Vargas AC, Reid L, Simpson PT, Lakhani SR, Chenevix-Trench G (2010) Gene expression profiling of formalin-fixed, paraffin-embedded familial breast tumours using the whole genome-DASL assay. *J Pathol.*221(4):452-461.
84. Wekerle H (1984) The lesion of acute experimental autoimmune encephalomyelitis. Isolation and membrane phenotypes of perivascular infiltrates from encephalitic rat brain white matter. *Lab Invest.*51(2):199-205.
85. Weng L, Wu X, Gao H, Mu B, Li X, Wang JH, Guo C, Jin JM, Chen Z, Covarrubias M, Yuan YC, Weiss LM, Wu H (2010) MicroRNA profiling of clear cell renal cell carcinoma by whole-genome small RNA deep sequencing of paired frozen and formalin-fixed, paraffin-embedded tissue specimens. *J Pathol.*222(1):41-51.

86. Xaus J, Comalada M, Cardo M, Valledor AF, Celada A (2001) Decorin inhibits macrophage colony-stimulating factor proliferation of macrophages and enhances cell survival through induction of p27(Kip1) and p21(Waf1). *Blood*.98(7):2124-2133.
87. Xi Y, Nakajima G, Gavin E, Morris CG, Kudo K, Hayashi K, Ju J (2007) Systematic analysis of microRNA expression of RNA extracted from fresh frozen and formalin-fixed paraffin-embedded samples. *RNA*.13(10):1668-1674.
88. Yamaguchi Y (2000) Lecticans: organizers of the brain extracellular matrix. *Cell Mol Life Sci*.57(2):276-289.
89. Yamaguchi Y, Mann DM, Ruoslahti E (1990) Negative regulation of transforming growth factor-beta by the proteoglycan decorin. *Nature*.346(6281):281-284.
90. Yasojima K, McGeer EG, McGeer PL (2001) High stability of mRNAs postmortem and protocols for their assessment by RT-PCR. *Brain Res Brain Res Protoc*.8(3):212-218.

7 Acknowledgement

Thank you

- ... Prof. Dr. Edgar Meinel for being a wonderful mentor
- ... Dr. Markus Krumbholz for valuable support with evaluation of data
- ... Dr. Hema Mohan for cooperation with ECM project
- ... Dr. Andreas Junker for guidance and support with the miRNA work
- ... Marie-Therese Fischer for contribution of the in situ hybridisation results
- ... Korcan Ayata for introduction to the FFPE RNA isolation protocol
- ... Angelika Henn for valuable technical advice regarding the work with FFPE tissue
- ... Dr. Thomas Arzberger for providing valuable archival brain samples
- ... Prof. Dr. Hans Lassmann for sharing his expertise with archival MS samples
- ... Prof. Dr. Reinhard Hohlfeld, Prof. Dr. Hartmut Wekerle for allowing a MD student in their department
- ... Berta, Manfred und Thomas Eisele for being a great family
- ... Sebastian Kurz for his never ending patience and always loving support

8 Curriculum Vitae

- 2003 **Abitur**
Erich-Kästner-Gymnasium Eislingen (Fils), Germany
- 2003 - 2010 **Medical Curriculum Munich (MeCuM)**
Ludwig-Maximilians-University Munich, Germany
- 2006 – 2008 **“Molecular Medicine and System Biology”**
Competitive research scholarship,
Ludwig-Maximilians-University Munich, Germany
- 2008 **Research Scholar**
Application of methodological advances to investigate the miRNA
expression pattern in autaptic FFPE MS lesions of different activity
Hans Lassmann, M.D., Center for Brain Research, Vienna, Austria
- 2009 - 2010 **Medical Subinternship**
Internal Medicine, University Hospitals, Cleveland, USA
Neurology, University Hospitals and Cleveland Clinic, Cleveland, USA
Neurosurgery, Metrohealth Medical Center, Cleveland, USA
General Surgery, Zentralklinikum Augsburg, Germany
- Medical Certification Examinations**
- 8/2005 1st State Exam Certification, Germany
6/2008 United States Medical License Examination Step 1
3/2009 United States Medical License Examination Step 2 CK
8/2009 United States Medical License Examination Step 2 CS
5/2010 2nd State Exam Certification, Germany
- since 2010 **Neurology Residency**
University Hospitals Case Medical Center
Case Western Reserve University, Cleveland, USA